

Extracellular Glutamate-GABA Balance in the Developing Neocortex

Dissertation

Zur Erlangung des Grades
Doktor der Naturwissenschaften

Am Fachbereich Biologie
Der Johannes Gutenberg-Universität Mainz

Petr Unichenko
geb. am 16.07.1983 in Novosibirsk,
Russische Föderation

Mainz, 2014

Dekan:

1. Berichterstatter:

2. Berichterstatter:

Tag der mündlichen Prüfung:

Table of contents

Table of contents	3
List of figures	6
List of symbols and abbreviations	9
Summary	11
1 Introduction	13
1.1 Neuroglia	13
1.2 Astrocytes.....	13
1.2.1 Main types and functional properties of astroglial cells.....	13
1.2.2 Electrophysiological properties of astroglial cells.....	14
1.2.3 Ionotropic and metabotropic receptors in astroglial cells	15
1.3 Glutamate and GABA transporters in CNS	15
1.3.1 Transporters in glial and neuronal cells	15
1.3.2 GABA transporters.....	16
1.3.3 Glutamate transporters	17
1.4 Na ⁺ homeostasis and dynamics in astrocytes	19
1.5 Ambient Glutamate and GABA concentrations in the cerebral cortex .	22
1.5 Aim of the study.....	23
2 Materials and Methods.....	25
2.1 Brain slices preparation.....	25
2.2 Electrophysiological recordings from Cajal-Retzius cells in acute slices	25
2.2.1 Whole cell recordings from Cajal-Retzius cells	25
2.2.2 Electrical stimulation	26
2.3 Electrophysiological recordings from astroglial cells in acute slices....	27
2.3.1 Astrocyte identification	27
2.3.2 Whole cell recordings from astrocytes	27
2.3.3. Electrical stimulation	28
2.4 Extracellular recordings.....	29
2.5 Ca ²⁺ imaging	31
2.6 [Na ⁺] _i measurements	31
2.7 Solutions and chemicals	33

2.8 Data evaluation and statistics	33
3 Results	34
3.2 Transporter-mediated replacement of extracellular glutamate for GABA in the developing murine neocortex	41
3.2.1 D-aspartate-induced effects differ from those produced by DL- TBOA	42
3.2.2 DL-TBOA abolishes presynaptic GABA _B R-mediated inhibition	43
3.2.2 D-aspartate potentiates GABA _B R-mediated inhibition.....	46
3.2.3 EAAT1 (GLAST) is the main glutamate transporter in this preparation.....	48
3.3 [Na ⁺] _i influences short-term plasticity of glutamate transporter-mediated currents in neocortical astrocytes	49
3.3.1 Synaptically activated, transporter-mediated currents (STCs) in cortical astrocytes	50
3.3.2 Paired-pulse plasticity of STCs	52
3.3.3 [Na ⁺] _i in cortical astrocytes	53
3.3.4 Paired-pulse plasticity of STCs in astrocytes dialyzed with the high [Na ⁺] _i solution	54
3.3.5 Transporter-mediated [Na ⁺] _i signals in cortical astrocytes.....	56
3.3.6 Exogenous GABA influence STCs in cortical astrocytes	57
3.3.7 Endogenous GABA can modulate STCs	61
3.3.8 Short-term plasticity of STCs at near physiological temperature ..	63
3.3.9 Cortical field potentials are influenced by astrocytic [Na ⁺] _i	64
4 Discussion	67
4.1 EAATs operate in the uptake mode	67
4.2 Presynaptic inhibition of GABAergic transmission.....	68
4.3 EAATs modulate GABA release.....	69
4.4 Physiological role of the EAAT-GAT-mediated glutamate-GABA exchange.....	71
4.5 Does the glutamate-GABA exchange occur in astrocytes?.....	72
4.6 Paired-pulse plasticity of STCs.....	72
4.7 [Na ⁺] _i influences paired-pulse plasticity of STCs	73

4.8 GATs may affect glutamate uptake under physiological conditions.....	76
5 References	78
Acknowledgments.....	92
Curriculum Vitae	Fehler! Textmarke nicht definiert.

List of figures

<i>Figure 1. Astrocytes in somatosensory cortex (sulphorhodamin 101 staining).</i>	14
<i>Figure 2. Glutamate and GABA transporters.</i>	17
<i>Figure 3. Na⁺ signalling in glial cells (Kirischuk et al., 2012).</i>	20
<i>Figure 4. Ambient GABA constrains the strength of GABAergic synapses at Cajal-Retzius cells in the developing visual cortex (Kirmse and Kirischuk, 2006a).</i>	22
<i>Figure 5. Paired-pulse plasticity of STCs does not depend on stimulus intensity.</i>	29
<i>Figure 6. Field potentials elicited in layer 2/3 by electrical stimulation in cortical layer 4.</i>	30
<i>Figure 7. [Na⁺]_i in cortical astrocytes.</i>	32
<i>Figure 8. EAAT blockade did not influence the frequency of Ca²⁺ in CR cells.</i>	34
<i>Figure 9. EAAT blockade reduced the frequency of spontaneous GPSCs in CR cells.</i>	35
<i>Figure 10. DL-TBOA decreases frequency, but not amplitude of miniature GABAergic PSCs.</i>	36
<i>Figure 11. DL-TBOA inhibits GABAergic transmission presynaptically.</i>	37
<i>Figure 12. DL-TBOA-induced inhibition of GABAergic transmission is mediated through presynaptic metabotropic receptors.</i>	38
<i>Figure 13. DL-TBOA-induced inhibition of GABAergic transmission is mediated through presynaptic mGluR-II/III.</i>	39
<i>Figure 14. LY341495 does not influence GABAergic transmission when applied under control conditions.</i>	40
<i>Figure 15. mGluR blockade potentiates eGPSCs in the presence of DL-TBOA.</i>	41
<i>Figure 16. D-Aspartate influences GABAergic transmission.</i>	42
<i>Figure 17. DL-TBOA abolishes presynaptic GABAB receptor-mediated inhibition of eGPSCs.</i>	44
<i>Figure 18. DL-TBOA abolishes GAT-2/3-mediated GABA release.</i>	45

<i>Figure 19. D-aspartate fails to abolish presynaptic GABA_B receptor-mediated inhibition of eGPSCs.....</i>	<i>46</i>
<i>Figure 20. D-aspartate fails to abolish GAT-2/3-mediated GABA release. ...</i>	<i>47</i>
<i>Figure 21. EAAT1/2 control extracellular glutamate concentration in the marginal zone.</i>	<i>48</i>
<i>Figure. 22 EAAT1 (GLAST) controls extracellular glutamate concentration in the marginal zone.</i>	<i>49</i>
<i>Figure 23. Cortical astrocytes.</i>	<i>50</i>
<i>Figure 24. Membrane currents in cortical astrocytes.</i>	<i>50</i>
<i>Figure 25. STCs in cortical astrocytes.</i>	<i>51</i>
<i>Figure 26. Short-term plasticity of STCs studied using the low [Na⁺]_i intracellular solution.</i>	<i>52</i>
<i>Figure 27. STCs elicited by the tetanic stimulation studied using the low [Na⁺]_i intracellular solution.</i>	<i>53</i>
<i>Figure 28. Short-term plasticity of STCs studied using the high [Na⁺]_i intracellular solution.</i>	<i>54</i>
<i>Figure 29. STCs elicited by the tetanic stimulation studied using the high [Na⁺]_i intracellular solution.....</i>	<i>55</i>
<i>Figure 30. Transporter-mediated [Na⁺]_i transients in cortical astrocytes.....</i>	<i>56</i>
<i>Figure 31. Mean [Na⁺]_i response elicited by 5 min bath application of GABA.....</i>	<i>57</i>
<i>Figure 32. Exogenous GABA influences STCs in cortical astrocytes.....</i>	<i>58</i>
<i>Figure 33. Exogenous GABA slowed the kinetics of STCs.....</i>	<i>59</i>
<i>Figure 34. GABA effects on STCs may be mediated by [Na⁺]_i.....</i>	<i>60</i>
<i>Figure 35. Negative correlation between the GABA-induced relative changes of mean STC amplitudes, PPR and [Na⁺]_i elevations.....</i>	<i>61</i>
<i>Figure 36. GABA effects on STCs is blocked by pre-application of NO-711 and SNAP-5114.....</i>	<i>61</i>
<i>Figure 37. GAT blockade influences STC short-term plasticity.....</i>	<i>62</i>
<i>Figure 38. GAT blockade influences STCs elicited by the tetanic stimulation.</i>	<i>62</i>
<i>Figure 39. Short-term plasticity at near physiological temperature.</i>	<i>63</i>

Figure 40. GAT blockade influences STC short-term plasticity at near physiological temperature. 64

Figure 41. Dialysis of an astrocyte with the low $[Na^+]_i$ solution influence evoked field potentials in the cortex. 65

Figure 42. EAAT-GAT-mediated glutamate-GABA exchange..... 70

List of symbols and abbreviations

(RS)-MCPG	(RS)- α -Methyl-4-carboxyphenylglycine
ACSF	Artificial Cerebrospinal Fluid
AMPA	α -Amino-3-hydroxy-5-methyl-4-isoxazolepropionic acid
APV	DL-2-Amino-5-phosphonopentanoic acid
CGP55845	(2S)-3-[[[(1S)-1-(3,4-Dichlorophenyl)ethyl]amino-2-hydroxypropyl](phenylmethyl)phosphinic acid hydrochloride
CNS	Central nervous system
CR-cells	Cajal-Retzius cells
DHK	Dihidrokainik acid
DL-TBOA	DL-threo- β -Benzyloxyaspartic acid
DNQX	6,7-Dinitroquinoxaline-2,3-dione
EAAC1	Exitatory amino acid carrier 1 (EAAT3)
EAAT	Excitatory aminoacid transporter
eGPSC	Evoked gabaergic postsynaptic current
EGTA	Ethylene glycol-bis(2-aminoethylether)-N,N,N',N'-tetraacetic acid
EOS	Glutamate-sensitive fluorescence indicator
GABA	γ -aminobutyric acid
GABA _A	γ -aminobutyric acid A receptor
GABA _B	γ -aminobutyric acid B receptor
GABA _C	γ -aminobutyric acid C receptor
GAT	γ -aminobutyric acid transporter
GLAST	Glutamate-aspartate transporter
GLT-1	Glutamate transporter 1
GPSC	GABAergic postsynaptic current
HEPES	4-(2-Hydroxyethyl)piperazine-1-ethanesulfonic acid
IC ₅₀	Half maximal inhibitory concentration
KB-R7963	2-[2-[4-(4-Nitrobenzyloxy)phenyl]ethyl]isothiourea mesylate
LY341495	(2S)-2-Amino-2-[(1S,2S)-2-carboxycycloprop-1-yl]-3-

	(xanth-9-yl) propanoic acid
LY379268	<i>(1R,4R,5S,6R)-4-Amino-2-oxabicyclo[3.1.0]hexane-4,6-dicarboxylic acid</i>
mGluR	Metabotropic glutamate receptors
mGPSC	Miniature GABAergic postsynaptic current
ISI	Interstimulus interval
NCX	Sodium/calcium exchanger
NEM	N-Ethylmaleimide
NMDA	N-Methyl-D-aspartic acid
NO-711	1,2,5,6-Tetrahydro-1-[2- [[[(diphenylmethylene)amino]oxy]ethyl]-3- pyridinecarboxylic acid hydrochloride
OGB-1	Oregon Green BAPTA-1
P	Postnatal day
PPD	Paired pulse depression
PPF	Paired pulse facilitation
PPR	Paired pulse ratio
S.E.M	Standard error of the mean
SBFI	Sodium-binding benzofuran isophthalate
sGPSC	Spontaneous GABAergic postsynaptic current
SNAP-5114	1-[2-[tris(4-methoxyphenyl)methoxy]ethyl]-(S)-3- piperidinecarboxylic acid
sPSC	Spontaneous postsynaptic current
SR101	Sulphorhodamin 101
STC	Synaptically-activated transporter-mediated current
TFB-TBOA	(3S)-3-[[3-[[4- (Trifluoromethyl)benzoyl]amino]phenyl]methoxy]-L- aspartic acid
TTX	Tetrodotoxin

Summary

During corticogenesis, radially migrating cells move from deeper zone to the marginal zone, but they do not invade the latter. This “stop” function of the marginal zone is mediated by a number of factors, including glutamate and GABA, two main neurotransmitters in the central nervous system (CNS). In the marginal zone, GABA has been shown to be released via GABA transporters (GAT)-2/3, whereas glutamate transporters (EAATs) operate in the uptake mode. In this study GABAergic postsynaptic currents (GPSCs) were recorded from Cajal-Retzius cells in the marginal zone of murine neonatal neocortex using whole-cell patch-clamp technique. Minimal electrical stimulation was applied to elicit evoked GPSCs using paired-pulse protocol. We report that EAAT blockade with DL-TBOA, a specific non-transportable EAAT antagonist, abolishes constitutive GAT-2/3-mediated GABA release. In contrast to DL-TBOA, D-aspartate, an EAAT substrate, fails to block GAT-2/3-mediated GABA release. SNAP-5114, a specific GAT-2/3 antagonist, induced an elevation of intracellular sodium concentration ($[Na^+]_i$) under resting conditions and in the presence of D-aspartate, indicating that GAT-2/3 operates in reverse mode. In the presence of DL-TBOA, however, SNAP-5114 elicited $[Na^+]_i$ decrease, demonstrating that GAT-2/3 operates in uptake mode. We conclude that EAATs via intracellular Na^+ signaling and/or cell depolarization can govern the strength/direction of GAT-mediated GABA transport. Next we investigated short-term plasticity of synaptically-activated, glutamate transporter-mediated currents (STCs) in cortical layer 2/3 astrocytes. STCs were elicited by local electrical stimulation in layer 4 in the presence of ionotropic glutamate (AMPA and NMDA), $GABA_A$, and $GABA_B$ receptor antagonists. In experiments with low $[Na^+]_i$ (5 mM) intrapipette solution, STCs elicited by paired-pulse stimulation demonstrated paired-pulse facilitation (PPF) at short (<250 ms) inter-stimulus intervals (ISIs) and paired-pulse depression (PPD) at longer ISIs. In experiments with close to physiological, high $[Na^+]_i$ (20 mM) intrapipette solution, PPF of STCs at short ISIs was significantly reduced, while PPD at longer ISIs was not affected. In

addition, the STC decay kinetics were slowed in the presence of high $[Na^+]_i$. Exogenous GABA increase astrocytic $[Na^+]_i$, reduced the mean STC amplitude, decreased PPF at short ISIs, and slowed STC decay kinetics. All GABA-induced changes were blocked by NO-711 and SNAP-5114, GABA transporters (GATs) antagonists. In experiments with the low intrapipette solution, GAT blockade decreased STC PPF at short ISIs both at room and at near physiological temperatures. Astrocyte dialysis with low $[Na^+]_i$ solution increased the amplitude and resulted in PPD of field potentials recorded in the vicinity of the astrocyte. Thus, we conclude that 1) short-term plasticity of STCs is dependent on $[Na^+]_i$ and 2) GATs may influence EAAT-mediated glutamate uptake and thus the rate and efficacy of glutamate removal (Dvorzhak et al., 2012;Unichenko et al., 2012;Unichenko et al., 2013).

1 Introduction

1.1 Neuroglia

A term "Neuroglia" was first introduced by Virchow in the middle of the XIX century. Virchow meant by "glia" a form of connective tissue which surrounds neurons. Since the "connective tissue" of the brain was different from that in other organs, Virchow used a term «Nervenkitt», or «neuroglia" (Somjen, 1988).

The main difference between neurons and glial cells is the ability for generation of action potentials (APs). Being unable to generate action potentials, glial cells had been considered as a passive element which had mainly trophic/homeostatic function (Bacci et al., 1999). The point of view on glial functions has dramatically changed during the recent decades (Halassa et al., 2007; Santello et al., 2012). Glial cells express a number of voltage- and ligand- activated ionic channels, as well as the metabotropic receptors (Porter and McCarthy, 1997). This allows glial cells to respond to neural activity (Rouach et al., 2004; Volterra and Steinhauser, 2004) and even modulate it (Araque et al., 1999; Poskanzer and Yuste, 2011; Rouach et al., 2008). Currently four main types of glial cells are identified in mature brain: oligodendrocytes, ependymal cells, microglial cells and astrocytes.

1.2 Astrocytes

1.2.1 Main types and functional properties of astroglial cells

The term "astrocyte" was first introduced by M. von Lenossek for description of star-shaped glial cells (Lenhossek, 1891). Astrocytes are very heterogeneous subpopulation of cells in the brain (Matyash and Kettenmann, 2010). Astrocytes are found in almost all parts of the CNS. In the cerebellum and retina are two types of extended radial-like glia: Bergman glia and retinal Muller cells, respectively. Despite morphological differences, Bergman glia

and Muller cells are quite similar to the cortical astrocytes, particularly in terms of their functions, microanatomic structure of perisynaptic processes and expression of receptors and neurotransmitter transporters. Astrocytes have a significant number of processes surrounding neuronal synapses (Danbolt, 2001). This is defined by one of the most important astrocytic function – neurotransmitter uptake from the synaptic space (Auger and Attwell, 2000; Diamond, 2005; Lopez-Bayghen and Ortega, 2011). Having a number of contacts with blood capillaries (Fig. 1), astrocytes can serve as part blood-brain barrier (Kovacs et al., 2012).

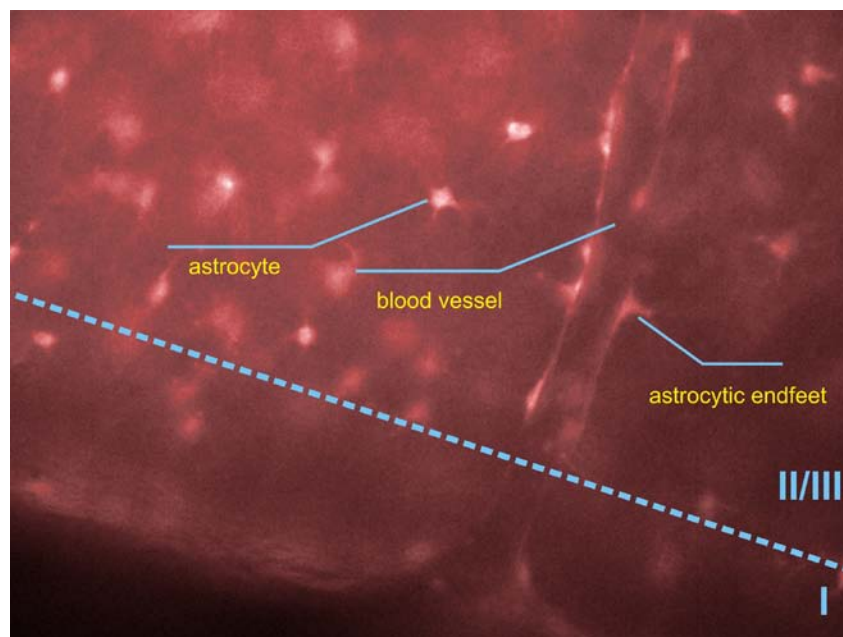


Figure 1. Astrocytes in somatosensory cortex (sulphorhodamin 101 staining).

The other major role of glial cells and, particularly, astrocytes in CNS is potassium uptake from the extracellular space (Kressin et al., 1995).

1.2.2 Electrophysiological properties of astroglial cells

Electrophysiological properties astroglial cells strongly vary depending on the type and age of an animal. The main electrophysiological difference between astrocytes and neurons is the inability of astrocytes to generate AP. Mature astrocytes are not able to generate APs, because astrocytes, unlike neurons, do not express a sufficient number of voltage gated sodium channels. In mature “simple” astrocytes potassium conductivity of cell membrane is

considerably higher than that in neurons. Hence the resting membrane potential in astrocytes is closer to the potassium equilibrium potential than that in neurons. If a typical neuronal resting membrane potential is approximately -70 mV, the resting membrane potential in astrocytes is approximately -80 mV (Kressin et al., 1995). Mature astrocytes have a very low membrane resistance, not more than tens of mega Ohms (Schroder et al., 1999). Low membrane resistance is a consequence of high potassium conductance (Kressin et al., 1995) significant expression of gap junctions with adjacent astrocytes (Giaume and McCarthy, 1996).

1.2.3 Ionotropic and metabotropic receptors in astroglial cells

Astrocytes express a large number of ionotropic and metabotropic receptors (Bowman and Kimelberg, 1984) glutamatergic, GABAergic, adrenergic, purinergic, serotonergic and other receptors. Activation of these receptors is functionally associated with a change in membrane potential or with activation of intracellular signaling cascades, such as activation of phospholipase C or adenylyl cyclase. Expression of the receptor by astrocytes extremely heterogeneous and dependent on astrocyte localization, age of animal, and can vary in reaction to the injury. It is also shown that the receptors can be activated by neurotransmitters released into the synaptic terminals of neurons (Porter and McCarthy, 1997). This means that neural activity has a direct effect on astroglia via membrane receptors (Giaume, 2009). Besides receptor astrocytes express various neurotransmitter transporters (Gadea and Lopez-Colome, 2001a;Gadea and Lopez-Colome, 2001b).

1.3 Glutamate and GABA transporters in CNS

1.3.1 Transporters in glial and neuronal cells

Neurotransmitter transporters on membrane of glial cells are responsible for uptake of released neurotransmitters (Bergles and Jahr, 1998) from synaptic cleft during the synaptic transmission. The need for effective glial neurotransmitter removal is dictated apparently by limited area available on

the presynaptic and postsynaptic membranes of neuronal cells. Physical limitations restrict the location of a large number of neuronal transporters near sites of neurotransmitter release. Surrounding glial cells provide additional surface for enhanced neurotransmitter clearance by high affinity transporters. It has a direct impact on the concentration of neurotransmitters in juxtasyaptic space. Controlling the excitation/inhibition balance in the brain astrocytic processes become an important part of synapse (Angulo et al., 2004). Thus, synapse nowadays is considered as tripartite synapse (Halassa et al., 2007;Perea et al., 2009;Santello et al., 2012). Since glutamate is the major excitatory neurotransmitter, and GABA is the major inhibitory neurotransmitter in the adult cortex, the most important transporters contributing to excitation/inhibition balance are glutamate and GABA transporters.

1.3.2 GABA transporters

There are four known GABA transporter to date: GAT-1, GAT-2, and GAT-3 and betaine-GABA transporter (BGT-1) (rat nomenclature). Molecular studies have shown that the GAT-1, GAT-2, and GAT-3 are high affinity GABA transporters; affinity of BGT-1 for GABA is lower. Activity of GABA transporters is strongly dependent on transmembrane sodium gradient. Chloride ion concentration is also important for the transport of the GABA. However, presence of chloride ions in the absence of Na^+ is not sufficient for the transporter functioning. Transporters GAT-1, GAT-2 and GAT-3 have the following stoichiometry: $2\text{Na}^+ : 1\text{Cl}^- : 1\text{GABA}$ (Eulenburg and Gomez, 2010) (Fig. 2).

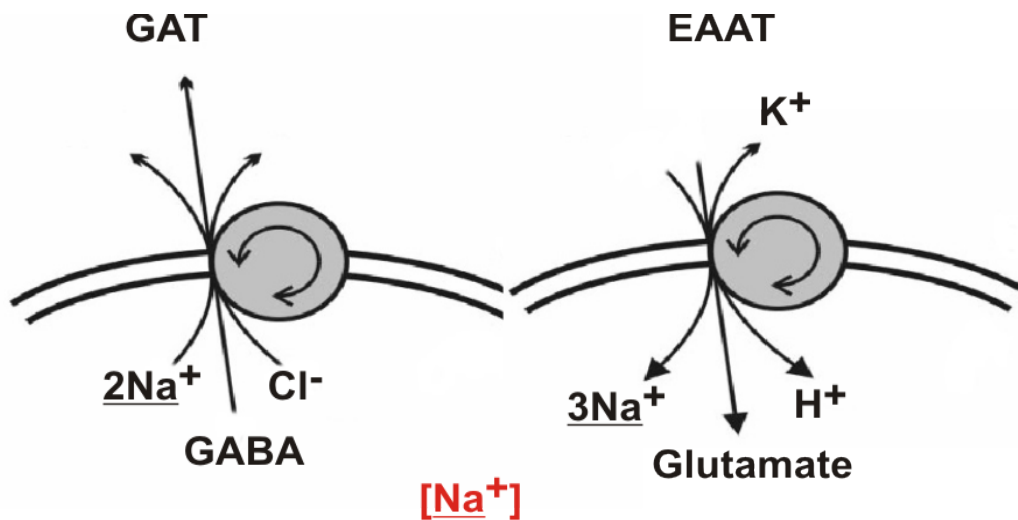


Figure 2. Glutamate and GABA transporters.

GAT -1 - the most common GABA transporter in the CNS. In situ hybridization showed that the vast majority of cells expressing GAT -1 are neurons, and a small number of the cells are astrocytes (Conti et al., 2004). According to the earlier immunohistochemical studies GAT-2 is expressed exclusively in ependymal and choroid plexus cells and in the leptomeninges (Conti et al., 1999). The highest expression level of GAT-3 is found in the cortex. GAT -3 was predominantly detected on the distal astrocytic process near the synaptic contacts (Minelli et al., 1996), thus contributing to the modulation of GABAergic synaptic transmission (Conti et al., 2004). Although glutamate level in the extracellular space is primarily controlled by glutamate transporters (Huang and Bergles, 2004), GABA transporters are probably also involved in the modulation of glutamatergic synaptic transmission, for example via release of GABA, which may tonically activate GABA_B receptors on presynaptic or postsynaptic compartments.

1.3.3 Glutamate transporters

In the CNS, glutamatergic neurotransmission proceeds with high temporal and spatial resolutions. Synaptically released glutamate diffuses through the synaptic cleft and activates postsynaptic receptors, eliciting a postsynaptic current. Glutamate effects on receptors are terminated by diffusion and by the actions of glutamate transporters (EAATs for excitatory amino acid transporters). To date, five subtypes of glutamate transporters are known:

EAAT1 or GLAST (glutamate-aspartate transporter), EAAT2 or GLT-1 (glutamate transporter 1), EAAT3 or EAAC (excitatory amino acid carrier), EAAT4 and EAAT5. EAATs localisation depending on the type is highly nonuniform: EAAT3, EAAT4, and EAAT5 are primarily located to neurons, whereas EAAT1 (GLAST) and EAAT2 (GLT-1) are primarily expressed in glial cells in adult animals (Danbolt et al., 1998; Levy et al., 1998; Rothstein et al., 1996). Glial EAATs shape the time course of postsynaptic responses and limit spillover of glutamate to adjacent synapses (Huang and Bergles, 2004; Tzingounis and Wadiche, 2007).

EAAT5 perhaps the most scantily explored transporter of EAAT family. EAAT5 expressed exclusively in bipolar cells of the retina. Also in this transporter was detected in some amount in Muller glia (Arriza et al., 1997). The other EAAT with the same specific localization area is EAAT4. EAAT4 is a major neuronal glutamate transporter in the cerebellum. Purkinje cells in the cerebellum also express EAAT3, but only in small amounts (Danbolt, 2001); (Otis and Jahr, 1998). EAAT3 in the greatest number found in hippocampus, cerebellum and basal ganglia. EAAT3 expressed in glutamatergic and GABAergic (e.g., cerebellar Purkinje cells and motor neurons of the spinal cord) neurons. It is also detected in retinal horizontal amacrine and ganglion cells, as well as in cones, but not in Muller glia cells. It is believed that EAAT3 localized mainly in neuronal rather than glial cells (Danbolt, 2001). However, in some studies EAAT3 was found in astrocytes (Conti et al., 1998). Interestingly, EAAT3 knockout mice do not demonstrate severe anatomical and behavioural deviation except dicarboxylic aciduria (Peghini et al., 1997). EAAT2 as well as EAAT1 is one of the most common glutamate transporters in the brain. EAAT2 in a large quantity is expressed in the hippocampus. Despite the fact that the EAAT2 mRNA was also detected in neurons the principal place of expression are astrocytes. EAAT2 was not found in neurons of the normal adult CNS (with the exception of retina). EAAT2 is expressed in the hippocampus, cerebellum, neocortex, striatum and thalamus (Danbolt, 2001). EAAT1 is widely expressed throughout the CNS. EAAT1 – the major transporter in the cerebellum, inner ear, near ventricular structures and in the retina. The EAAT1/EAAT2 ratio varies in astrocytes from different regions of the CNS (Danbolt, 2001). According to Anderson and colleagues, EAAT1 is

present in the cerebral cortex and cerebellum of rodents from birth, whereas EAAT2 can be detected only after the third postnatal week, reaching an amount of typical adult brain to the 5th week (Anderson and Swanson, 2000). In the greatest number EAAT1 was found in areas near various parts of neurons, and to a less extent – close to blood capillaries, endothelial or pia mater (Danbolt, 2001). As EAAT2, EAAT1 is an important transporter in the CNS. Although EAAT1-deficient mice survive and are able to fulfil simple tasks in behavioural experiments, but these mice are not able to solve more complex motor tasks. These mice are significantly more vulnerable to various injuries and brain ischemia (Watase et al., 1998).

Effective glutamate clearance from the synaptic cleft makes possible precise synaptic transmission with high frequency and resolution. Turning off one of the elements of reuptake leads to functional and developmental deviations in the CNS. Although the single EAAT1 or EAAT2 knockout is viable in mice, Double EAAT1 and EAAT2 deficient mice do not survive at all (Stoffel et al., 2004). Because transport of one glutamate anion is coupled to the co-transport of three Na^+ ions and one proton and to the counter-transport of one potassium ion (Levy et al., 1998; Zerangue and Kavanaugh, 1996), EAATs are electrogenic and its efficacy is highly dependent on transmembrane Na^+ ion gradient (Fig. 2).

1. 4 Na^+ homeostasis and dynamics in astrocytes

Na^+ ion concentration in astrocytes is regulated by Na^+ permeable channels, exchangers and transporters (Fig. 3, (Kirschuk et al., 2012)).

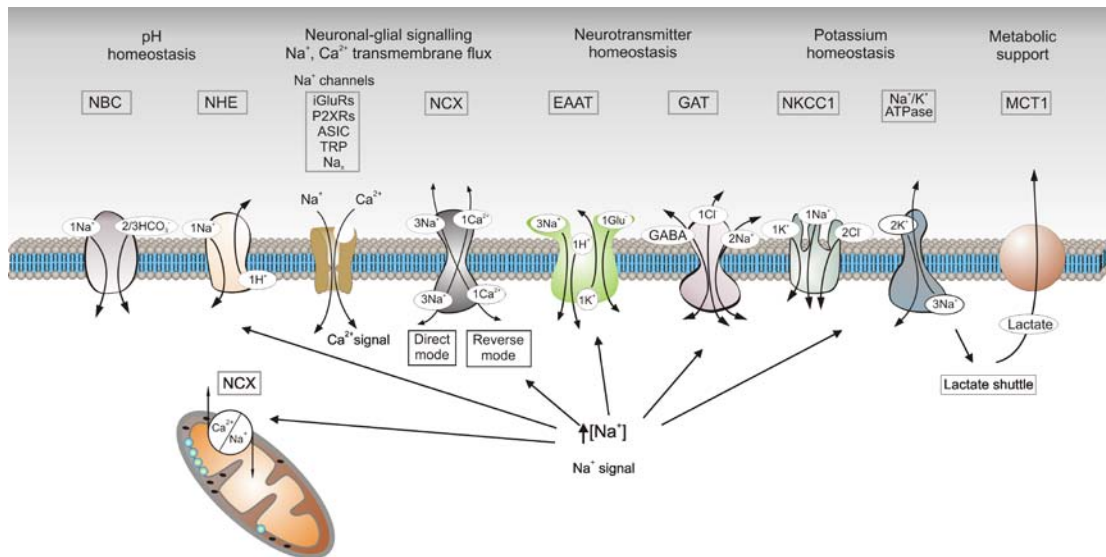


Figure 3. Na⁺ signalling in glial cells (Kirischuk et al., 2012).

First of all $[Na^+]_i$ is regulated by transmembrane Na⁺/K⁺ ATPase which exchanges 3 sodium ions by 2 potassium ion. This is a basic mechanism for Na⁺ removal from astrocytic cytosol. The other three main mechanisms mediating Na⁺ dynamics in glial cells are activation of ligand-gated ionotropic receptors, activity of transporters and sodium-calcium exchangers (NCX).

During elevated neuronal activity, NCX is supposed to extrude the high level of Ca²⁺ ions from the neuronal synaptic terminal. Since in this process Ca²⁺ ion is exchanged with 3 Na⁺ ions, activity of NCX is one of the major sources of Na⁺ influx in neurons (Lee et al., 2002). Glial cells do not generate action potentials, and so far even though astrocytes express NCX, its activity should not strongly influence $[Na^+]_i$.

Experiments with specific glutamate transporter blocker DL-TBOA showed that EAAT block leads to an increase of extracellular glutamate concentration in cortex and following activation of NMDA receptors and generation of epileptic-like discharges (Demarque et al., 2004) (the effect was also observed in immature hippocampus (Cattani et al., 2007)). This data demonstrates that glutamate transporters are constantly active in the brain, mediating glutamate clearance from extracellular space. Hence, glutamate transporters are the source of persistent Na⁺ influx in astrocytes. Na⁺ influx can be also strongly increased during elevated neuronal activity and glutamate release, like in up-

states in cerebral cortex, during epileptic discharges and during electrical stimulation in *in vitro/in vivo* conditions. Glutamate transport, being electrically charged, besides the elevation of somatic $[Na^+]_i$, can also induce measurable electrical transmembrane currents (Barbour et al., 1991). Indeed, EAAT mediated currents (STCs for synaptically induced transporter mediated currents), induced by electrically evoked glutamate release from Schaffer collateral fiber terminals in CA1 region of hippocampus were detected in astrocytes via whole cell recordings (Diamond et al., 1998). The amplitude of synaptically-induced $[Na^+]_i$ transients in astrocytes can reach 10 mM and their time course is surprisingly slow. The decay time constant amounts to tens of seconds (Bennay et al., 2008; Langer and Rose, 2009; Barbour et al., 1991). This effect provides a tool for monitoring the process of glutamate uptake and synaptic release of glutamate in various brain structures (Unichenko et al., 2012; Unichenko et al., 2013).

However it seems that the largest changes in Na^+ concentrations take place not in somatic region of astrocytes, but in near membrane regions on distant astrocytic processes close to synaptic contacts. In this case local Na^+ concentration changes can be hardly detected by optical imaging technique. According to the calculations EAATs reverse potential is near +60mV, that means that EAATs can be reversed only in pathophysiological conditions (Rossi et al., 2000), meanwhile theoretical reverse potential for GATs is near -68 mV (Wu et al., 2007). This means that direction of GABA transport is strongly dependent on transmembrane Na^+ gradient, which is in turn dependent on $[Na^+]_i$. Consequently, elevation of $[Na^+]_i$ might change the direction of GABA transport (Richerson and Wu, 2003; Wu et al., 2007). Interestingly, GAT-2/3 does operate in the reverse mode in the marginal zone of the neonatal neocortex (Dvorzhak et al., 2010; Kirmse and Kirischuk, 2006a). GABAergic synapses at Cajal-Retzius (CR) cells, the principal neurons in the marginal zone of the neonatal murine cortex, experience presynaptic GABA_B receptor-mediated tonic inhibition, because GABA is constitutively released via GAT-2/3 (Fig. 4) (Kirmse & Kirischuk, 2006a).

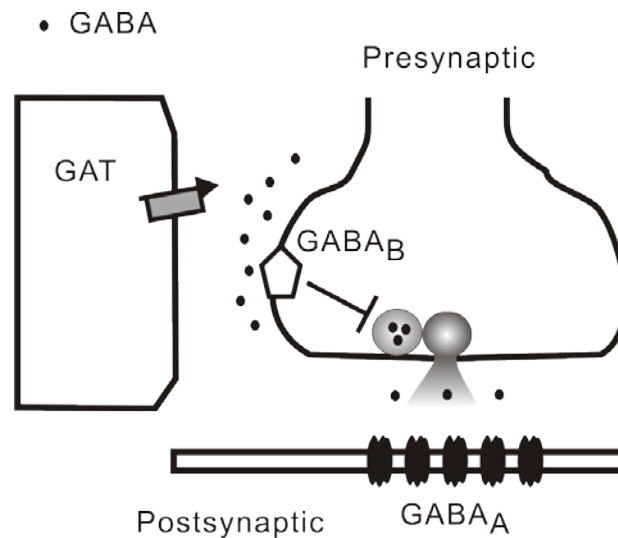


Figure 4. Ambient GABA constrains the strength of GABAergic synapses at Cajal-Retzius cells in the developing visual cortex (Kirmse and Kirischuk, 2006a).

From the other hand, as EAATs are Na^+ -dependent, an increase of $[\text{Na}^+]_i$, i.e. decreasing of electrochemical gradient for Na^+ , directly reduces glutamate uptake (Barbour et al., 1991). Moreover, intracellular Na^+ also influences the cycling time, or turn-over rate, of EAATs (Wadiche et al., 2006). Because synaptically-induced $[\text{Na}^+]_i$ transients demonstrate slow kinetics, EAAT-mediated Na^+ entry and/or $[\text{Na}^+]_i$ changes induced by activity of other Na^+ -coupled mechanisms, like GABA transporters (Attwell et al., 1993), can potentially modulate short-term plasticity of STCs and in turn the efficacy of glutamate removal. Thus, glial transporters are an essential part excitatory amino acid homeostasis in the CNS. Neuronal and glial glutamate and GABA transporters represent a single system which controls glutamate and GABA concentrations in the extracellular space in the brain. However the interaction between EAATs and GATs, being of great importance and interest, is poorly investigated (Unichenko et al., 2012).

1.5 Ambient Glutamate and GABA concentrations in the cerebral cortex

The major excitatory and inhibitory neurotransmitters in the adult brain, glutamate and GABA, influence various developmental processes well before mature synaptic patterns have been established (Owens and Kriegstein, 2002; Represa and Ben-Ari, 2005). Low concentrations of GABA operating via high affinity GABA_C and GABA_B (GABA_BRs) receptors regulate cell migration in the cortical plate (Behar et al., 1999a; Lopez-Bendito et al., 2003; Denter et al., 2010; Behar et al., 2000), while low affinity GABA_A receptors appear to provide a stop signal to end migration (Behar et al., 2000). Blockade of GABA_A receptors with antagonists or their desensitization by agonists causes heterotopias in the most superficial cortical layers *in vivo*, presumably because the stop signal is missing (Heck et al., 2007). Similarly to GABA, glutamate is released well before the formation of glutamatergic synapses (Demarque et al., 2004). Migration of embryonic neocortical neurons in slice cultures is stimulated by activation of NMDA receptors (Behar et al., 1999b) and inhibited by blocking NMDA receptors (Hirai et al., 1999). Local blockade of NMDA receptors *in vivo* in P0 rat pups disturbs cortical lamination and causes heterotopic cell clusters in the superficial layer (Reiprich et al., 2005). Interestingly, there is no deficit in cortical layering and synapse formation in mice in which vesicular release has been deleted (Varoqueaux et al., 2002; Verhage et al., 2000). Moreover, both NMDA and GABA receptors are activated by endogenous neurotransmitters even when vesicular release was genetically ablated (Manent et al., 2005). Thus, both GABA and glutamate acting on various receptor subtypes play an important modulatory role during corticogenesis. Although the exact origin of neurotransmitters remains unknown, extracellular glutamate and GABA levels are supposed to be mainly determined by Na⁺-dependent glutamate and GABA transporters (Unichenko et al., 2012).

1.5 Aim of the study

During perinatal development of the brain, GABAergic and glutamatergic systems involved in many developmental processes. Both increased and decreased GABA/glutamate levels in the extracellular space lead to severe

brain cortical malformations. As astroglial cells express Na⁺ dependent glutamate and GABA transporters, these cells are mainly responsible for the setting of the actual GABA/glutamate balance in the extracellular space. To uncover the astroglial contribution to extracellular glutamate/GABA homeostasis, the following questions were addressed:

1. What are the maintenance mechanisms of extracellular GABA/glutamate balance in superficial layers of neocortex?
2. Is there any interaction between EAAT and GAT? If yes, what is the mechanism(s)?
3. Can astrocytic [Na⁺]_i changes influence neuronal network activity?

2 Materials and Methods

2.1 Brain slices preparation

All experiments were carried out according to the guidelines for the care and use of laboratory animals of University Medical Center of the Johannes Gutenberg University Mainz and the European Communities Council Directive of 24 November 1986 (86/609/EEC). The study was approved by the ethics committee of the University Medical Center Mainz. Experiments were designed to minimize the number of animals used.

All experiments were conducted with pigmented C57BL/6 mice pups of postnatal days 5-7 (the day of birth was designated as P0) for recordings from Cajal-Retzius cells and P16-20 mice for recordings from astrocytes. Animals were decapitated under deep isoflurane anaesthesia. The brain was removed quickly and transferred into ice-cold saline that contained (in mM): 125 NaCl, 4 KCl, 10 glucose, 1.25 NaH₂PO₄, 25 NaHCO₃, 0.5 CaCl₂, and 2.5 MgCl₂ constantly aerated with a 5% CO₂/95% O₂ mixture (pH = 7.3). The brain was separated into two hemispheres. Sagittal slices of both hemispheres were cut on a vibratome (Campden Instruments Ltd., UK). After preparation, slices (200 µm thick) were stored for at least 1 h at room temperature in artificial cerebrospinal fluid (ACSF) that contained (in mM): 125 NaCl, 4 KCl, 10 glucose, 1.25 NaH₂PO₄, 25 NaHCO₃, 2 CaCl₂, and 1 MgCl₂. pH was buffered to 7.3 by continuous bubbling with a 5% CO₂/95% O₂ mixture. The osmolarity was 330 mOsm.

2.2 Electrophysiological recordings from Cajal-Retzius cells in acute slices

2.2.1 Whole cell recordings from Cajal-Retzius cells

For recordings, slices were placed into a recording chamber (~0.4 ml volume) on the microscope stage (Axioscope FS, Zeiss) equipped with phase contrast optics. Slices were submerged with a constant flow of oxygenated ACSF.

Flow rate was set to 1 ml/min. A 40x water immersion objective was used in all experiments. Cajal-Retzius (CR) cells were visually selected according to morphological criteria: 1) location in layer I; 2) horizontal orientation; 3) large ovoid soma and 4) one thick tapered dendrite typically extended in parallel to the pial surface. 10 μ M 6,7-dinitroquinoxaline-2,3-dione (DNQX, an AMPA/kainate receptor antagonist) and 50 μ M DL-2-amino-5-phosphonopentanoic acid (APV, an NMDA receptor blocker) were added to the ACSF to block glutamatergic currents, unless otherwise stated. GABAergic postsynaptic currents (GPSCs) were recorded using the whole-cell configuration of patch-clamp technique. Intra-pipette solution contained (in mM): 100 potassium gluconate, 50 KCl, 5 NaCl, 0.5 CaCl₂, 5 EGTA, 25 HEPES, 2 MgATP, 0.3 NaGTP, pH was set to 7.2 with KOH. The chloride reversal potential was about -20 mV. Relatively high intrapipette Cl⁻ concentration was used to mimic elevated [Cl⁻]_i observed in CR cells (Achilles et al., 2007). Pipette resistance was 3-5 M Ω , when filled with the above saline. Electrophysiological signals were acquired using an EPC-10 amplifier and TIDA 5.24 software (HEKA Elektronik, Lambrecht, Germany). The signals were filtered at 3 kHz and sampled at a rate of 10 kHz. Hyperpolarizing pulses of 10 mV were used to control the access resistance. Only recordings with a series resistance below 40 M Ω were accepted. Series resistance compensation was not applied. Cells exhibiting more than 20% changes in the access resistance during an experiment were discarded. The holding potential was set to -70 mV.

2.2.2 Electrical stimulation

Evoked GABAergic postsynaptic currents (eGPSCs) were elicited by focal electrical stimulation through a glass pipette filled with the ACSF (about 10 M Ω). The stimulation pipette was always positioned within layer I. N-(2,6-dimethylphenylcarbamoylemethyl)-triethylammonium bromide (QX 314, 2 mM) was added to the intracellular solution to prevent generation of action potentials in the tested neurons. An isolated stimulation unit was used to generate rectangular electrical pulses. Pulse duration was set to 0.5 ms. Pulse intensity was adjusted to activate a unitary synaptic input (minimal

stimulation). Stimulation was accepted as minimal if the following criteria were satisfied: 1) eGPSC latency remained stable (< 20% fluctuations); 2) lowering stimulus intensity by 20% resulted in a complete failure of eGPSCs; 3) an increase in stimulus intensity by 20% changed neither mean eGPSC amplitude nor eGPSC shape (Kirmse and Kirischuk, 2006a). Typical pulse intensity required for minimal stimulation was between one and two μ A.

CR cells receive two types of GABAergic inputs characterized as fast and slowly rising eGPSCs. Because inputs generating the slowly rising eGPSCs experience weak tonic GABA β R-mediated inhibition (Kirmse et al., 2007a), only fast rising eGPSCs (10-90 % rise time less than 1 ms, the mean value - 0.7 ms) have been selected in this study.

2.3 Electrophysiological recordings from astroglial cells in acute slices.

2.3.1 Astrocyte identification

Sulforhodamine 101 (SR101) was used to visualize cortical astrocytes. The detailed description of the method is given elsewhere (Nimmerjahn et al., 2004). Briefly, slices were incubated in the ACSF supplemented with 2 μ M SR101 for 20 min at 36 °C. After loading, slices were stored in the ACSF for at least one hour at room temperature to ensure SR101 washout from the extracellular space. Excitation wavelength was controlled by a fast monochromator system, and a cooled CCD camera was used to record fluorescence signals (TILL Photonics, München, Germany). SR101 was excited at 590 nm. The excitation and emission light was separated using a 610 nm dichroic mirror. Emitted light was filtered using a 630 nm long-pass filter.

2.3.2 Whole cell recordings from astrocytes

For recordings, slices were placed to the recording chamber (~0.4 ml volume) on an upright microscope (Axioscope FS, Zeiss, Oberkochen, Germany).

Slices were submerged with a constant flow of oxygenated ACSF. 10 μM 6,7-dinitroquinoxaline-2,3-dione (DNQX), an AMPA/kainate receptor antagonist, 50 μM DL-2-amino-5-phosphonopentanoic acid (APV), an NMDA receptor blocker, 20 μM gabazine, a GABA_A receptor antagonist and 1 μM CGP55845, a GABA_B receptor blocker, were added to the ACSF, unless otherwise stated. Flow rate was set to 1 ml/min using a gravity-driven superfusion system. A 40x water immersion objective (Zeiss, Oberkochen, Germany) was used in all experiments. STCs were recorded using the whole-cell configuration of patch-clamp technique. Two intrapipette solutions were used. Low $[\text{Na}^+]_i$ solution contained (in mM): 100 potassium gluconate, 50 KCl, 5 NaCl, 0.5 CaCl₂, 5 EGTA, 25 HEPES, 2 MgATP, 0.3 NaGTP. High $[\text{Na}^+]_i$ solution contained (in mM): 100 potassium gluconate, 35 KCl, 20 NaCl, 0.5 CaCl₂, 5 EGTA, 25 HEPES, 2 MgATP, 0.3 NaGTP. pH was set to 7.2 with KOH. Pipette resistance was 3-5 M Ω , when filled with the above saline. Electrophysiological signals were acquired using an EPC-10 amplifier and TIDA 5.24 software (HEKA Elektronik, Lambrecht, Germany). The signals were filtered at 3 kHz and sampled at a rate of 10 kHz. Liquid junction potentials (about 5 mV) were not corrected. The holding potential was set to -80 mV. Series resistance was controlled by applying hyperpolarizing pulses of 10 mV. Cell capacitance and membrane resistance values were obtained from capacitance artifacts by mono-exponential fitting. Only recordings with series resistance below 20 M Ω were accepted. Series resistance compensation was not applied. Cells exhibiting more than 20% changes in the access resistance during an experiment were discarded.

2.3.3. Electrical stimulation

STCs in layer 2/3 cortical astrocytes were elicited by focal electrical stimulation in layer 4. Pulses were applied through a glass pipette filled with ACSF (about 10 M Ω). Isolated stimulation unit was used to generate rectangular electrical pulses. Pulse duration was set to 0.5 ms. In case of extracellular stimulation, the number of activated fibers remains unknown and vary from cell to cell. Because the main goal of this work was to investigate

paired-pulse plasticity of STCs, we inspected whether paired-pulse ratio (PPR) is dependent on the stimulus intensity. As expected, STC amplitudes increased as the stimulus intensity raised from 1 to 5 μA . The relationship between pulse intensity and STC amplitude was approximately linear (Fig. 5A,B), but both STC decay time constant and PPR did not depend on the pulse intensity (Fig. 5C,D).

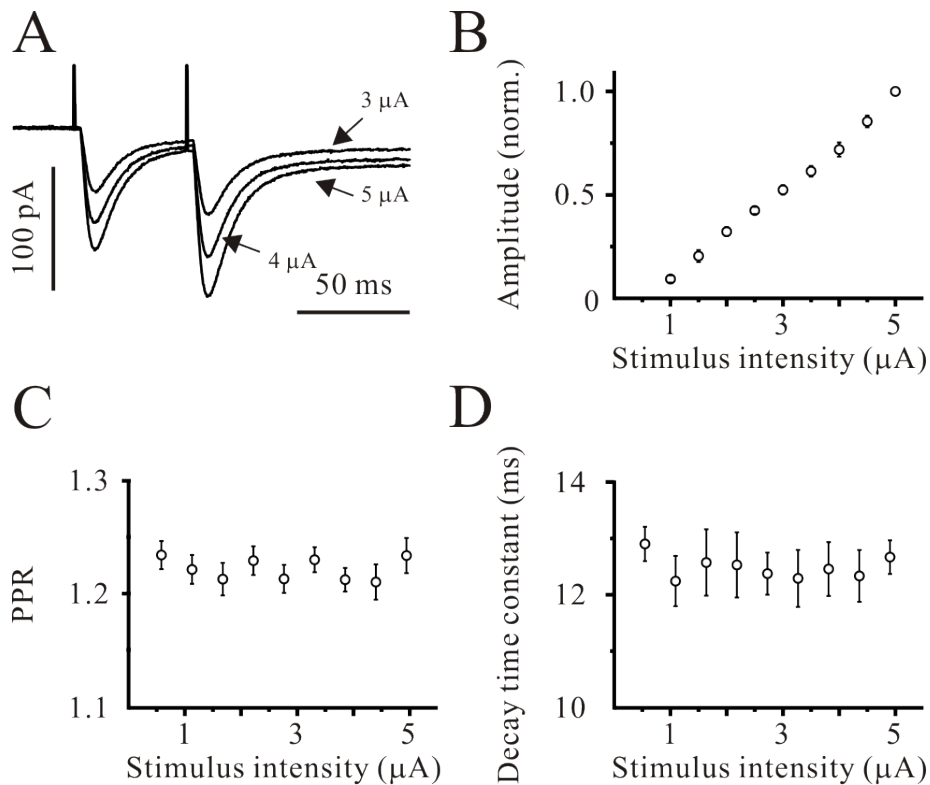


Figure 5. Paired-pulse plasticity of STCs does not depend on stimulus intensity. (A) STCs elicited by paired-pulse stimulation at 50 ms inter-stimulus intervals using different pulse intensities. Each trace is an average of 10 responses. Recordings were performed in the presence of DNQX, APV, gabazine, and CGP55845. (B) Relationship between pulse intensity and corresponding STC amplitude. (C-D) PPR (C) and STC decay time constant (D) do not depend on the stimulus intensity ($n=9$).

Thus, the number of activated fibers does not significantly contribute to STC short-term plasticity. To prevent possible cell/fiber damage, a relatively weak stimulation current (4 μA) was applied in all experiments. Paired stimuli were applied at frequency of 0.14 Hz (once per 7 s).

2.4 Extracellular recordings

In this set of experiments the standard ACSF without any receptor blocker was used. For local field potential recordings a glass pipette filled with ACSF (3-5 M Ω) was placed into layer 2/3 at a distance of 50-100 μm from a SR101-positive astrocyte. The latter was approached with a patch pipette filled with either low or high $[\text{Na}^+]_i$ intracellular solution and cell-attached configuration was established. Electrical stimulation in layer 4 was similar to that used to elicit STCs (4 μA , 0.5 ms). Ten paired-pulse stimuli (50 ms inter-stimulus interval, ISI) were applied at frequency of 0.14 Hz to acquire control field potential responses. Then the whole-cell configuration was established by means of a gentle suction. After at least 10 min of cell dialysis 10 paired-pulse stimuli (50 ms ISI) were applied at frequency of 0.14 Hz to acquire field potential responses. Finally, ACSF containing DNQX (10 μM), an AMPA receptor blocker, and APV (50 μM), an NMDA receptor antagonist, was applied to block ionotropic glutamatergic transmission. In some experiments we have also applied TTX (1 μM) to test whether the recorded activity is action potential dependent (Fig. 6A). Averaged response recorded in the presence of DNQX and APV was subtracted from the averaged control response (Fig. 6B).

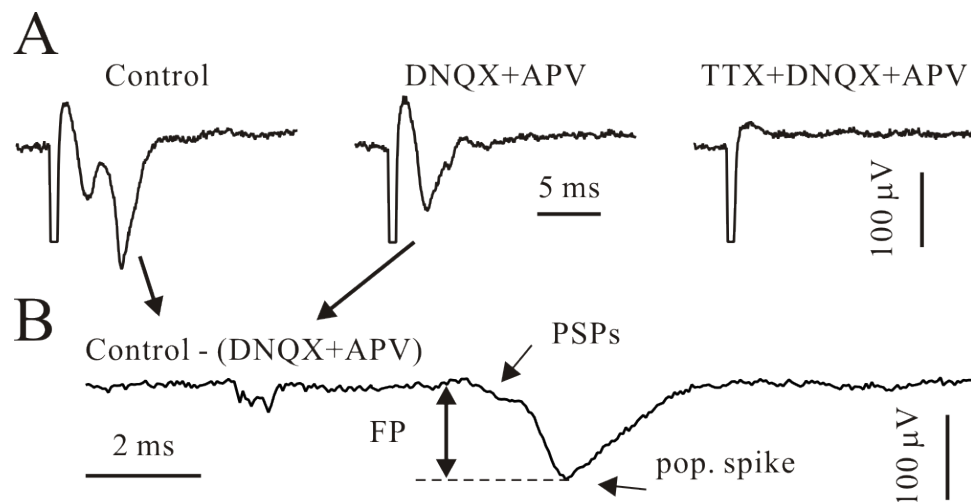


Figure 6. Field potentials elicited in layer 2/3 by electrical stimulation in cortical layer 4. (A) Field potentials induced in control (left), in the presence of DNQX (10 μM) and APV (50 μM , middle) and TTX+DNQX+APV (right trace). Each trace is an average of 10 recordings. (B) Trace obtained by subtraction of the response obtained in the presence of DNQX+APV from the control response. PSP is for postsynaptic potentials. “Pop. spike” means a population spike. Field potential (FP), i.e. an amplitude of compound response, has been taken for further comparisons.

Local field potential response consisted of two phases: a slow and small first deviation (PSPs) presumably reflecting an activation of postsynaptic receptors followed by a fast response presumably reflecting postsynaptic action potentials (population spike). Because the first component was relatively small we were unable to use its slope for comparison. Instead the amplitude of compound response has been used.

2.5 Ca²⁺ imaging

The detailed description of the method is given elsewhere (Kirischuk and Verkhratsky, 1996). In this study, we used Oregon Green 488 BAPTA-1 (OGB1) to measure intracellular [Ca²⁺] changes. Slices were incubated in ACSF supplemented with 5 μ M OGB-1-AM and 0.02% Pluronic F-127 (Molecular Probes, Ore., USA) for 20 min at 36 °C. After loading, slices were washed twice with ACSF and stored in ACSF for at least 20 min at room temperature to ensure deesterification. For recording slices were transferred to the experimental chamber. Excitation wavelength was controlled by a fast monochromator system, and a cooled CCD camera was used to record fluorescence signals (TILL Photonics, München, Germany). OGB-1 was excited at 490 nm. The excitation and emission light was separated using a 510 nm dichroic mirror. Emitted light was filtered using a 530 nm long-pass filter. Images were acquired and evaluated using Vision 4.0 software (TILL Photonics). All measurements were performed using 4x4 binning. Exposure time was set to 400 ms. Acquisition rate was one image per 1 s. The background fluorescence was calculated from a region in the immediate vicinity of the tested cell and subtracted. Fluorescence signals were expressed as relative changes from pre-stimulus levels ($\Delta F/F_0$).

2.6 [Na⁺]_i measurements

Sodium-binding benzofuran isophthalate (SBFI), a Na⁺-sensitive indicator, was used to measure [Na⁺]_i changes. Using patch-clamp technique we have

shown that SBFI stains mostly astrocytes in the neonatal neocortex (Unichenko et al., 2012). The detailed description of the bulk-loading method is given elsewhere (Rose and Ransom, 1996). Briefly, slices were incubated in the ACSF supplemented with 15 μM SBFI-AM and 0.02% Pluronic F-127 for 40 min at 36 $^{\circ}\text{C}$. After loading, slices were washed twice with the ACSF and stored in the ACSF for one hour at room temperature. Excitation wavelength was controlled by a fast monochromator system, and a cooled CCD camera was used to record fluorescence signals (TILL Photonics, München, Germany). SBFI was alternatively excited at 360 and 380 nm. The excitation and emission light was separated using a 510 nm dichroic mirror. Emitted light was filtered using a 530 nm long-pass filter. Images were acquired and evaluated using Vision 4.0 software (TILL Photonics). Exposure time was set to 400 ms. Acquisition rate was one image per 1 s. The background fluorescence was calculated from a region in the immediate vicinity of the tested cell and subtracted. Fluorescence signals were expressed as a ratio ($R = F_{360}/F_{380}$).

To calculate resting $[\text{Na}^+]_i$ in cortical astrocytes, we performed the following calibration experiments (Rose and Ransom, 1996). After the resting fluorescence had been measured, the ACSF supplemented with 3 μM gramicidin, 10 μM monensin and 1 mM ouabain was washed in to equilibrate extra- and intracellular Na^+ , K^+ and pH. In the presence of the above substances, brain slices were perfused with calibration solutions containing different $[\text{Na}^+]_i$ and calibration curve was plotted (Fig. 7).

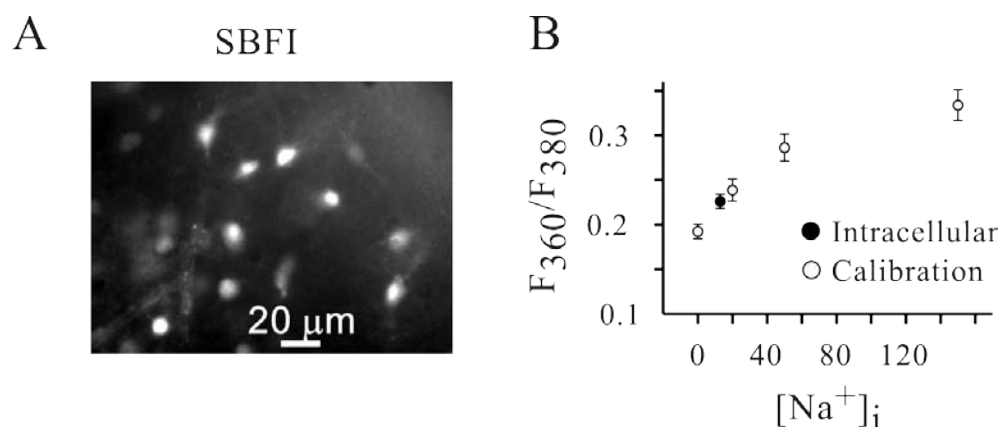


Figure 7. $[\text{Na}^+]_i$ in cortical astrocytes. (A) Sample image demonstrates SBFI-stained cells in a cortical slice. (B) Mean F_{360}/F_{380} ratio obtained from cortical

astrocytes (filled circle) and F_{360}/F_{380} ratios obtained with calibration extracellular solutions containing zero, 20, 40 and 150 mM $[Na^+]_i$ in the presence of gramicidin (3 μM), monensin (10 μM) and ouabain (1 mM, open circles).

In line with (Rose and Ransom, 1996), absolute $[Na^+]_i$ showed linear dependence on F_{360}/F_{380} ratio provided the former was below 40 mM. Therefore, we used the mean F_{360}/F_{380} ratio to obtain the mean $[Na^+]_i$ in cortical astrocytes (Fig. 7B).

2.7 Solutions and chemicals

All experiments were performed at room temperature (22-25 °C). Tetrodotoxin (TTX), CGP55845, SNAP-5114 and NO-711 were obtained from Tocris (Bristol, UK). All other chemicals were from Sigma-Aldrich (Munich, Germany).

2.8 Data evaluation and statistics

Data were evaluated off-line using TIDA 5.24 (HEKA Elektronik, Lambrecht, Germany). mGPSCs were analyzed using PeakCount V3.2 software (C. Henneberger, Institute of Neurophysiology, Berlin). The program employs a derivative threshold-crossing algorithm to detect individual mGPSCs. Each automatically detected event is displayed for visual inspection. mGPSC rise times and decay time constants (a single exponential fit) can be also obtained. All results are presented as mean \pm S.E.M. The error bars in all figures indicate S.E.M. Differences between means were tested for significance using paired Student's *t*-test, unless otherwise stated.

3 Results

3.1 Glutamate transporters and presynaptic metabotropic glutamate receptors protect neocortical Cajal-Retzius cells against over-excitation

Elevation of extracellular glutamate concentration can result in an activation of high affinity glutamate receptors and synchronous cell discharges. DL-TBOA, a specific EAAT blocker, has been shown to induce slow oscillations in layer 4/5 neurons of the neonatal cerebral cortex (Demarque et al., 2004). The DL-TBOA-produced oscillations were blocked by APV, an NMDA-receptor blocker, showing that they depend on NMDA receptor activation. To investigate whether EAAT blockade results in slow oscillations in the marginal zone, we bulk loaded brain slices with the Ca^{2+} indicator Oregon Green BAPTA-1 and recorded intracellular $[\text{Ca}^{2+}]$ changes using the calcium imaging technique (Fig. 1A). In this set of experiments, the ACSF did not contain APV and DNQX, blockers of ionotropic glutamate receptors. DL-TBOA (40 μM) induced NMDA receptor-dependent oscillations in layer 2/3 cells, but failed to affect the frequency of Ca^{2+} transients in Cajal-Retzius (CR) cells in the marginal zone (0.022 ± 0.012 and 0.019 ± 0.011 Hz in control and in the presence of DL-TBOA, respectively, $p > 0.7$, $n = 7$, Fig. 8).

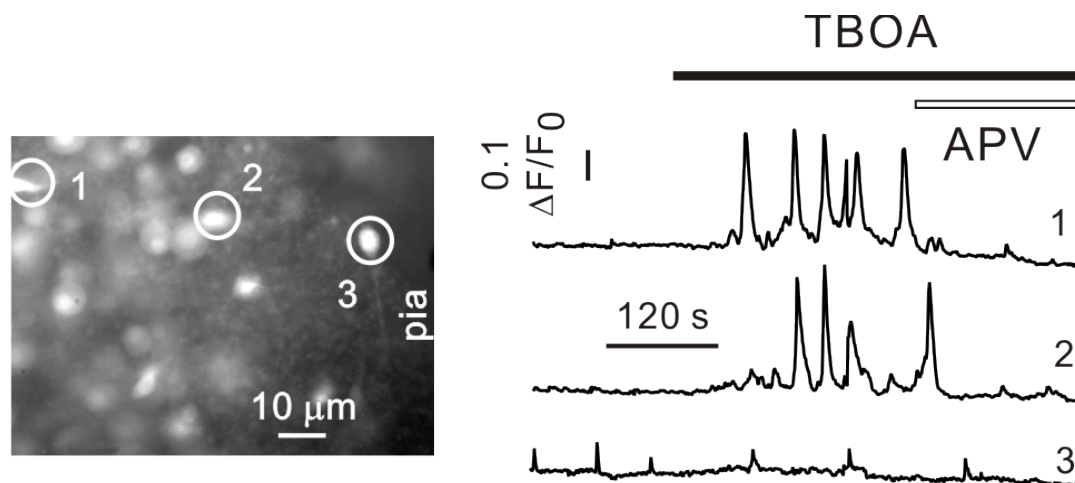


Figure 8. EAAT blockade did not influence the frequency of Ca^{2+} in CR cells. Cortical slice loaded with Ca^{2+} -sensitive indicator Oregon Green BAPTA-1 (left) and DL-TBOA-induced responses in layer 2/3 (1-2) and CR cells (3, right). * $P < 0.05$, ** $P < 0.01$, *** $P < 0.001$, ns not significant.

Whole-cell patch-clamp recordings demonstrated that DL-TBOA elicited repetitive barrages of sPSCs in layer 2/3 cells, but reduced the frequency of

spontaneous GPSCs (sGPSCs) in CR cells (0.11 ± 0.05 and 0.07 ± 0.03 Hz in control and in the presence of DL-TBOA, respectively, $p < 0.05$, $n = 9$, Fig. 9). (Dvorzhak et al., 2012)

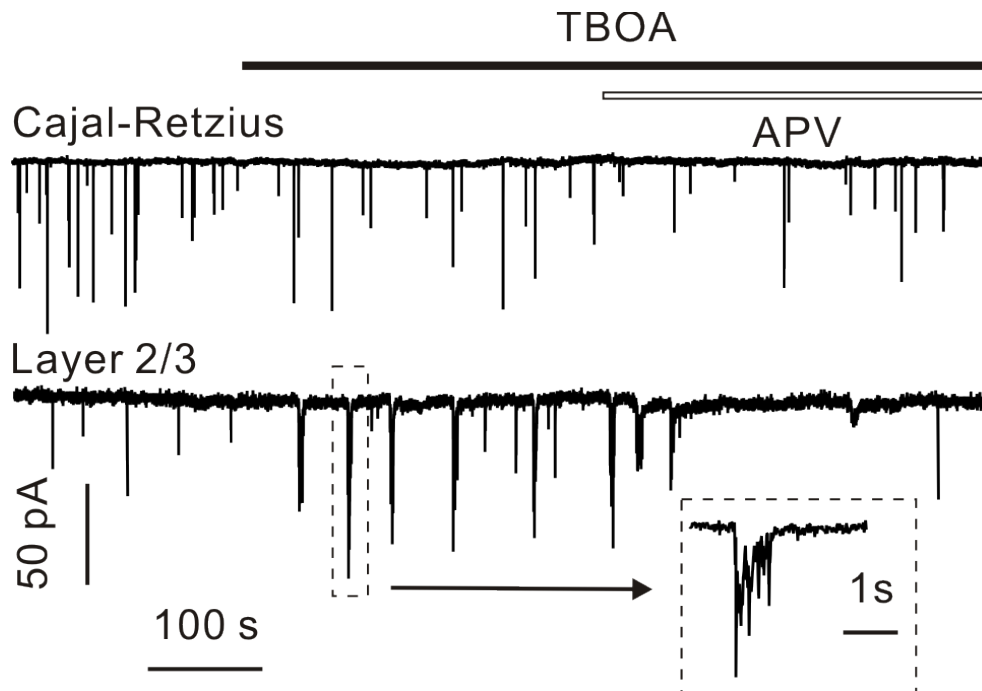


Figure 9. EAAT blockade reduced the frequency of spontaneous GPSCs in CR cells. Whole-cell patch-clamp recordings from a layer 2/3 pyramidal cell (bottom) and CR cell (top). A single discharge is illustrated in the inset. * $P < 0.05$, ** $P < 0.01$, *** $P < 0.001$, ns not significant.

3.1.1 EAAT blockade presynaptically inhibits GABAergic transmission

To prevent oscillatory responses in the cortical plate, all following experiments were performed in the presence of DNQX and APV. Although application of DL-TBOA slightly hyperpolarized CR cells from -51 ± 2 to -53 ± 2 mV ($p < 0.05$, $n = 74$), it did not significantly change the membrane resistance (440 ± 31 versus 425 ± 29 M Ω , $p > 0.2$) or holding current (15 ± 6 versus 11 ± 6 pA, $p > 0.3$, $n = 74$, data not shown). These results favour the suggestion that EAAT blockade leads to a presynaptic suppression of GABAergic transmission to CR cells. (Dvorzhak et al., 2012)

To corroborate the suggestion, miniature GPSCs (mGPSCs) from CR cells were recorded in the presence of tetrodotoxin (TTX, 1 μ M), a specific blocker of voltage-sensitive Na⁺ channels. DL-TBOA significantly decreased mGPSC frequency from 0.08 ± 0.03 to 0.03 ± 0.01 Hz ($n = 6$, $p < 0.05$, Fig. 10A,B), but failed to affect the median mGPSC amplitude (28 ± 4 versus 29 ± 5 pA, $n = 6$, $p > 0.7$, Fig. 10A,C).

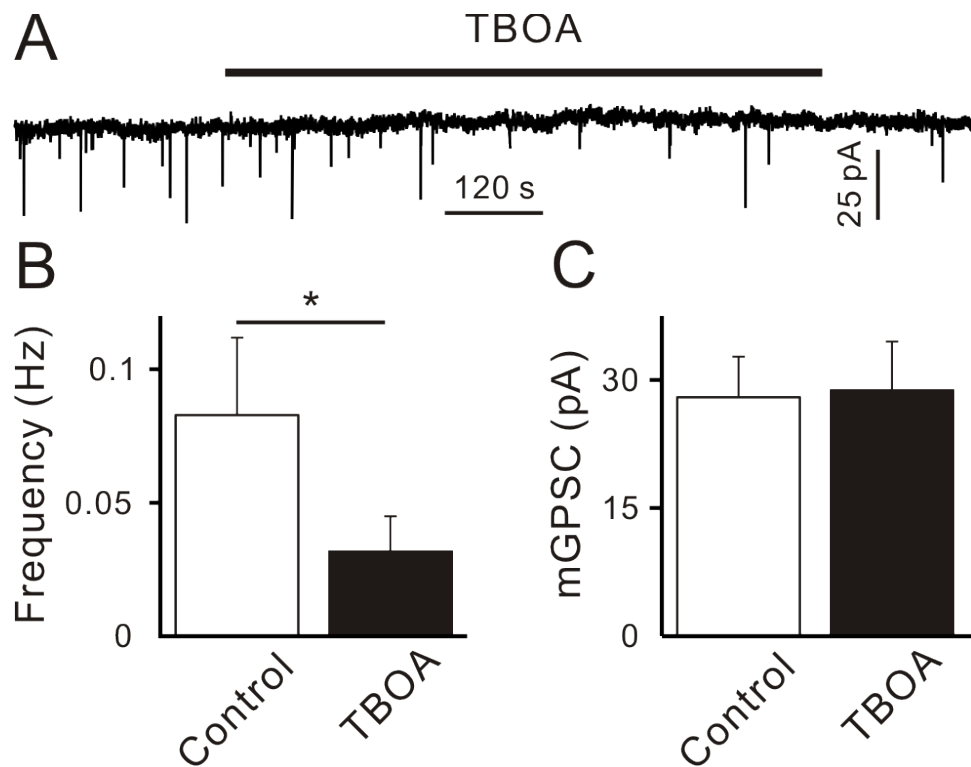


Figure 10. DL-TBOA decreases frequency, but not amplitude of miniature GABAergic PSCs. A, Sample trace demonstrates mGPSCs recorded before and during DL-TBOA application. B-C, Statistical data shows DL-TBOA-induced effects on the frequency (B) and median amplitude of mGPSCs (C). * $P < 0.05$, ** $P < 0.01$, *** $P < 0.001$, ns not significant.

Neither the rise time ($t_{10-90\%}$, 0.69 ± 0.07 versus 0.68 ± 0.06 ms, $p > 0.5$) nor the half-decay time (10.3 ± 0.8 versus 10.7 ± 0.9 ms, $p > 0.2$, $n = 6$, data not shown) was affected by DL-TBOA. Next we recorded evoked GPSCs (eGPSCs) using a paired-pulse stimulation protocol (50 ms inter-stimulus interval). DL-TBOA significantly reduced the mean eGPSC amplitude (114 ± 8 and 51 ± 5 pA, $p < 0.0001$) and increased paired-pulse ratio (PPR, 1.15 ± 0.06 and 1.75 ± 0.12 in control and in the presence of DL-TBOA, respectively, $p < 0.0001$, $n = 55$, Fig. 11D-F).

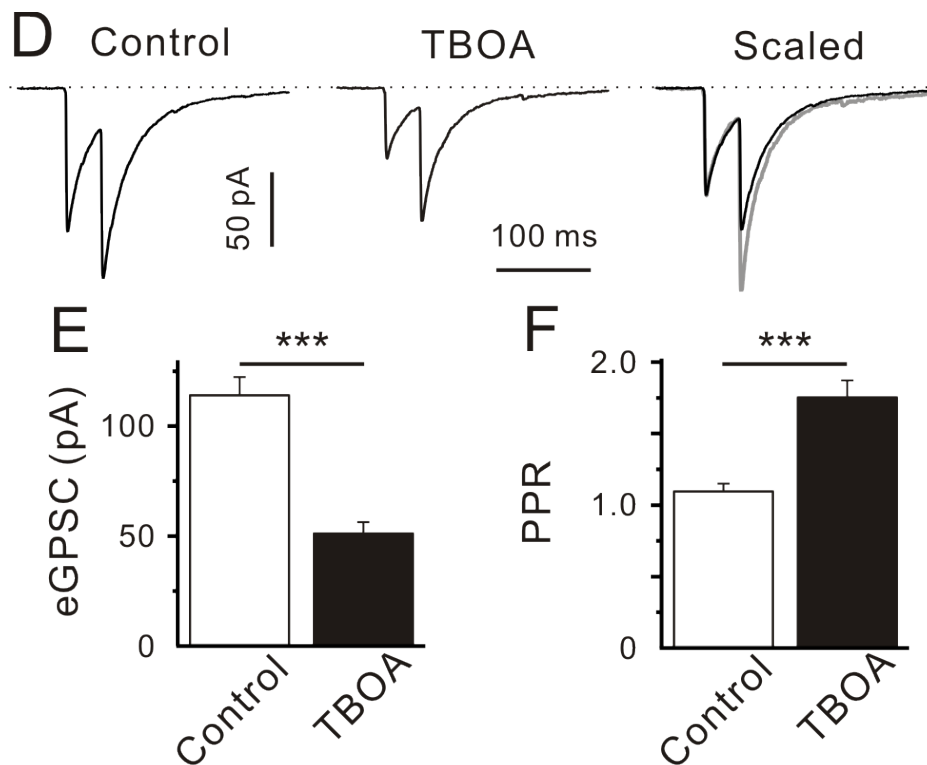


Figure 11. DL-TBOA inhibits GABAergic transmission presynaptically. *D*, Sample traces demonstrate eGPSCs elicited by paired-pulse stimulation in control (left) and in the presence of DL-TBOA (40 μ M, middle). Right panel shows scaled responses (black line - control, grey line - DL-TBOA). Traces represent an average of 40 responses. *E-F*, Statistical data shows DL-TBOA-induced effects on the mean eGPSC amplitude (*E*) and PPR (*F*). * $P < 0.05$, ** $P < 0.01$, *** $P < 0.001$, ns not significant.

Thus, we conclude that EAAT blockade results in a presynaptic inhibition of GABAergic transmission. (Dvorzhak et al., 2012)

3.1.2 Presynaptic mGluRs mediate TBOA-induced effects

Blockade of EAATs leads to an elevation of extracellular glutamate concentration. Because both AMPA and NMDA receptors are blocked throughout the experiments, the DL-TBOA-induced effects are presumably mediated by metabotropic glutamate receptors (mGluRs). Next, we applied N-ethylmaleimide (NEM), an uncoupler of pertussis toxin-sensitive G-proteins (Jakobs et al., 1982; Kirmse and Kirischuk, 2006b). NEM (50 μ M) completely blocked DL-TBOA-mediated effects (Fig. 12A-C).

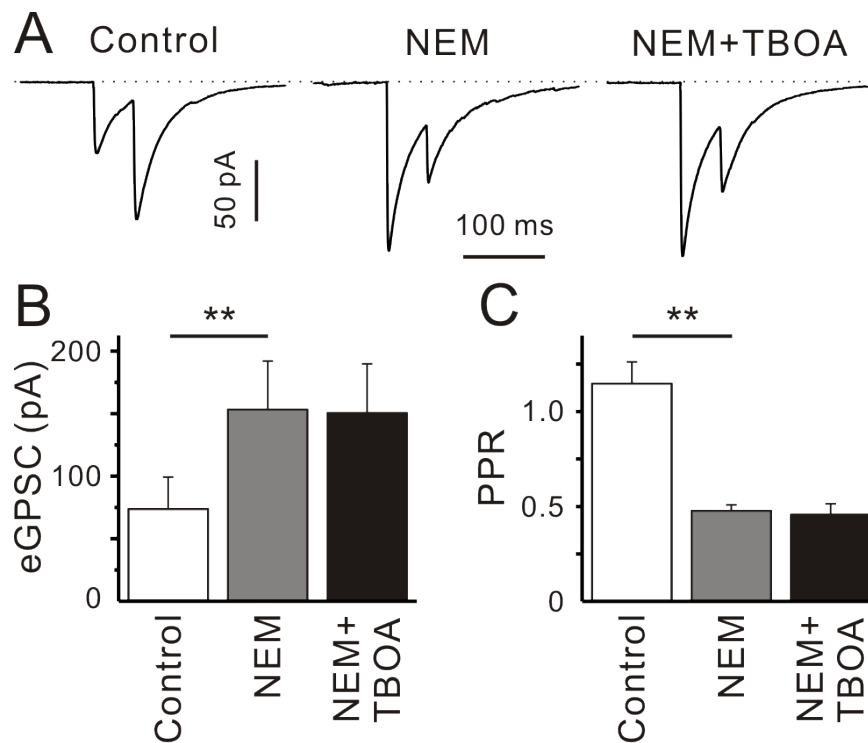


Figure 12. DL-TBOA-induced inhibition of GABAergic transmission is mediated through presynaptic metabotropic receptors. A Sample traces demonstrate eGPSCs elicited by paired-pulse stimulation in control (left), in the presence of NEM (50 μ M, middle) and NEM plus DL-TBOA (40 μ M, right). B-C, Statistical data shows NEM- and NEM plus DL-TBOA-induced effects on the mean eGPSC amplitude (B) and PPR (C). * $P < 0.05$, ** $P < 0.01$, *** $P < 0.001$, ns not significant.

The corresponding values were 73 ± 25 , 153 ± 37 , and 151 ± 38 pA ($p < 0.01$ - control versus NEM, $p > 0.7$ - NEM versus NEM plus DL-TBOA) for the mean eGPSC amplitudes and 1.15 ± 0.11 , 0.48 ± 0.03 , and 0.46 ± 0.06 ($n = 8$, $p < 0.01$ - control versus NEM, $p > 0.7$ - NEM versus NEM plus DL-TBOA, ANOVA test and post hoc Student's *t*-test with Bonferroni correction) for PPRs. Thus, EAAT blockade results in an activation of $G_{i/o}$ -coupled receptors, i.e. metabotropic group II and III glutamate receptors (mGluR-II/III). Next, we applied LY379268, a selective mGluR-II/III agonist. LY379268 (1 μ M) reversibly reduced the mean eGPSC amplitude (77 ± 21 versus 26 ± 11 pA, $p < 0.01$) and increased PPR (1.24 ± 0.11 versus 1.83 ± 0.2 , $p < 0.01$, $n = 7$, in control and in the presence of LY379268, respectively, Fig. 13A-C).

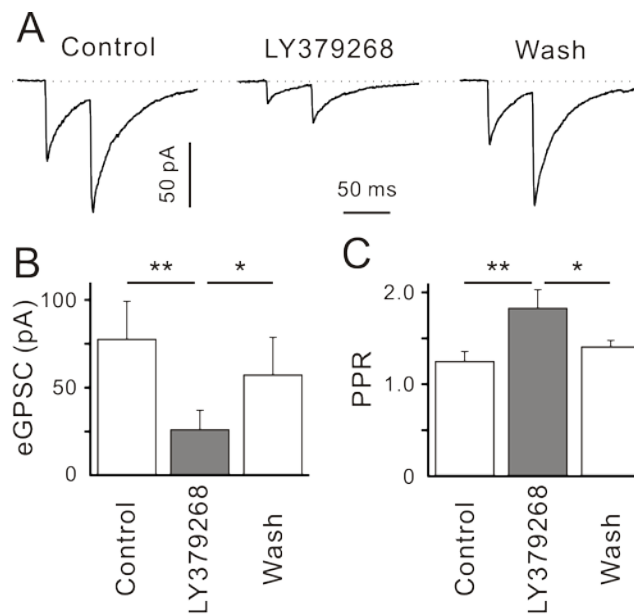


Figure 13. DL-TBOA-induced inhibition of GABAergic transmission is mediated through presynaptic mGluR-II/III. A, Sample traces show that LY379268 (1 μ M) reversibly suppresses eGPSCs. B-C, Statistical data shows LY379268 influence on the mean eGPSC amplitude (B) and PPR (C). Traces represent an average of 40 responses. * $P < 0.05$, ** $P < 0.01$, *** $P < 0.001$, ns not significant.

We conclude that GABAergic synapses on CR cells express functional presynaptic mGluR-II/III receptors. (Dvorzhak et al., 2012)

Next, we applied LY341495. At low concentrations (tens of nM) this is a specific antagonist of mGluR-II/III. However, because pharmacological characterization of mGluRs was not the main goal of this study, we used rather high (40 μ M) concentration of LY341495 to block all (or almost all) mGluRs. In the presence of DL-TBOA LY341495 (40 μ M) increased the mean eGPSC amplitude from 53 ± 12 to 132 ± 24 pA ($p < 0.001$) and decreased PPR from 1.51 ± 0.09 to 0.79 ± 0.06 ($p < 0.001$, $n = 9$, Fig. 14A-C).

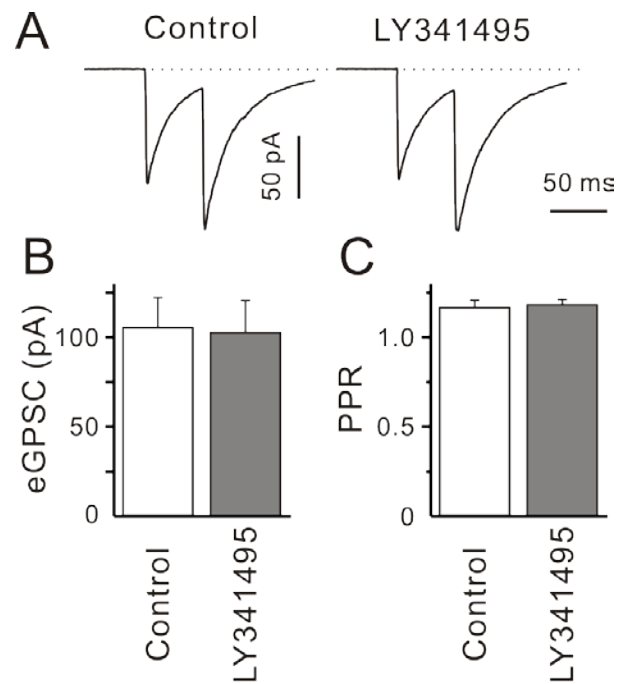


Figure 14. LY341495 does not influence GABAergic transmission when applied under control conditions. A-C, Sample traces (A) and statistical data (B, C), amplitude (B) and PPR (C). * $P < 0.05$, ** $P < 0.01$, *** $P < 0.001$, ns not significant.

Surprisingly, in the presence of DL-TBOA plus LY341495 the mean eGPSC amplitudes increased beyond the control values (98 ± 19 and 132 ± 24 pA in control and in the presence of DL-TBOA plus LY341495, respectively, $n=9$, $p < 0.01$, paired Student's t -test with Bonferroni correction). PPR in turn was significantly smaller in the presence of DL-TBOA plus LY341495 (0.79 ± 0.06) as compared to control (1.15 ± 0.07 , $n=9$, $p < 0.001$, paired Student's t -test with Bonferroni correction, Fig. 14A-C). Tonic activation of mGluR-II/III under resting conditions might be an explanation for the obtained data. If this were the case, LY341495 would block both tonic and DL-TBOA-induced components resulting in an increase of eGPSC amplitudes beyond the controls. But if tonic activation of mGluR-II/III exists, LY341495 should potentiate eGPSCs under resting conditions. However, LY341495 ($40 \mu\text{M}$) alone failed to affect either the mean eGPSC amplitude (105 ± 17 and 103 ± 59 pA, $n=11$, $p > 0.7$) or PPR (1.17 ± 0.04 and 1.18 ± 0.03 , $n=11$, $p > 0.8$, in control and in the presence of LY341495, respectively, Fig. 15D-F).

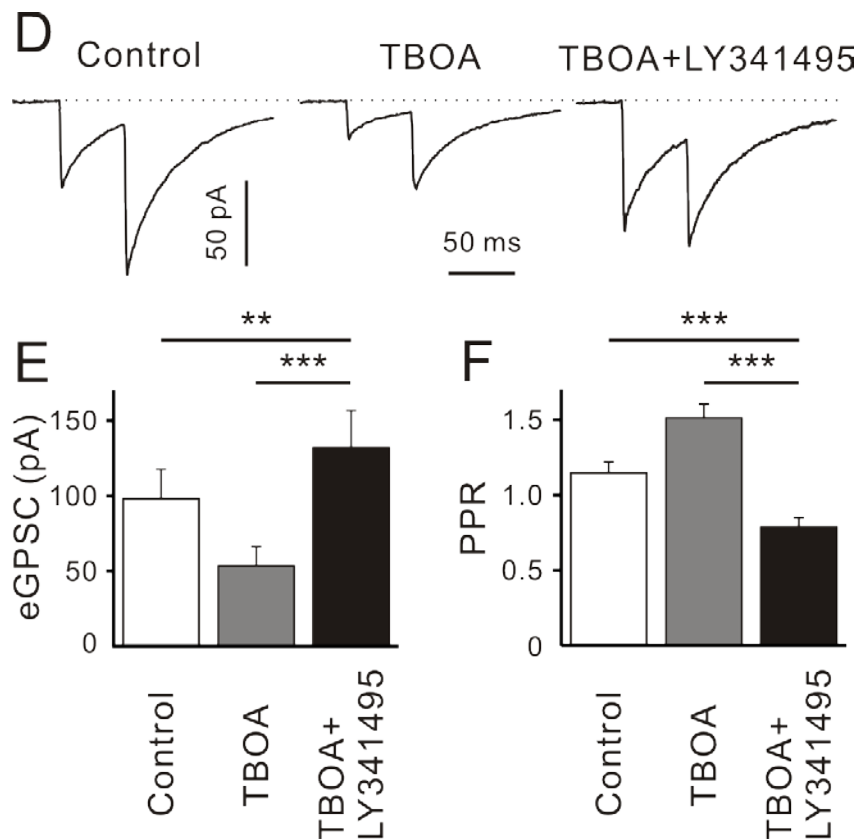


Figure 15. mGluR blockade potentiates eGPSCs in the presence of DL-TBOA. D-F, Sample traces (D) and statistical data (E-F) show that LY341495 (40 μ M) not only eliminates DL-TBOA-mediated inhibition of eGPSCs, but results in a potentiation of GABAergic transmission as compared to controls. * $P < 0.05$, ** $P < 0.01$, *** $P < 0.001$, ns not significant.

These results argue against tonic activation of mGluR-II/III by ambient glutamate. Considering that not all mGluRs are blocked by LY341495, we applied (RS)-MCPG (500 μ M), an antagonist of group I and II mGluRs. However, in the presence of DL-TBOA and LY341495 (RS)-MCPG did not influence either the mean ePSC amplitude ($97 \pm 5\%$, $p > 0.4$) or PPR ($98 \pm 3\%$, $p > 0.7$, $n=5$, data not shown). We conclude that the observed potentiation of GABAergic transmission in the presence of DL-TBOA and LY341495 is not mediated by mGluRs. (Dvorzhak et al., 2012)

3.2 Transporter-mediated replacement of extracellular glutamate for GABA in the developing murine neocortex

3.2.1 D-aspartate-induced effects differ from those produced by DL-TBOA

To further investigate the above observation, we applied D-aspartate, a transportable glutamate uptake blocker. Similar to DL-TBOA, D-aspartate slightly hyperpolarized CR cells from -52 ± 3 to -54 ± 2 mV ($p=0.17$, $n=32$) and did not significantly change either the membrane resistance (431 ± 22 versus 446 ± 17 M Ω , $p>0.4$) or holding current (17 ± 8 versus 14 ± 7 pA, $p>0.4$, $n=32$, data not shown). D-aspartate (100 μ M) suppressed the mean amplitude of eGPSCs (from 128 ± 31 to 56 ± 15 pA, $n=9$, $p<0.05$) and increased PPR (from 1.16 ± 0.11 to 1.71 ± 0.18 , $n=9$, $p<0.01$, Fig. 16A-C).

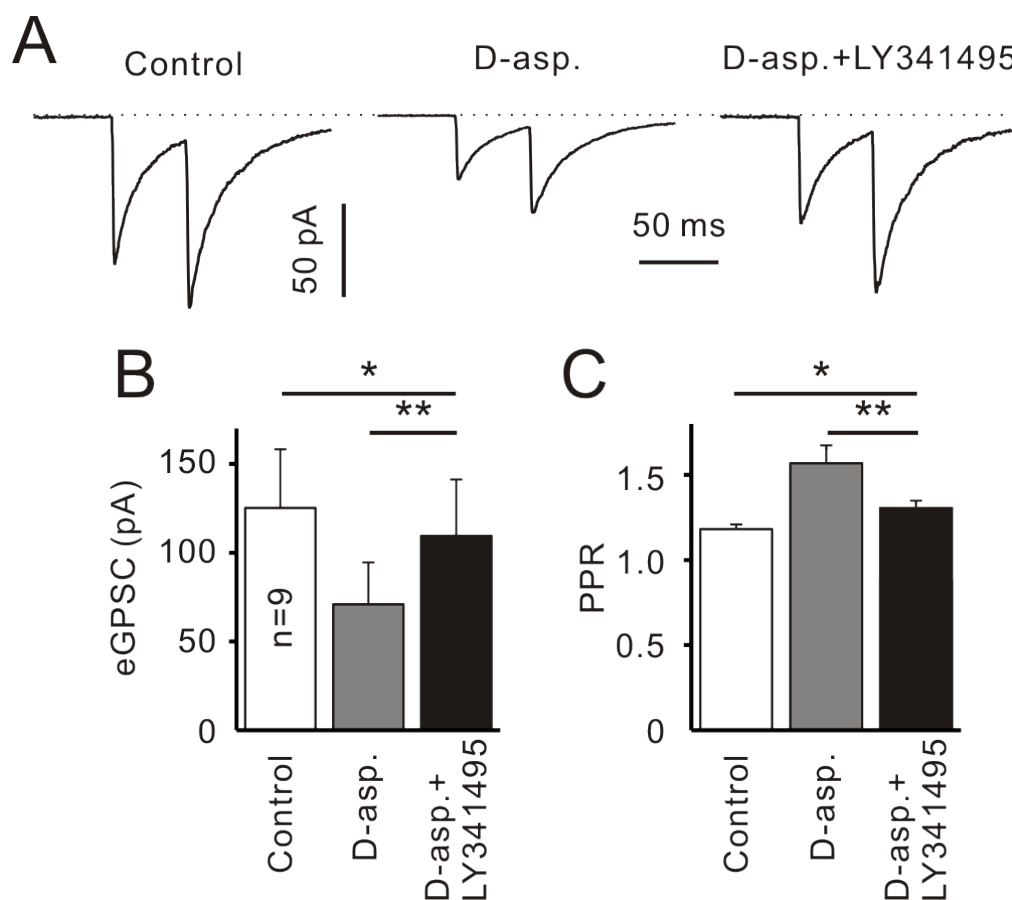


Figure 16. D-Aspartate influences GABAergic transmission. (A) Representative traces demonstrating eGPSCs elicited by paired-pulse stimulation in control, and in the presence of D-aspartate (100 μ M) and d-aspartate plus LY341495. (B, C) Statistical data demonstrating D-aspartate- and D-aspartate plus LY341495-induced effects on the mean eGPSC amplitude (B) and PPR (C). * $P < 0.05$, ** $P < 0.01$, *** $P < 0.001$, ns not significant.

However, although LY341495 (40 μ M) in the presence of D-aspartate resulted in an increase of the mean eGPSC amplitude, the latter was smaller as compared to the control value (125 ± 32 and 110 ± 32 pA in control and in the

presence of D-aspartate plus LY341495, $n=9$, $p<0.05$, Fig. 16 A-C). PPR in the presence of D-aspartate plus LY341495 (1.33 ± 0.06) was significantly higher than in control (1.18 ± 0.03 , $n=9$, $p<0.05$, paired Student's *t*-test with Bonferroni correction, Fig. 5 D, F). (RS)-MCPG (500 μM) applied in the presence of D-aspartate and LY341495 did not change either the mean ePSC amplitude ($98\pm 4\%$, $p>0.4$) or PPR ($99\pm 4\%$, $p>0.6$, $n=4$, data not shown). D-aspartate not only blocks EAAT-mediated glutamate uptake, but it can stimulate glutamate release via the hetero-exchange mode of EAATs (Volterra and Steinhauser, 2004) or through cystine-glutamate exchanger (Bannai and Tateishi, 1986). As a consequence, D-aspartate-induced elevation of extracellular glutamate level might be higher as compared to DL-TBOA-induced glutamate increase. To investigate this question, we added exogenous glutamate (10 μM) in the presence of DL-TBOA plus LY341495. Exogenous glutamate failed to affect either the mean eGPSC amplitude ($103\pm 6\%$ of control, $p>0.6$) or PPR (98 ± 3 , $p>0.5$, $n=3$, data not shown) suggesting that glutamate levels do not underlie the observed difference between DL-TBOA- and D-aspartate-induced effects of eGPSCs. Thus, unexpectedly two glutamate uptake blockers differently affected GABAergic transmission. (Unichenko et al., 2013)

3.2.2 DL-TBOA abolishes presynaptic GABA_BR-mediated inhibition

We have recently reported that GABAergic transmission on Cajal-Retzius cells is tonically inhibited via GABA_BRs (Kirmse and Kirischuk, 2006a). To inspect whether EAAT blockade influences tonic GABA_BR-mediated presynaptic inhibition, we applied CGP55845, a GABA_BR blocker. Unexpectedly, CGP55845 (1 μM) failed to influence GABAergic transmission in the presence of DL-TBOA (Fig. 17A-C).

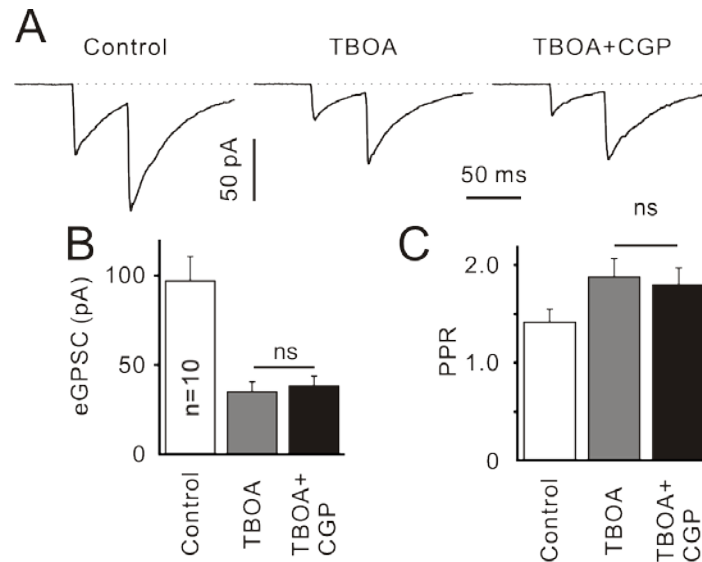


Figure 17. DL-TBOA abolishes presynaptic GABAB receptor-mediated inhibition of eGPSCs. (A) Representative traces demonstrating eGPSCs elicited in control, and in the presence of DL-TBOA and DL-TBOA plus CGP55845. (B–C) Statistical data showing DL-TBOA and DL-TBOA plus CGP55865-induced effect on the mean eGPSC amplitude (B) and PPR (C). ns not significant. * $P < 0.05$, ** $P < 0.01$, ns not significant.

The mean eGPSC amplitude was 35 ± 6 and 38 ± 6 pA ($n=11$, $p > 0.2$) and PPR was 1.87 ± 0.19 and 1.79 ± 0.17 ($n=11$, $p > 0.3$) in the presence of DL-TBOA and DL-TBOA plus CGP55845, respectively. These results allow suggesting that ambient GABA concentration is decreased in the presence of DL-TBOA. Because GAT-2/3 releases GABA in the neonatal neocortex (Kirmse and Kirischuk, 2006a), we asked whether GAT-2/3-mediated GABA release persists in the presence of DL-TBOA. Surprisingly, this was not the case. SNAP-5114 ($40 \mu\text{M}$), a specific GAT-2/3 blocker, applied in the presence of DL-TBOA changed neither the mean eGPSC amplitude (22 ± 5 versus 23 ± 6 pA, $n=8$, $p > 0.9$) nor PPR (1.62 ± 0.10 versus 1.53 ± 0.09 , $n=8$, $p > 0.4$, Fig. 18A).

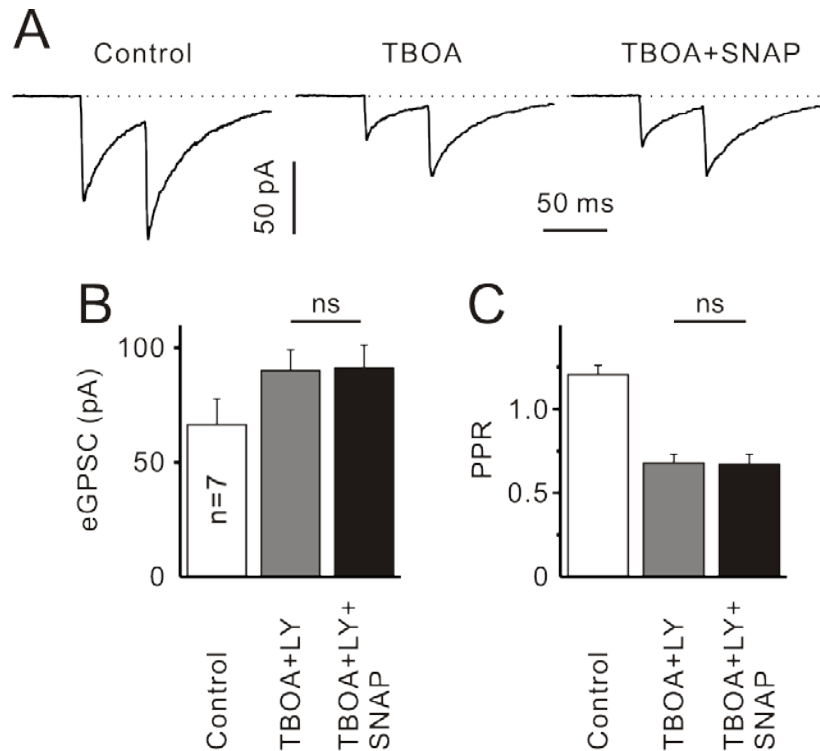


Figure 18. DL-TBOA abolishes GAT-2/3-mediated GABA release. (A) Sample traces demonstrating eGPSCs elicited in control, and in the presence of DL-TBOA and DL-TBOA plus SNAP-5114 (SNAP, 40 μ M). (B,C) Statistical data showing DL-TBOA plus LY341495- and DL-TBOA plus LY341495 plus SNAP-5114-induced effects on the mean eGPSC amplitude (B) and PPR (C). * $P < 0.05$, ** $P < 0.01$, ns not significant.

Similar results were obtained when SNAP-5114 was applied in the presence of DL-TBOA plus LY341495 (40 μ M). Fig. 18B,C show that also in this case SNAP-5114 failed to influence either the mean eGPSC amplitude (90 ± 9 versus 91 ± 11 pA, $n=7$, $p > 0.8$) or PPR (0.68 ± 0.05 versus 0.67 ± 0.06 , $n=7$, $p > 0.8$). Can the DL-TBOA-mediated removal of GABA_BR-mediated inhibition explain the observed potentiation of GABAergic transmission in the presence of DL-TBOA plus LY341495 (Fig. 15)? To answer this question, we applied DL-TBOA plus LY341495 in the presence of CGP55845. As expected, CGP55845 (1 μ M) increased the mean eGPSC amplitude from 87 ± 13 to 138 ± 19 pA ($p < 0.05$) and decreased PPR from 1.23 ± 0.07 to 0.87 ± 0.06 ($p < 0.05$, $n=6$). But DL-TBOA plus LY341495 applied in the presence of CGP55845 failed to change either the mean eGPSC amplitude ($92 \pm 7\%$, $p > 0.2$) or PPR ($102 \pm 6\%$ of control, $p > 0.7$, $n=6$, one population Student's t-test, data not shown). We conclude that EAAT blockade with DL-TBOA eliminates or at least strongly reduces GAT-2/3-mediated GABA release. (Unichenko et al., 2013)

3.2.2 D-aspartate potentiates GABA_BR-mediated inhibition

Both EAATs and GATs are electrogenic and Na⁺-dependent transporters. EAATs co-transport three Na⁺ ions with one glutamate molecule, while GATs co-transport two Na⁺ ions with one GABA. GAT reversal potential appears to be close to the resting potential of neurons under normal conditions and elevation of intracellular Na⁺ concentration can change the direction of GABA transport (Richerson and Wu, 2003; Wu et al., 2007). EAAT-blockade by DL-TBOA eliminates both EAAT-mediated Na⁺ influx and depolarization and can potentially reduce GAT-2/3-mediated GABA release. If this is the case, then D-aspartate, a transportable glutamate uptake blocker, which increases the EAAT-mediated Na⁺ influx/depolarization, should potentiate GAT-2/3-mediated GABA release. Indeed, CGP55845 (1 μM) in the presence of D-aspartate (100 μM) significantly increased the mean eGPSC amplitude (from 52±8 to 99±10 pA, n=6, p<0.01) and decreased PPR (from 1.78±0.15 to 1.38±0.07, n=6, p<0.01, Figure 19A-C) suggesting that presynaptic GABA_BRs are activated in the presence of D-aspartate.

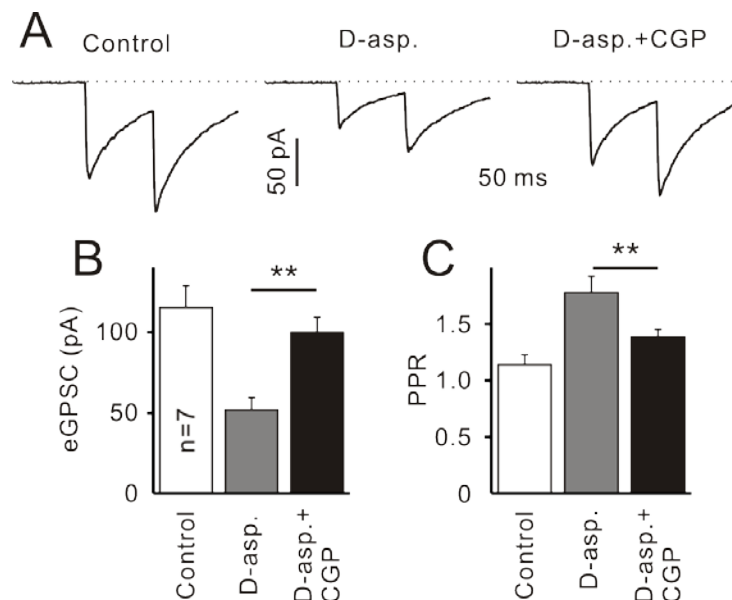


Figure 19. D-aspartate fails to abolish presynaptic GABA_B receptor-mediated inhibition of eGPSCs. (A) Sample traces demonstrating eGPSCs elicited by paired-pulse stimulation in control, and in the presence of D-aspartate and D-aspartate plus CGP55845. (B–C) Statistical data showing D-aspartate and D-aspartate plus CGP55845-induced effects on the mean eGPSC amplitude (B) and PPR (C). *P < 0.05, **P < 0.01, ns not significant.

Similar to CGP55845, SNAP-5114 (40 μ M) significantly increased the mean eGPSC amplitude (from 41 ± 5 to 82 ± 12 pA, $n=6$, $p < 0.01$) and decreased PPR (from 1.71 ± 0.06 to 1.4 ± 0.1 , $n=6$, $p < 0.01$, Fig. 20A) validating that GAT-2/3 releases GABA in the presence of D-aspartate.

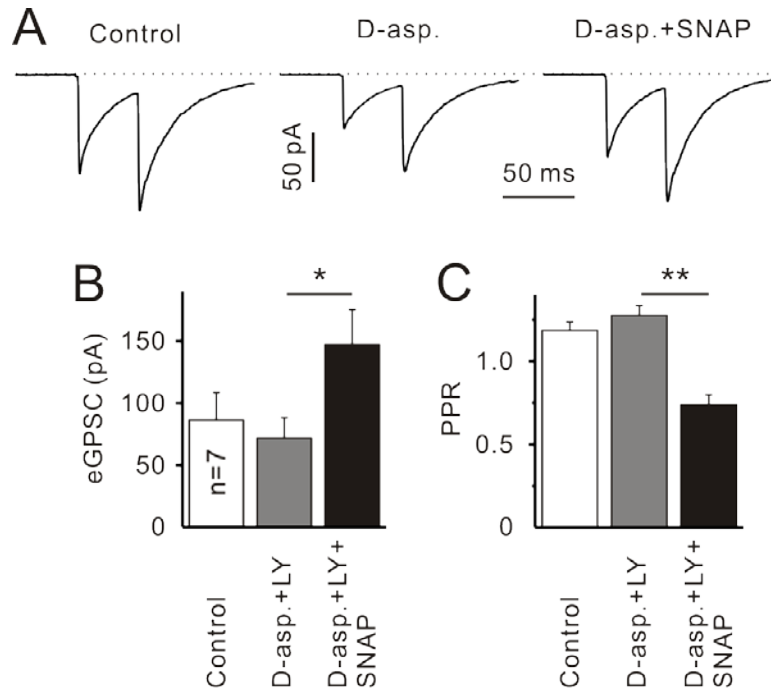


Figure 20. D-aspartate fails to abolish GAT-2/3-mediated GABA release. (A) Representative traces demonstrating eGPSCs elicited by paired-pulse stimulation in control, and in the presence of D-aspartate plus LY341495 and D-aspartate plus LY341495 plus SNAP-5114. (B,C) Statistical data showing d-aspartate plus LY341495- and D-aspartate plus LY341495 plus SNAP-5114-induced effects on the mean eGPSC amplitude (B) and PPR (C). * $P < 0.05$, ** $P < 0.01$, ns not significant.

Also in the presence of D-aspartate plus LY341495 (40 μ M) SNAP-5114 enlarged the mean eGPSC amplitude (72 ± 15 versus 147 ± 28 pA, $n=6$, $p < 0.05$) and reduced PPR (1.27 ± 0.06 versus 0.73 ± 0.06 , $n=6$, $p < 0.01$, Fig. 20B,C). Thus, in contrast to DL-TBOA, glutamate uptake blockade with an EAAT substrate does not eliminate tonic GABA β R-mediated presynaptic inhibition. Moreover, SNAP-5114 increased the mean eGPSC amplitude to 169 ± 13 % in ACSF ($n=9$, (Dvorzhak et al., 2010)) and to 201 ± 14 % ($n=6$, $p < 0.05$, unpaired Student's t -test) in the presence of D-aspartate plus LY341495. Similarly, SNAP-5114 decreased PPR to 66 ± 4 % in control ($n=9$) and to 56 ± 4 % ($n=6$, $p < 0.05$, unpaired Student's t -test) in the presence of D-aspartate plus LY341495. These results suggest that D-aspartate potentiates GAT-2/3-mediated GABA release. We conclude that EAAT-mediated

glutamate transport is capable to modulate or may be even change the direction of GAT-mediated GABA transport. (Unichenko et al., 2013)

3.2.3 EAAT1 (GLAST) is the main glutamate transporter in this preparation

Finally, we asked what type of EAATs mediates the observed EAAT-GAT interaction. To date, five different EAATs have been cloned (EAAT1-5, (Danbolt, 2001)), three of them (EAAT1-3) are expressed in the embryonic mouse brain (Shibata *et al.*, 1996). DL-TBOA is a blocker of all known EAATs. Therefore, we next applied TFB-TBOA (100 nM), a selective antagonist of EAAT1 (GLAST) and EAAT2 (GLT1 (Shimamoto et al., 2004). TFB-TBOA reduced the mean amplitude of eGPSCs 82 ± 8 to 32 ± 9 pA ($p < 0.001$, $n=7$) and increased PPR from 1.18 ± 0.09 to 1.64 ± 0.15 ($p < 0.01$, $n=7$, Fig. 21A,B).

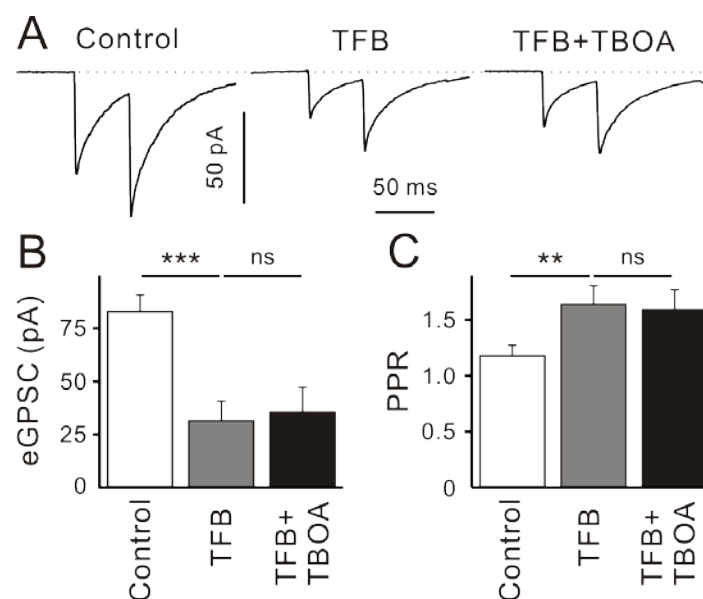


Figure 21. EAAT1/2 control extracellular glutamate concentration in the marginal zone. A–C Sample traces (A) and statistical data show that TFB-TBOA (TFB, 100 nM) inhibits GABAergic transmission as efficiently as DL-TBOA (TBOA). * $P < 0.05$, ** $P < 0.01$, *** $P < 0.001$, ns not significant.

Moreover, DL-TBOA (40 μ M) applied in the presence of TFB-TBOA failed to affect either the mean eGPSC amplitude (32 ± 9 versus 35 ± 11 , $p > 0.5$, $n=7$) or PPR (1.64 ± 0.15 versus 1.59 ± 0.18 , $p > 0.4$, $n=7$, paired Student's *t*-test with Bonferroni correction, Fig. 8A-C). These results suggest that EAAT3 (EAAC1) plays a minor role in this preparation. Next, we applied dihydrokainic acid

(DHK), a specific antagonist of EAAT2 (GLT1). DHK (200 μ M) failed to affect either the mean eGPSC amplitude (81 ± 19 versus 80 ± 17 pA, $p>0.8$) or PPR (1.11 ± 0.06 versus 1.10 ± 0.05 , $p>0.9$, $n=6$, Fig. 22A-C).

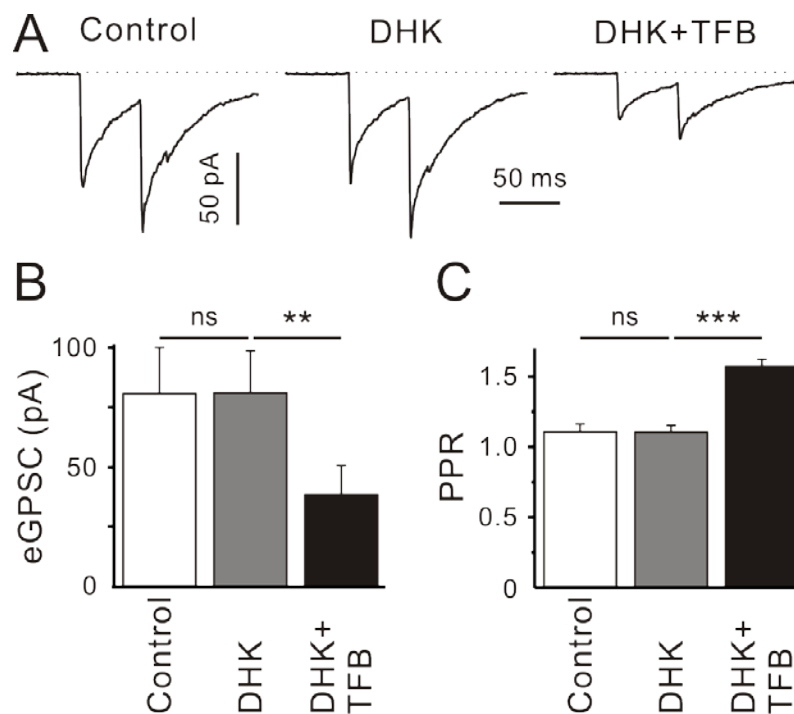


Figure 22 EAAT1 (GLAST) controls extracellular glutamate concentration in the marginal zone. A–C Sample traces (A) and statistical data (C, B) demonstrate that dihydrokainic acid (DHK, 200 μ M) fails to influence GABAergic transmission, whereas TFB-TBOA (TFB) strongly suppresses it. * $P < 0.05$, ** $P < 0.01$, *** $P < 0.001$, ns not significant.

TFB-TBOA (100 nM) in the presence of DHK strongly suppressed the mean amplitude (from 80 ± 17 to 38 ± 11 pA, $p<0.01$, $n=6$) and increased PPR (from 1.10 ± 0.05 to 1.57 ± 0.05 ($p<0.001$, $n=6$, paired Student's t -test with Bonferroni correction, Fig. 22A-C). Thus, we conclude that EAAT1 (GLAST) is the glutamate transporter that in concert with GAT-2/3 controls the glutamate-GABA balance in the vicinity of GABAergic synapses on CR cells. (Dvorzhak et al., 2012)

3.3 $[Na^+]_i$ influences short-term plasticity of glutamate transporter-mediated currents in neocortical astrocytes

3.3.1 Synaptically activated, transporter-mediated currents (STCs) in cortical astrocytes

Evoked transmembrane currents were recorded from layer 2/3 cortical cells pre-stained with sulforhodamine 101 (SR101, Fig. 23A). All tested SR101-positive cells demonstrated passive current-voltage relationships (Fig. 23B), high-negative resting potentials (-81 ± 5 mV, $n=75$) and low input membrane resistances (21 ± 5 M Ω , $n=75$).

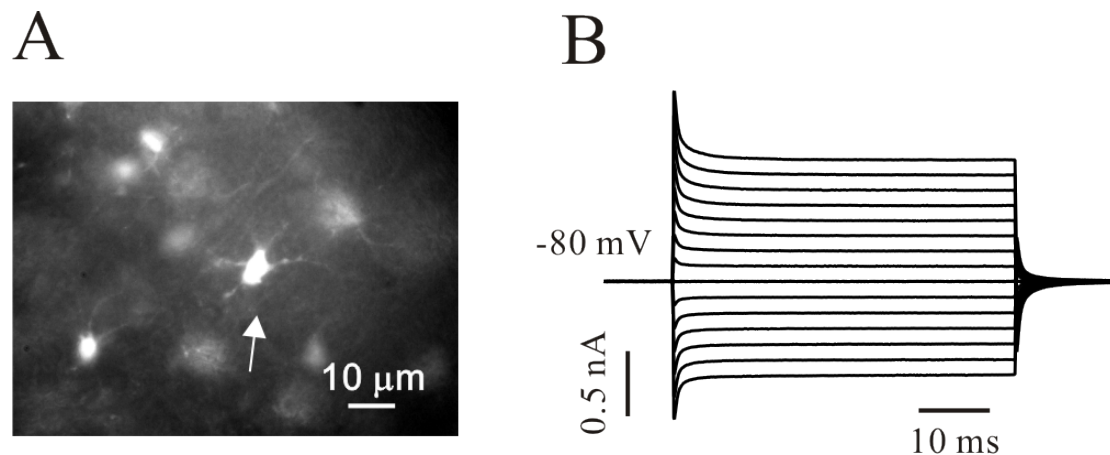


Figure 23. Cortical astrocytes. (A) Sample image shows cortical astrocytes labelled with SR101. (B) Current responses to 10 mV voltage steps recorded from an SR101-positive cell (an arrow in panel A).

These results confirm that SR101 stains exclusively astrocytes in the neocortex (Nimmerjahn et al., 2004). Electrical stimulation in layer 4 elicited a complex current response in layer 2/3 astrocytes. After initial very fast deviations due to the extracellular-recorded volley response (Clark and Barbour, 1997)(blacked for clarity in most shown recordings), an inward current comprising of fast and slow components was observed (Fig. 24).

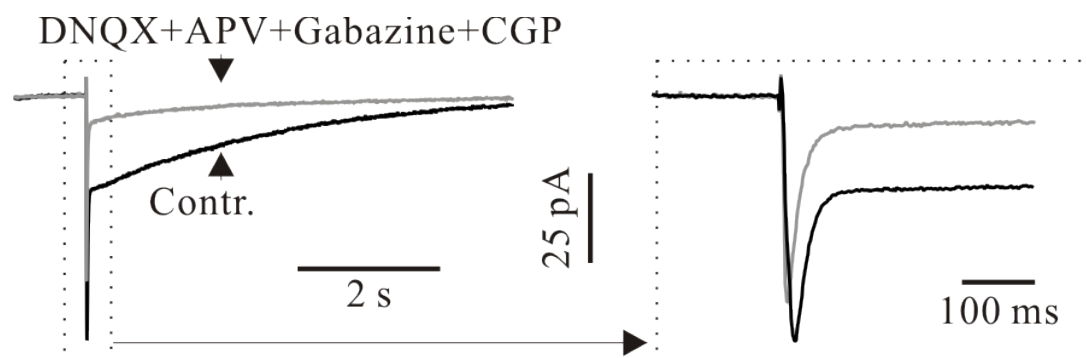


Figure 24. Membrane currents in cortical astrocytes. Membrane currents elicited in layer 2/3 astrocytes by electrical stimulation in layer 4. Addition of DNQX, APV, Gabazine and CGP55845 to the ACSF (grey line) strongly reduced the slow component of STC (left panel), but the fast STC response was only slightly reduced by the blocker cocktail (right panel). Each trace is an average of 10 responses.

Both components of the evoked responses were completely blocked by either TTX (1 μ M, n=3), an antagonist of voltage-gated Na⁺ channels, or Cd²⁺ (100 μ M, n=3, data not shown), an unspecific blocker of voltage-gated Ca²⁺ channels. Thus, the evoked currents in cortical astrocytes depend on the action potential-driven neurotransmitter release. Blockade of AMPA (DNQX, 10 μ M), NMDA (APV, 50 μ M), GABA_A (Gabazine, 20 μ M) and GABA_B (CGP55845, 1 μ M) receptors only slightly reduced the fast component (to 85 \pm 5 % of control, p<0.01, n=7, one population Student's *t*-test), while the slow component was decreased to 31 \pm 5 % of its control value (p<0.001, n=7, one population Student's *t*-test, Fig. 24). DL-TBOA (40 μ M), a specific EAAT antagonist, completely blocked the fast component, identifying it as a synaptically-induced, transporter-mediated current (STC, Fig. 25, (Bergles and Jahr, 1997; Clark and Barbour, 1997)). Isolated STCs (Fig. 25, right panel) showed the 20-80% rise time of 2.1 \pm 0.2 ms and 12.6 \pm 0.4 ms (n=29) decay time constant.

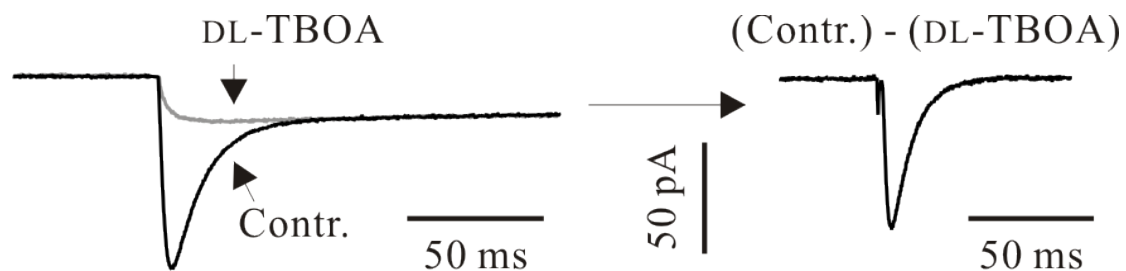


Figure 25. STCs in cortical astrocytes. In the presence of DNQX, APV, Gabazine, and CGP55845, the fast STC component was blocked by DL-TBOA (40 μ M, grey line). Each trace is an average of 10 responses. The right panel shows the fast STC component isolated by subtraction.

The slow components recorded in the presence of DL-TBOA displayed 5.3 \pm 0.6 ms 20-80% rise time and 930 \pm 109 ms decay time constant (n=9). Although the nature of slow component is still far from understanding (Bellamy and Ogden, 2005), in this work we investigated only fast STCs. (Unichenko et al., 2012)

3.3.2 Paired-pulse plasticity of STCs

All following experiments in this study were performed in the presence of AMPA, NMDA, GABA_A, and GABA_B receptor antagonists. STCs recorded from different astrocytes showed highly variable amplitudes (range from 25 to 250 pA, n=75). As the number of axons activated by electrical stimulus is unknown, this parameter presumably underlies the observed variability of STC amplitudes. However, when the stimulus intensity remained constant, STCs recorded from a single astrocyte demonstrated minor amplitude fluctuations and no time drift throughout the experiment (Fig. 26A,B). Coefficient of variation (the standard deviation divided by the mean amplitude of STCs) was 0.12 ± 0.3 (n=25). Next, we investigated the paired-pulse behavior of STCs. Paired-pulse facilitation (PPF) was observed at short inter-stimulus intervals (ISIs, 10-250 ms), while at longer ISIs (500-5000 ms) STCs displayed paired-pulse depression (PPD, Fig. 26A,C).

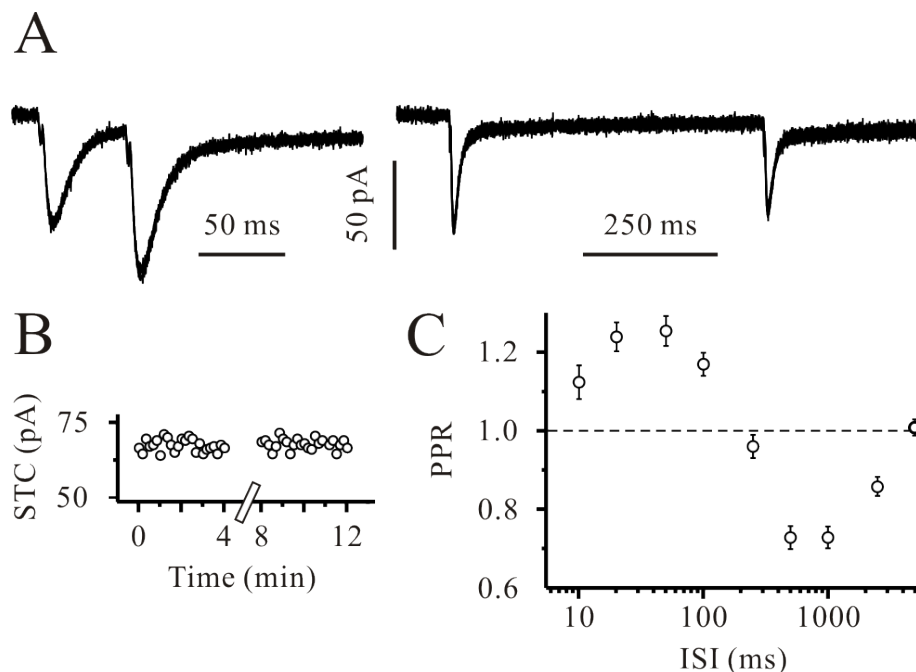


Figure 26. Short-term plasticity of STCs studied using the low $[Na^+]_i$ intracellular solution. (A) STCs elicited by paired-pulse stimulation at 50 and 500 ms inter-stimulus intervals (ISIs). Each panel is an overlay of five individual responses, not an average of several recordings. Note a very small variability of STC amplitude. (B) STCs recorded from an astrocyte show minor variability and no time drift. (C) Dependence of PPR on ISI. Note that the X axis is logarithmic.

The corresponding paired-pulse ratios (PPRs) at 50 and 500 ms ISIs were 1.25 ± 0.4 and 0.73 ± 0.03 , respectively (n=8). A train of 10 pulses delivered at

20 Hz resulted in initial facilitation of STC amplitude followed by depression (Fig. 27A,B).

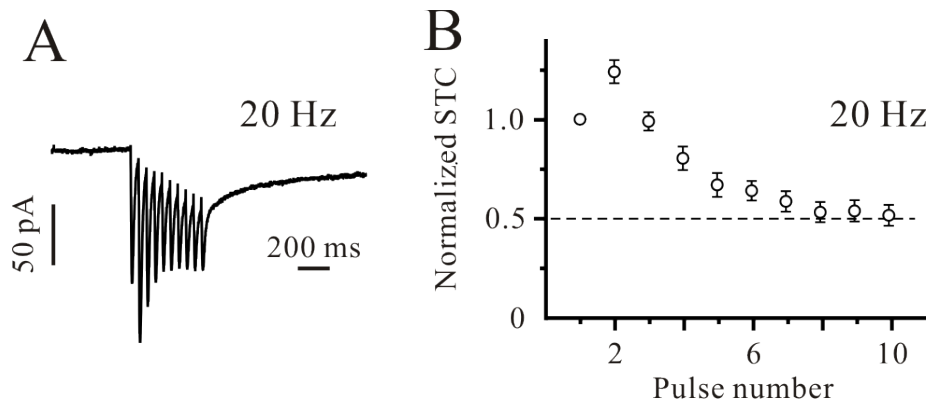


Figure 27. STCs elicited by the tetanic stimulation studied using the low $[Na^+]_i$ intracellular solution. (A) Sample trace shows STCs recorded in response to a 20 Hz, 10 pulses tetanic stimulation. (B) Relationship between the mean STC amplitude (normalized to the first STC) elicited by the tetanic stimulation and pulse number.

The mean amplitude of the 10th STC amounted to $51 \pm 7\%$ of the mean amplitude of the first STC ($n=8$). (Unichenko et al., 2012)

3.3.3 $[Na^+]_i$ in cortical astrocytes

As EAATs are mainly driven by the electrochemical gradient of Na^+ , we asked whether the STC paired-pulse plasticity is modulated $[Na^+]_i$. Moreover, to be closer to physiological conditions, we suggested to set $[Na^+]_i$ near its physiological concentration. In order to measure $[Na^+]_i$ in cortical astrocytes, we used the Na^+ -sensitive fluorescent indication SBFI. Electrophysiological experiments showed that more than 95% of SBFI-positive cells in layer 2/3 (25 out of 26 cells tested) demonstrated passive current-voltage relationships, high-negative resting membrane potentials and low input membrane resistances. Thus, SBFI similar to SR101 stains predominantly astrocytes in this preparation. Applying in situ calibration protocol (see Method), $[Na^+]_i$ in cortical astrocytes was measured to be 17 ± 5 mM ($n=56$, four slices, Fig. 7). (Unichenko et al., 2012)

3.3.4 Paired-pulse plasticity of STCs in astrocytes dialyzed with the high $[\text{Na}^+]_i$ solution

According to the above data, in the next set of experiments we recorded STCs with the intra-pipette solution containing 20 mM Na^+ . Fig. 28 A,B shows that similar to the data obtained with the low $[\text{Na}^+]_i$ solution (Fig. 26), slight PPF was observed at short intervals (20 to 100 ms), while STCs displayed PPD at longer ISIs (250-5000 ms) (Fig. 28A,C, n=7).

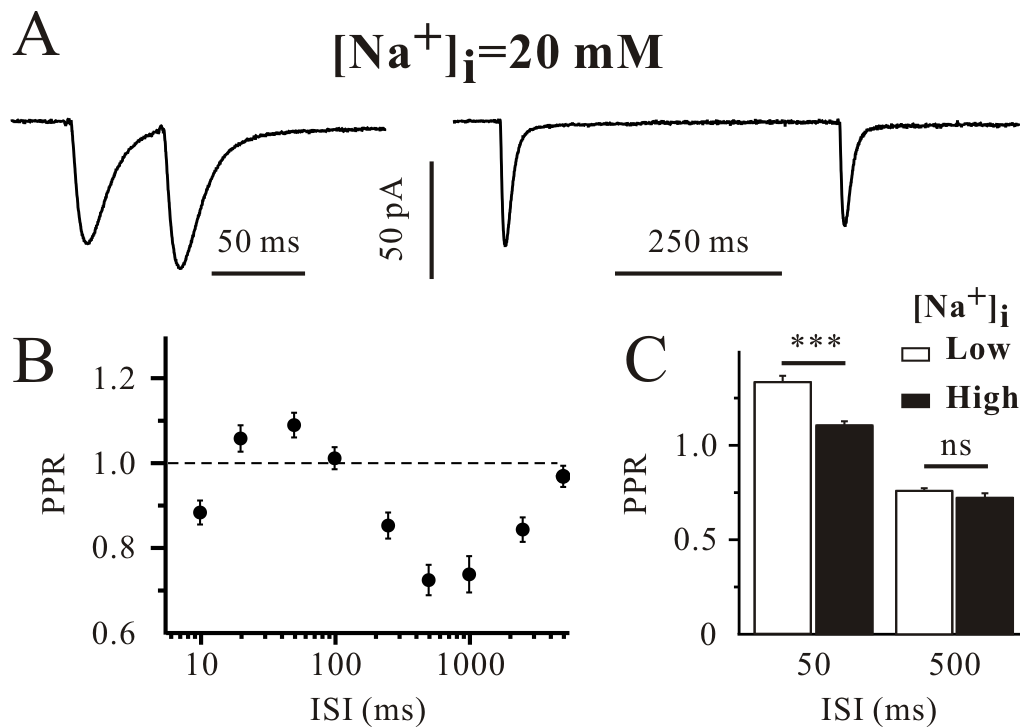


Figure 28. Short-term plasticity of STCs studied using the high $[\text{Na}^+]_i$ intracellular solution. (A) STCs elicited by paired-pulse stimulation at 50 and 500 ms inter-stimulus intervals (ISIs). Each trace is an average of 10 responses. (B) Dependence of PPR on ISI. Note that the X axis is logarithmic. (C) Bar graph shows the mean PPR values at 50 and 500 ms ISIs obtained with the low (open) and the high (filled bars) $[\text{Na}^+]_i$ intrapipette solutions. * $P < 0.05$, ** $P < 0.01$, *** $P < 0.001$, ns not significant.

Interestingly, PPRs at short but not at long (> 250 ms) ISIs were significantly smaller as compared to corresponding PPRs obtained with the low $[\text{Na}^+]_i$ solution (Fig. 26). To be sure that the observed difference in PPRs is not a consequence of sampling, we performed more experiments determining PPRs only at 50 and 500 ms ISIs. Fig. 28C shows that PPR at 50 ms ISI was strongly dependent on $[\text{Na}^+]_i$ (1.33 ± 0.04 and 1.10 ± 0.03 in the low and high

[Na⁺]_i intrapipette solutions, respectively, $p < 0.001$, $n = 35$ and 27), but not at 500 ms ISI (0.75 ± 0.02 and 0.73 ± 0.03 in the low and high [Na⁺]_i solutions, respectively, $p > 0.19$, $n = 35$ and 27 , unpaired Student's *t*-test). A train of 10 pulses delivered at 20 Hz resulted in initial facilitation of STC amplitude followed by depression (Fig. 29A,B).

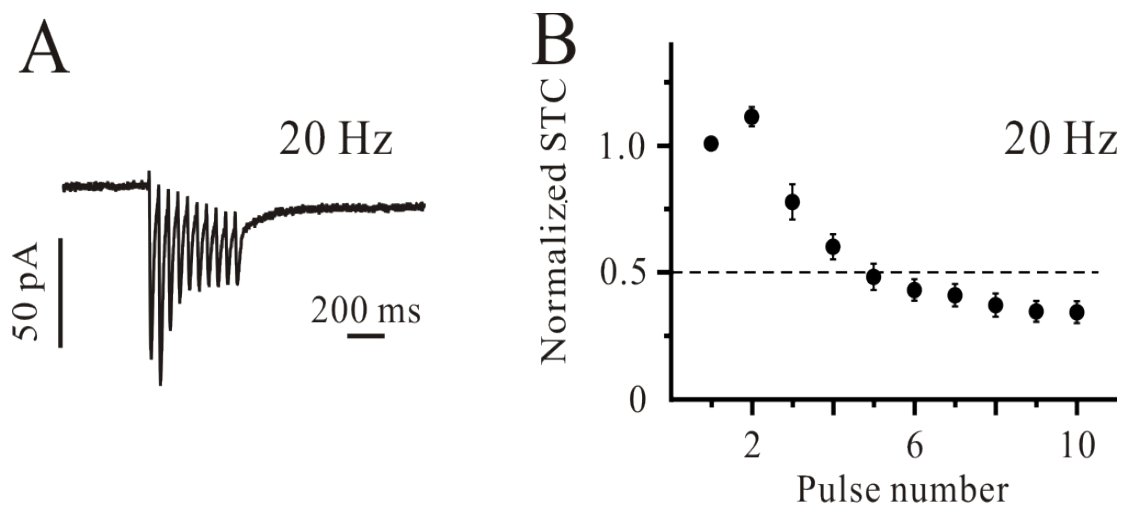


Figure 29. STCs elicited by the tetanic stimulation studied using the high [Na⁺]_i intracellular solution. (A) Sample trace shows STCs recorded in response to a 20 Hz, 10 pulses tetanic stimulation. (B) Relationship between the mean STC amplitude (normalized to the first STC) elicited by the tetanic stimulation and pulse number.

Interestingly, the mean amplitude of the 10th STC was $34 \pm 4\%$ of the first STC ($n = 7$), i.e. significantly smaller than the mean amplitude of the 10th STC recorded with the low [Na⁺]_i solution (Fig. 27, $51 \pm 7\%$, $n = 8$, $p < 0.01$, unpaired Student's *t*-test). In addition, the decay time constants of STCs recorded with the low (12.6 ± 0.4 ms, $n = 29$) and the high (15.3 ± 1.1 ms, $n = 22$) [Na⁺]_i solutions were significantly different ($p < 0.01$, unpaired Student's *t*-test). As high [Na⁺]_i may switch the Na⁺/Ca²⁺ exchanger (NCX) into the reverse mode, we checked whether the NCX contributes to the observed PPR changes. In the presence of high [Na⁺]_i, we applied KB-R7963, a selective inhibitor of the reverse mode of the NCX. KB-R7963 (10 μM) failed to affect either STC amplitude ($94 \pm 8\%$ of control, $p > 0.5$) or PPR at 50 ms ISI ($101 \pm 5\%$ of control, $p > 0.8$, $n = 5$, one population Student's *t*-test, data not shown). Thus, [Na⁺]_i seems to influence short-termed STC plasticity in an NCX independent

manner. However, because the above recordings of STCs with the low and high $[Na^+]_i$ solutions were performed from different cells, one can not exclude the possibility that the observed difference in STC kinetics is a result of sampling. Therefore, next we tried to manipulate $[Na^+]_i$ in the same cell. (Unichenko et al., 2012)

3.3.5 Transporter-mediated $[Na^+]_i$ signals in cortical astrocytes

Similar to EAATs, GABA transporters (GATs) are also driven by the electrochemical gradient of Na^+ . To investigate whether GAT activation can significantly change $[Na^+]_i$ in cortical astrocytes, we loaded astrocytes with the Na^+ -sensitive indicator SBFI (Fig. 30A).

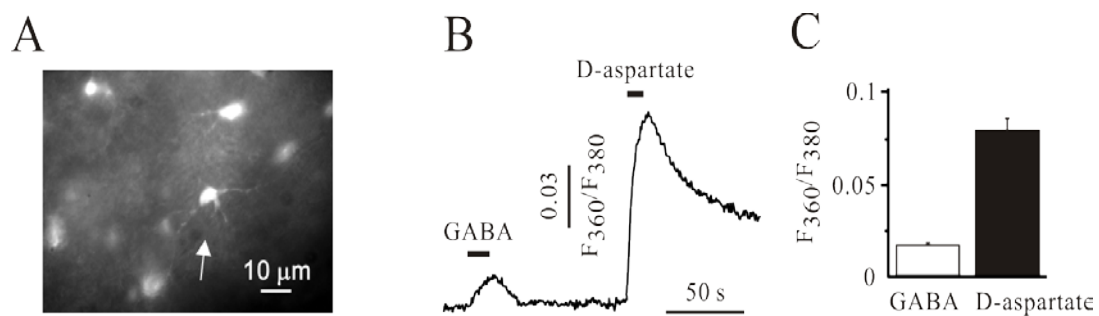


Figure 30. Transporter-mediated $[Na^+]_i$ transients in cortical astrocytes. (A) Image demonstrates SBFi-loaded cells in a neocortical mouse slice. Responses in panel (C) were obtained from the marked cell (an arrow). (B) Sample trace shows astrocytic $[Na^+]_i$ responses elicited by puff applications of GABA (100 μM) and D-aspartate (100 μM). Substances were applied in the presence of TTX, DNQX, APV, Gabazine, and CGP55845. (C) Column graph demonstrates the mean amplitudes of GABA- and D-aspartate-induced $[Na^+]_i$ responses in cortical astrocytes.

GABA (100 μM) and D-aspartate (100 μM), an EAAT substrate, were applied in the presence of TTX (1 μM), DNQX (10 μM), APV (50 μM), Gabazine (20 μM) and CGP55845 (1 μM). Puff application of D-aspartate (10 s) induced $[Na^+]_i$ elevation in all tested cells. Puff application of GABA (20 s) elicited $[Na^+]_i$ responses in a majority of cells tested (19 out of 26, Fig. 30B). After D-aspartate and GABA applications each cell was patched and electrophysiologically characterized. 25 out 26 cells tested demonstrated passive voltage-current relationships, possessed high-negative resting potentials (-76 ± 3 mV) and low membrane resistances (23 ± 2 M Ω). One cell

showed action potentials and was excluded from the further analysis. The mean amplitude of GABA-elicited $[Na^+]_i$ elevations (0.017 ± 0.001 , $n=19$) was much smaller as compared with the mean amplitude of D-aspartate-induced $[Na^+]_i$ responses (0.081 ± 0.007 , $n=25$, Fig. 30C). D-aspartate-elicited $[Na^+]_i$ responses were completely blocked by DL-TBOA ($40 \mu M$), an EAAT antagonist ($n=4$), whereas GABA-induced $[Na^+]_i$ transients were blocked by NO-711 ($10 \mu M$) plus SNAP-5114 ($40 \mu M$), GAT-1 and -2/3 blockers, respectively ($n=4$, data not shown). These results show that in most cases cortical astrocytes express both GATs and EAATs and exogenous GABA can significantly change astrocytic $[Na^+]_i$. (Unichenko et al., 2012)

3.3.6 Exogenous GABA influence STCs in cortical astrocytes

Bath application of GABA ($100 \mu M$) also induced astrocytic $[Na^+]_i$ increase. Moreover, $[Na^+]_i$ remained elevated as long as GABA was applied (Fig. 31).

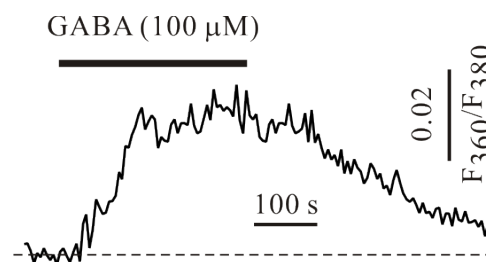


Figure 31. Mean $[Na^+]_i$ response elicited by 5 min bath application of GABA ($n=14$, 3 slices).

Thus, in the following experiments we applied long bath GABA application to keep $[Na^+]_i$ elevated. Despite the fact that GABA elicited somatic $[Na^+]_i$ signals, exogenous GABA induced a very tiny ($<5 \text{ pA}$, $n=21$) inward current and did not significantly change the membrane resistance (data not shown) independently on intracellular solution. However, in experiments with the low $[Na^+]_i$ solution, GABA reduced the mean amplitude of the first STC from $74 \pm 12 \text{ pA}$ to $62 \pm 9 \text{ pA}$ ($n=12$, $p < 0.05$, Fig. 32A-C). GABA also decreased PPR at 50 ms ISI from 1.24 ± 0.04 to 1.14 ± 0.05 ($n=12$, $p < 0.01$, Fig. 32A,D), but

failed to affect PPR at 500 ms ISI (0.81 ± 0.02 and 0.83 ± 0.02 in control and in the presence of GABA, respectively, $n=12$, $p>0.2$, Fig. 32A,D).

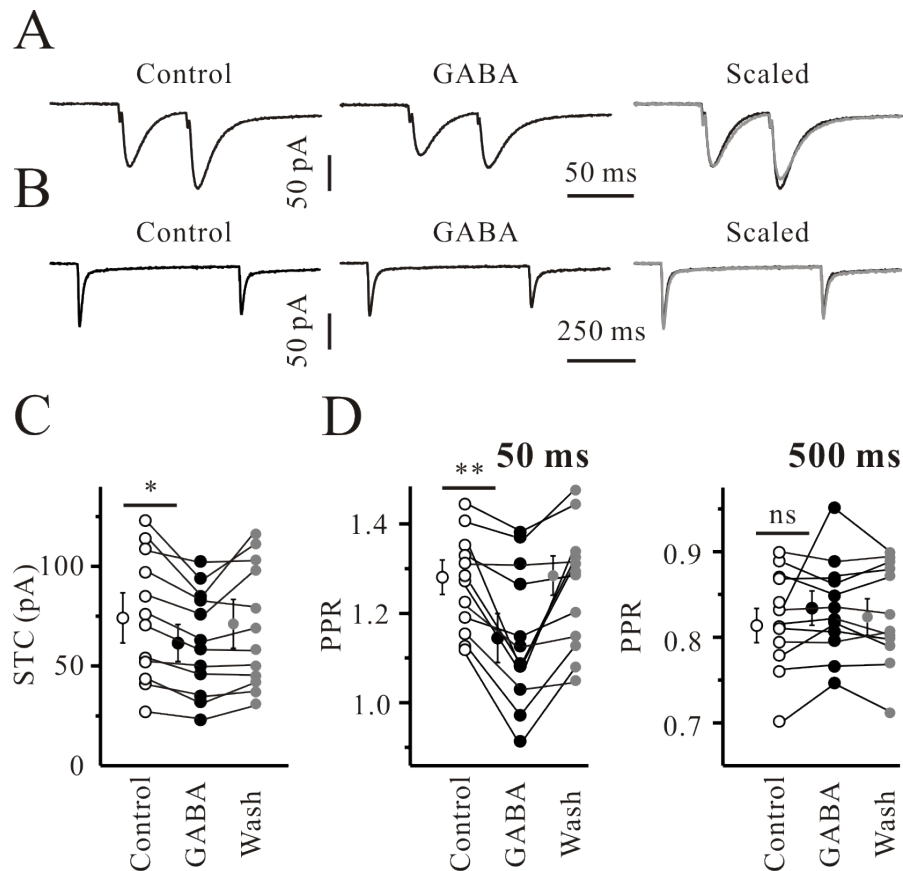


Figure 32. Exogenous GABA influences STCs in cortical astrocytes. (A) Paired-pulse STCs recorded at ISI of 50 ms in control (left) and in the presence of GABA (100 μ M). Each trace is an average of 10 responses. The right panel shows scaled STCs (grey line - in the presence of GABA). (B) Paired-pulse STCs recorded at ISI of 500 ms in control (left) and in the presence of GABA (100 μ M). Each trace is an average of 10 responses. The right panel shows scaled STCs (grey line - in the presence of GABA). (C-D) GABA effects on the mean amplitude of the first STCs (C) and PPRs (D). * $P < 0.05$, ** $P < 0.01$, *** $P < 0.001$, ns not significant.

In addition, exogenous GABA slowed the kinetics of STCs. It increased both the 20-80% rise time (from 2.11 ± 0.15 to 2.26 ± 0.18 ms, $p<0.001$) and decay time constant of STCs (from 11.9 ± 0.9 to 13.2 ± 1.1 ms in control and in the presence of GABA, respectively, $p<0.001$, $n=12$).

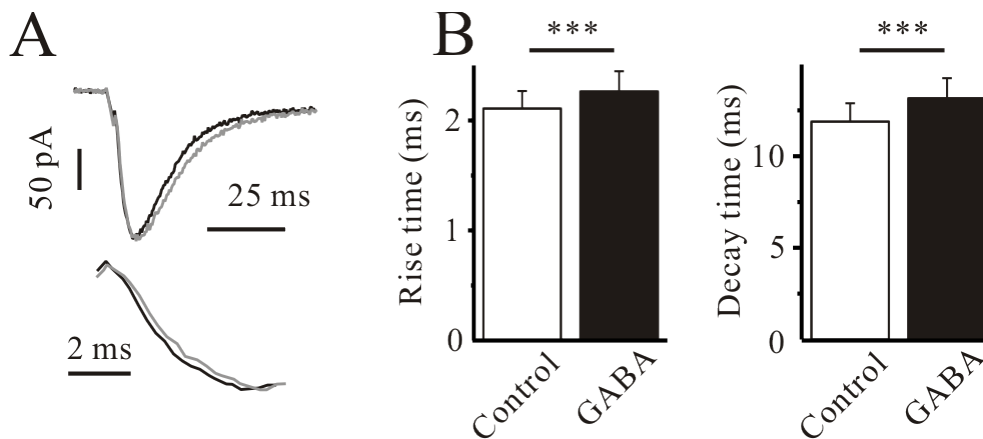


Figure 33. Exogenous GABA slowed the kinetics of STCs. (A) Scaled STCs (top) and their rising phase (bottom) recorded in control (black) and in the presence of GABA (grey line). (B) Column graphs show the effects of exogenous GABA on the 20-80% rise time (left) and decay time constant (right panel) of STCs. * $P < 0.05$, ** $P < 0.01$, *** $P < 0.001$, ns not significant.

The observed effects were reversible, but full washout required about 15-20 min. We also controlled whether exogenous GABA affects the slow component of evoked responses. Its amplitude was measured 100 ms after the stimulus application. In the presence of GABA the mean amplitude of the slow response amounted to $99 \pm 5\%$ of the control amplitude ($p > 0.9$, $n = 12$), i.e. this component was not modified by GABA. Similar results were obtained in experiments with the high $[Na^+]_i$ solution, but the effects were smaller. 100 μM GABA only slightly decreased the first amplitude of STCs (from 80 ± 18 to 75 ± 16 pA, $n = 9$, $p > 0.1$), but it significantly changed PPR at 50 ms ISI (from 1.09 ± 0.08 to 1.04 ± 0.05 , $n = 9$, $p < 0.05$, data not shown). Exogenous GABA increased the 20-80% rise time (from 2.9 ± 0.2 to 3.3 ± 0.3 ms, $p < 0.05$) and decay time constant of STCs (from 14.6 ± 0.5 to 15.3 ± 0.4 ms in control and in the presence of GABA, respectively, $p < 0.05$, $n = 8$, data not shown). Thus, exogenous GABA is capable to influence amplitude, kinetics, and short-termed plasticity of STCs. (Unichenko et al., 2012)

To check whether the above effects of exogenous GABA on STCs are mediated by GATs, the latter were blocked by NO-711 (10 μM), an antagonist of GAT-1, and SNAP-5114 (40 μM), a blocker of GAT-2/3. The low $[Na^+]_i$ intracellular solution was used to maximize the GABA-mediated effects. In the presence of GAT antagonists exogenous GABA failed to influence either the mean amplitude of the first STCs ($97 \pm 11\%$ of the control value, $p > 0.9$) or

PPR (102 ± 3 % of the control value, $p > 0.4$, $n = 4$, one population Student's t -test, data not shown). GABA also did not affect STC kinetics (data not shown). These results suggest that GATs mediate the effects of exogenous GABA on STCs. (Unichenko et al., 2012)

The above data shows that GAT antagonists block both the GABA-induced $[Na^+]_i$ elevations and the GABA effects on STCs. To investigate whether there is a correlation between $[Na^+]_i$ and STC changes, we applied the following approach. SBFI was added to the intracellular solution, allowing simultaneous recordings of $[Na^+]_i$ changes and transmembrane currents (Fig. 34A,B).

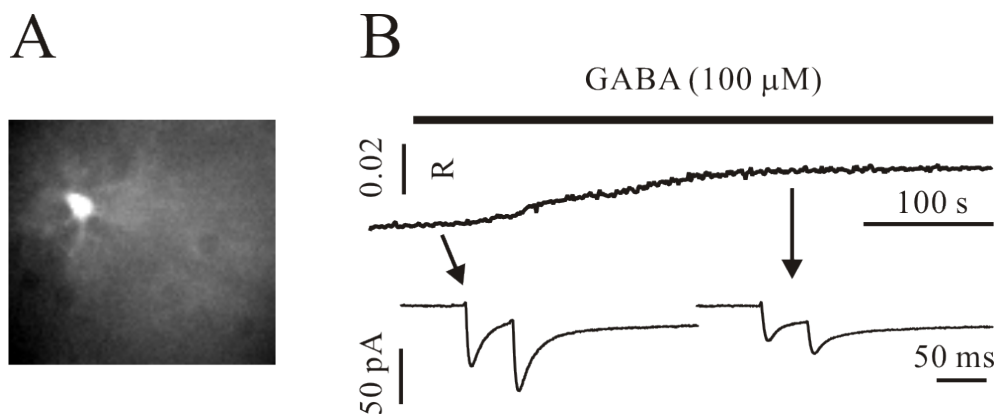


Figure 34. GABA effects on STCs may be mediated by $[Na^+]_i$. (A) An astrocyte filled with SBFI via a patch pipette. (B) Exogenous GABA ($100 \mu M$) induces a $[Na^+]_i$ elevation and modulates STCs. STC traces (bottom) are 10 response averages. R means the F_{360}/F_{380} ratio.

Fig. 35A demonstrates a negative correlation between the GABA-induced relative changes of mean STC amplitudes and $[Na^+]_i$ elevations ($n = 10$, $p < 0.05$). Similarly, a negative correlation between $[Na^+]_i$ and PPR of STCs have been observed (Fig. 35B).

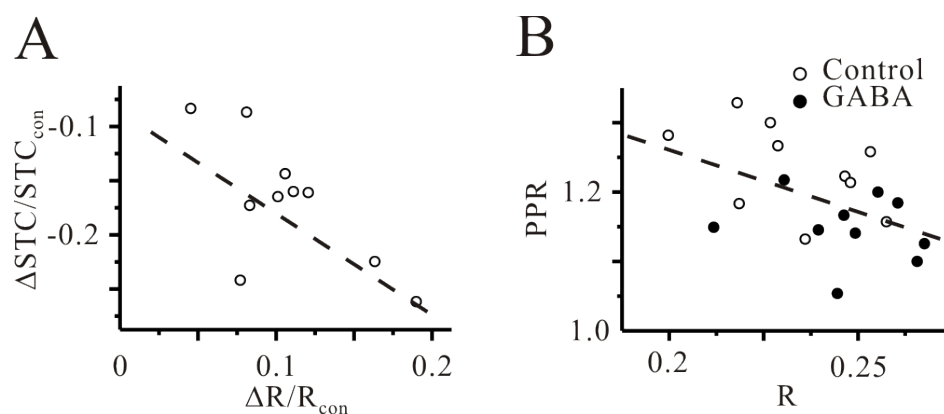


Figure 35. Negative correlation between the GABA-induced relative changes of mean STC amplitudes, PPR and $[Na^+]_i$ elevations. (A) Correlation between the relative changes of $[Na^+]_i$ and the relative changes of STC amplitudes induced by GABA. (B) Relationship between $[Na^+]_i$ and PPR of STCs. R means the F_{360}/F_{380} ratio.

As expected, GABA-mediated effects were completely blocked by pre-application of NO-711 (10 μ M) and SNAP-5114 (40 μ M, $n=4$, Fig. 36).

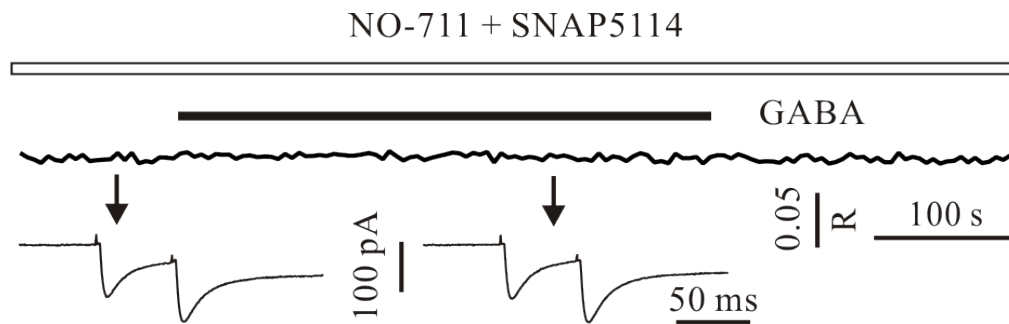


Figure 36. GABA effects on STCs is blocked by pre-application of NO-711 and SNAP-5114. (E) In the presence of NO-711 (10 μ M) and SNAP-5114 (40 μ M) GABA failed to change either $[Na^+]_i$ or STCs. R means the F_{360}/F_{380} ratio.

Thus, we conclude that the GAT-mediated $[Na^+]_i$ increase might contribute to the GABA-induced changes in the STC paired-pulse plasticity. (Unichenko et al., 2012)

3.3.7 Endogenous GABA can modulate STCs

Interestingly, GAT blockade with NO-711 and SNAP-5114 alone influenced STCs. In experiments with the low $[Na^+]_i$ solution, NO-711 plus SNAP-5114 did not change the first amplitude of STCs (73 ± 14 to 75 ± 15 pA, $n=9$, $p > 0.65$, Fig. 37A,B). PPR at 50 ms ISI, however, was decreased from 1.24 ± 0.08 in control to 1.15 ± 0.07 in the presence of NO-711 plus SNAP-5114 ($n=9$, $p < 0.01$), whereas PPR at 500 ms ISI was not significantly affected (0.73 ± 0.05 and 0.75 ± 0.05 in control and in the presence of NO-711 plus SNAP-5114, respectively, $n=9$, $p > 0.09$, Fig. 37A,C).

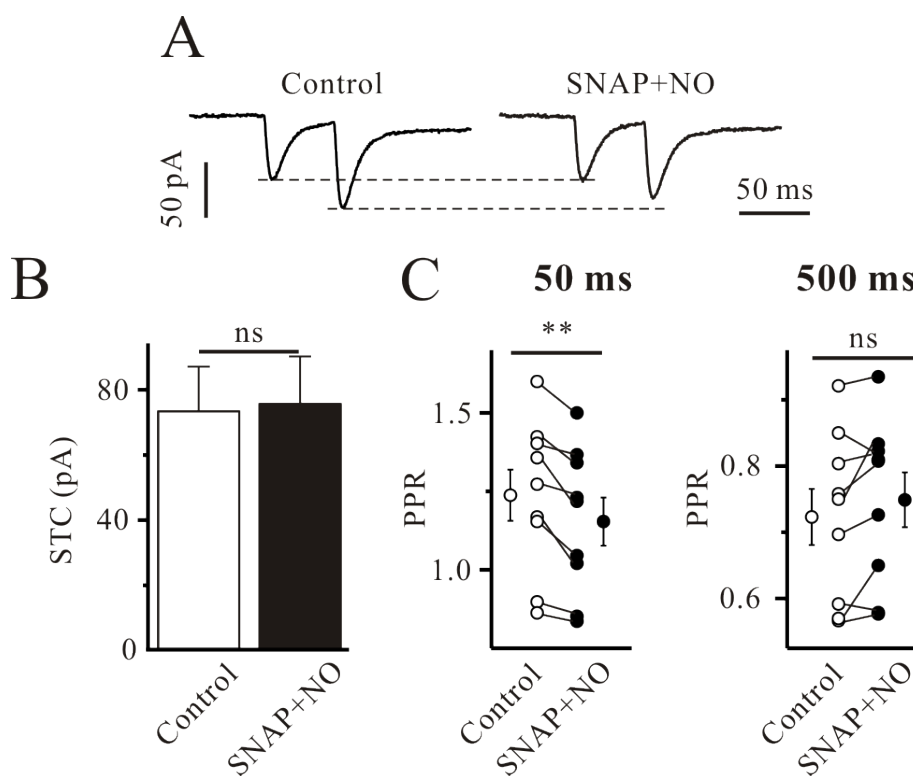


Figure 37. GAT blockade influences STC short-term plasticity. (A) Paired-pulse STCs recorded at 50 ms ISI in control and in the presence of NO-711 (NO, 10 μ M) and SNAP-5114 (SNAP, 40 μ M). Each trace is an average of 10 responses. (B and C) Column graphs demonstrate GAT blockade effects on the mean amplitude of the first STCs (B) and PPRs (C). * $P < 0.05$, ** $P < 0.01$, *** $P < 0.001$, ns not significant.

Similar to exogenous GABA, NO-711 plus SNAP-5114 did not influence the slow component of evoked responses (98 ± 5 % of the control amplitude, $p > 0.8$, $n = 9$). A train of 10 pulses delivered at 20 Hz resulted in initial facilitation of STC amplitude followed by depression (Fig. 38).

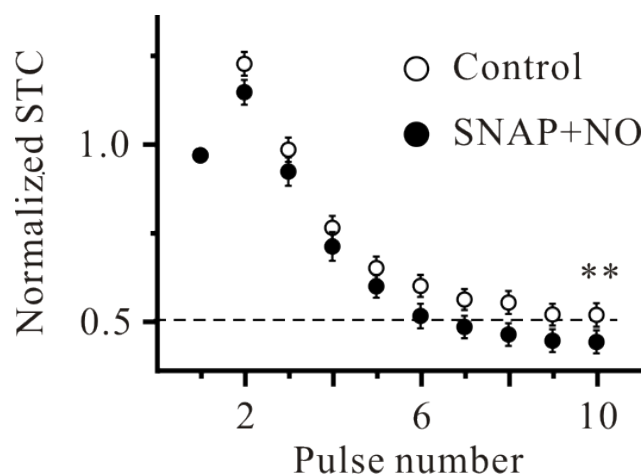


Figure 38. GAT blockade influences STCs elicited by the tetanic stimulation. Relationship between the mean STC amplitude (normalized to the first STC amplitude) elicited by the tetanic (20 Hz, 10 pulses) stimulation and pulse number. * $P < 0.05$, ** $P < 0.01$, *** $P < 0.001$, ns not significant.

The mean amplitude of the 10th STC normalized to the mean amplitude of the first STC amounted to $52\pm 4\%$ and $45\pm 3\%$ in control and in the presence of NO-711 plus SNAP-5114 ($p < 0.01$, $n = 9$, Fig. 38). In experiments with the high $[Na^+]_i$ intrapipette solution, NO-711 plus SNAP-5114 failed to change either the first amplitude of STCs (54 ± 9 and 61 ± 12 pA, $p > 0.1$) or PPR at 50 ms ISI (1.09 ± 0.04 and 1.06 ± 0.03 in control and in the presence of NO-711 plus SNAP-5114, respectively, $p > 0.3$, $n = 8$, data not shown). Thus, we conclude that GATs activated by endogenous GABA are capable to affect short-term plasticity of STCs, and this influence is dependent on $[Na^+]_i$. (Unichenko et al., 2012)

3.3.8 Short-term plasticity of STCs at near physiological temperature

Because the above experiments were performed at room temperature, we asked whether endogenous GABA can influence PPR of STCs at near physiological (31 °C) temperature. STCs recorded under these conditions demonstrated faster kinetics. Their rise time and decay time constant amounted to 1.9 ± 0.3 ms and 9.6 ± 0.4 ms ($n = 17$), respectively. Similar to the data obtained at room temperature (Fig. 26), PPR of STCs recorded using the low $[Na^+]_i$ solution showed PPF at short ISIs (<250 ms) and PPD at longer ISIs (Fig. 39A,B).

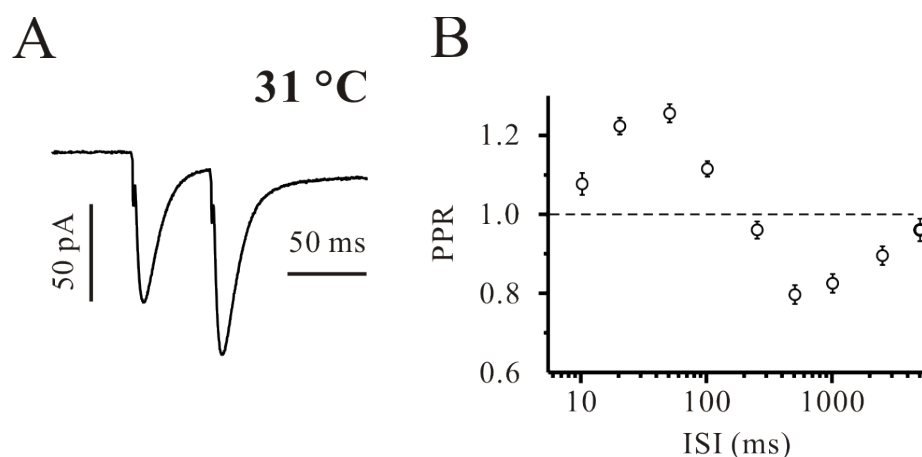


Figure 39. Short-term plasticity at near physiological temperature. (A) Paired-pulse STCs recorded at ISI of 50 ms at near physiological (31°C) temperature. The trace is an average of 10 responses. (B) Dependence of PPR on ISI. Note that the X-axis is logarithmic.

At 50 ms ISI, PPR at near physiological temperature (1.26 ± 0.02 , $n=15$) was not significantly different from PPR at room temperature (Fig. 26, 1.25 ± 0.04 , $n=8$, $p > 0.7$, unpaired Student's t -test). PPR at 500 ms ISI was slightly but significantly higher (0.80 ± 0.02 , $n=15$) as compared to PPR at room temperature (Fig. 26, 0.73 ± 0.03 , $n=8$, $p < 0.01$, unpaired Student's t -test). NO-711 ($10 \mu\text{M}$) plus SNAP-5114 ($40 \mu\text{M}$) did not change either the first STC amplitude (62 ± 5 versus 65 ± 6 pA, $p > 0.8$) or PPR at 500 ms ISI (0.81 ± 0.02 and 0.80 ± 0.02 , $p > 0.6$), but significantly reduced PPR at 50 ms ISI (1.29 ± 0.04 and 1.21 ± 0.03 in control and in the presence of NO-711 plus SNAP-5114, respectively, $p < 0.05$, $n=7$, Fig. 40A,B).

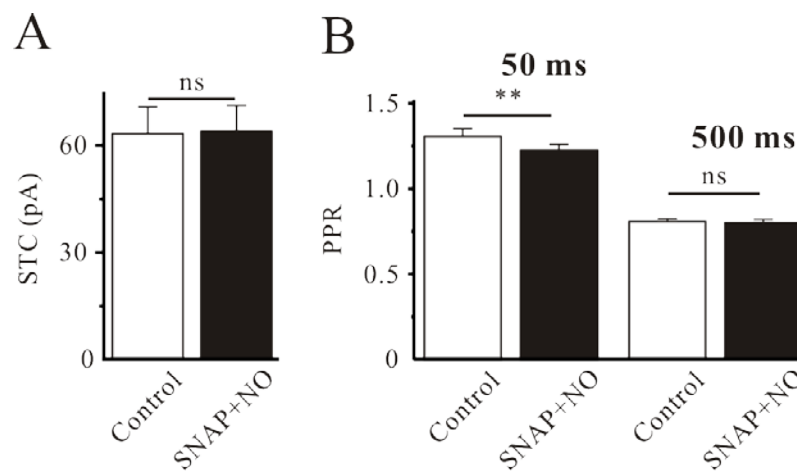


Figure 40. GAT blockade influences STC short-term plasticity at near physiological temperature. (A and B) GAT blockade did not change the mean STC amplitude (A) and PPR at 500 ms ISI (B), but significantly reduced PPR at 50 ms ISI (D). * $P < 0.05$, ** $P < 0.01$, *** $P < 0.001$, ns not significant.

In experiments with the high $[\text{Na}^+]_i$ solution, NO-711 plus SNAP-5114 failed to change PPR at 50 ms ISI (1.11 ± 0.03 and 1.09 ± 0.04 in control and in the presence of NO-711 plus SNAP-5114, respectively, $p > 0.7$, $n=5$, data not shown). Thus, we conclude that GATs activated by endogenous GABA modulate short-term plasticity of STCs at near physiological temperature, but only when $[\text{Na}^+]_i$ is relatively low. (Unichenko et al., 2012)

3.3.9 Cortical field potentials are influenced by astrocytic $[\text{Na}^+]_i$

The above data shows that astrocytic $[\text{Na}^+]_i$ can influence both STC amplitude and kinetics. If STCs reflect glutamate removal from the

extracellular space, their changes should result in alterations of extracellular glutamate levels and, in turn, could affect the neuronal network activity. To investigate whether this is the case, we recorded local field potentials in the vicinity of an SR-positive astrocyte. After recording the control responses the astrocyte was dialysed with either the low or the high $[Na^+]_i$ intracellular solution. Fig. 41 shows that intracellular perfusion of astrocytes with the high $[Na^+]_i$ solution recorded affected neither the amplitude of evoked field potential (177 ± 29 versus 166 ± 27 μV , $p > 0.6$) nor its paired-pulse ratio (1.02 ± 0.11 versus 1.01 ± 0.12 , $n = 6$, $p > 0.8$, paired Student's t -test).

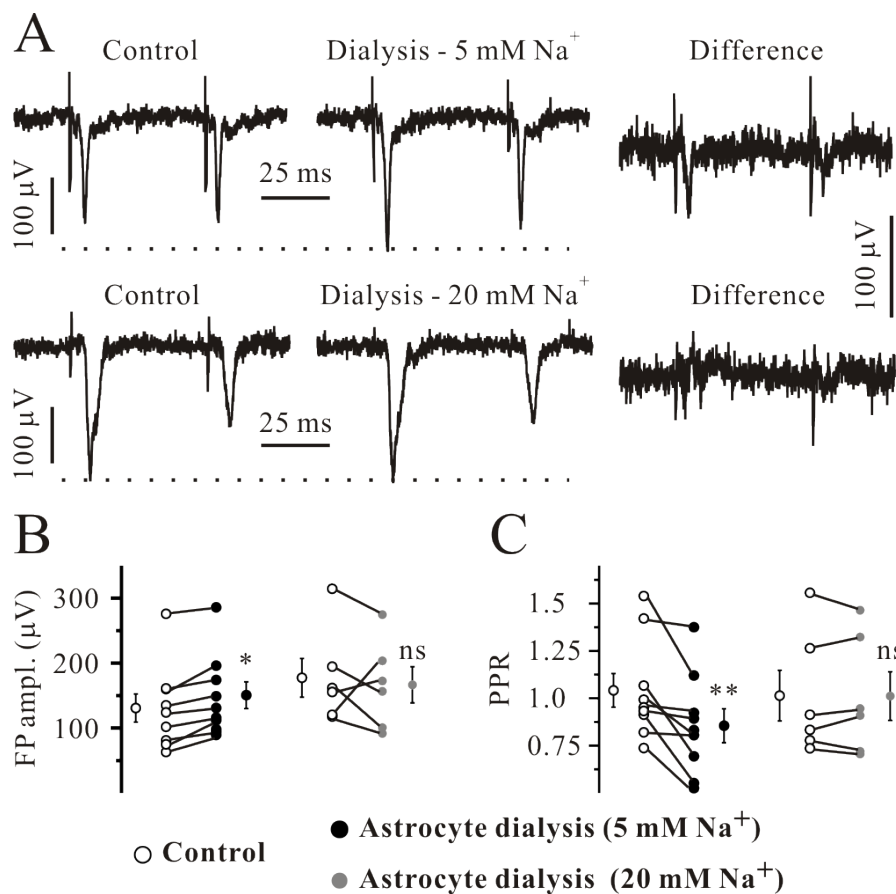


Figure 41. Dialysis of an astrocyte with the low $[Na^+]_i$ solution influence evoked field potentials in the cortex. (A) Field potentials recorded in controls (left), after 10 min of astrocyte dialysis with low (top) and high (bottom) pipette solutions (middle traces). Right traces demonstrate changes induced by the dialysis. (B and C) Effects of astrocyte dialysis with low (filled symbols) and high (gray symbols) $[Na^+]_i$ on the mean amplitude of the first field potential (B) and PPRs (C). * $P < 0.05$, ** $P < 0.01$, *** $P < 0.001$, ns not significant.

In contrast to this data, astrocyte dialysis with the low $[Na^+]_i$ solution resulted in an increase of the field potential amplitude from 131 ± 21 to 151 ± 20 μV ($p < 0.05$) and a decrease of PPR from 1.04 ± 1.13 to 0.85 ± 0.09 ($n=9$, $p < 0.01$, paired Student's *t*-test, Fig. 41). These results give a support to the hypothesis that changes in astrocytic $[Na^+]_i$ can influence cortical neuronal activity. (Unichenko et al., 2012)

4 Discussion

In this work we have shown that glutamate uptake is capable to modulate GABA transport. We have demonstrated that DL-TBOA, a non-transportable EAAT antagonist, eliminates GAT-2/3-mediated GABA release, while D-aspartate, an EAAT substrate, fails to block the latter. Thus, the strength or even the operating mode of GATs might be influenced by the status of EAATs. The observed interaction between EAATs and GATs also suggests that ambient glutamate and GABA levels are mutually dependent. The EAAT-GAT crosstalk observed in this study is mediated by EAAT1 and GAT-2/3. Since both transporters are Na⁺ dependent and mainly glial, next we investigated the role of [Na⁺]_i in astrocytic-mediated glutamate uptake. We tested whether [Na⁺]_i changes affect paired-pulse plasticity of STCs recorded from cortical layer 2/3 astrocytes. We report that an elevation of [Na⁺]_i induced either by using a high [Na⁺]_i intrapipette solution or by application of GABA slows STCs kinetics and decrease paired-pulse facilitation (PPF) of STCs at short inter-stimulus intervals. Moreover, GAT inhibitors decrease PPF of STCs under control conditions, suggesting that endogenous GABA operating via GATs influences EAAT-mediated transport. (Dvorzhak et al., 2012;Unichenko et al., 2012;Unichenko et al., 2013)

4.1 EAATs operate in the uptake mode

DL-TBOA has been shown to elicit slow oscillations in layer 4/5 pyramidal cells in neonatal rat cortical slices. The observed neuronal network discharges were triggered by glutamate and by activation of NMDA receptors (Demarque et al., 2004). In this study, EAAT blockade with DL-TBOA produced bursts of spontaneous PSCs in layer 2/3 pyramidal cells (Fig. 9), and this activity was completely blocked by APV, an NMDA receptor antagonist. In contrast to layer 2/3 pyramidal cells, EAAT blockade failed to increase the frequency of either Ca²⁺ transients or sGPSCs in CR cells.

Although CR cells express NMDA receptors (Mienville and Pesold, 1999), DL-TBOA did not produce any significant depolarization of CR cells. However, EAAT blockade significantly decreased the frequency of mGPSCs and the mean eGPSC amplitude. Because LY379268, an agonist of mGluR-II/III strongly reduced eGPSC amplitude, elevation of extracellular glutamate concentration and activation of presynaptic mGluR-II/III most probably underlies the DL-TBOA-elicited effects. Thus, in the marginal zone EAATs operate in the uptake mode under control conditions and their blockade results in an increase of extracellular glutamate concentration. Because DHK, a specific antagonist of EAAT2, failed to produce any effect and TFB-TBOA, a specific antagonist of EAAT1 and EAAT2, was as effective as DL-TBOA, an antagonist of all EAATs (Fig. 21, 22), EAAT1 appears to be the main EAAT that controls ambient glutamate concentration in the vicinity of GABAergic synapses on CR cells. Interestingly, according to immunohistochemical data EAAT1 expression in the perinatal neocortex is rather low as compared to that of EAAT2 and EAAT3 (Furuta et al., 1997). On the other hand, normal development of the CNS was observed in mutant mice lacking EAAT2/EAAT3, while EAAT1/EAAT2 double knockout mice died *in utero* and exhibited abnormal brain development (Matsugami et al., 2006). These results suggest that EAAT1 and EAAT2 are major glutamate transporters during prenatal development. Relatively low levels of EAAT1 immunoreactivity may point to a highly non-homogeneous spatial distribution of EAAT1, for instance their location might be primarily perisynaptic. (Dvorzhak et al., 2012)

4.2 Presynaptic inhibition of GABAergic transmission

Perisynaptic location of EAAT1 may be physiologically important. CR cells are highly vulnerable to excitotoxicity (Super et al., 1998). However, our data shows that DL-TBOA-induced increase of extracellular glutamate concentration does not lead to their hyperexcitability. Although CR cells express NMDA receptors (Mienville and Pesold, 1999; Mienville, 1998), EAAT blockade did not depolarize but slightly hyperpolarized CR cells. Thus, moderate and/or short-lasting elevation of extracellular glutamate does not

increase CR cell excitability. However, not only augmentation of cell excitability, but potentiation of synaptic inputs may also increase cell firing and potentially lead to excitotoxic damage. CR cells in the murine neocortex receive only excitatory GABAergic inputs (Kirmse and Kirischuk, 2006a; Soda et al., 2003; Kirmse et al., 2007b). Perisynaptic location of EAAT1 combined with presynaptic location of mGluR-II/III provides an effective protection mechanism against the neuronal network-mediated runaway excitation. In case of EAAT dysfunction, for instance during epilepsy (During et al., 1995; Hu et al., 1991), excitatory inputs to CR cells will be strongly suppressed through activation of presynaptic mGluR-II/III (Fig. 9). The observation that presynaptic mGluR-II/III are not activated under control conditions supports the suggestion that this mechanism represents a kind of “brakes” which will be activated under pathophysiological conditions. Physiologically, however, the GABAergic system controls the strength of excitatory GABAergic synaptic inputs to CR cells. Interestingly, tonic activation of presynaptic GABA_BRs is mediated by GABA released via GAT-2/3 operating in the reverse mode (Kirmse and Kirischuk, 2006a). (Dvorzhak et al., 2012)

4.3 EAATs modulate GABA release

Although the main function of GATs is believed to be GABA uptake, the existence of Ca²⁺ independent GABA release via GATs has been also suggested (Haycock et al., 1978). Several drugs known to increase [Na⁺]_i, i.e. veratridine, ouabain, excitatory amino acid agonists, have been shown to stimulate this form of GABA release (Cunningham and Neal, 1981; Sandoval, 1980; Schwartz, 1982). Because EAATs co-transport three Na⁺ ions with one glutamate molecule, they can potentially provide intracellular Na⁺ required for GATs to reverse (Fig. 42).

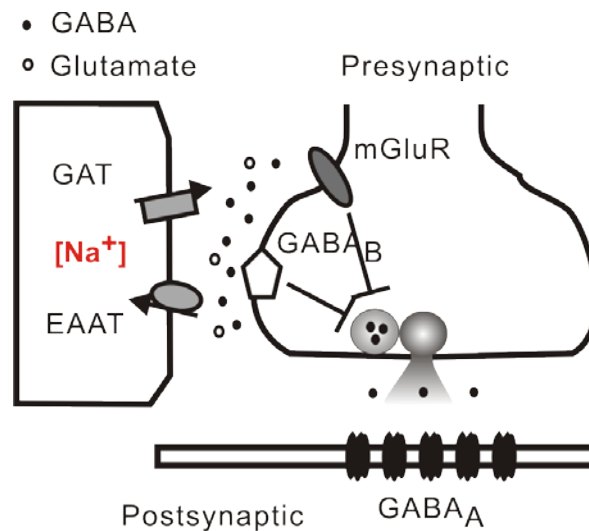


Figure 42. EAAT-GAT-mediated glutamate-GABA exchange

Recently, this hypothesis has been confirmed in the adult hippocampus. Application of 100 μM glutamate for 10 min has been shown to increase extracellular GABA concentration both *in vivo* and in hippocampal slices. Ambient GABA elevation was produced by all tested EAAT substrates, but not by non-transportable antagonists suggesting that EAAT-mediated transport is a prerequisite for GAT reversal (Heja et al., 2009). Our results are in line with this data, but there is an important difference. In the adult hippocampus, strong glutamate stimulation (100 μM , 10 min) was applied to initiate GABA release suggesting that transporter-mediated glutamate-GABA exchange occurs rather under pathophysiological conditions. In the current study, EAAT blockade by DL-TBOA reduced GAT-2/3-mediated GABA release suggesting that EAATs modulate GAT-2/3-mediated GABA release under control conditions. The question whether the “resting” EAAT-GAT crosstalk takes place in other brain structures needs further investigations. EAAT-GAT interaction presumably requires precise spatial co-localization of glutamate and GABA transporters, and most probably occurs in small cellular compartments, like small dendrites or astrocytic processes, where relatively small Na^+ influx can produce relatively large Na^+ concentration changes. In the current study, usage of presynaptic metabotropic receptors as detectors of extracellular GABA makes the spatial resolution of the approach close to synapse dimension. Héja et al. (Heja et al., 2009) used radioactive assay and

microdialysis to measure extracellular GABA levels. Both approaches, however, provide GABA concentrations averaged over reasonably large volumes. Definitely, EAAT-mediated GAT modulation at cell somata would require much larger Na^+ influx and would presumably occur under pathophysiological conditions, for instance during epileptic discharges. (Unichenko et al., 2013)

4.4 Physiological role of the EAAT-GAT-mediated glutamate-GABA exchange

In the marginal zone GABA acting on reasonably low-affinity GABA_A receptors mediates a “stop” signal for radially migrating neurons (Behar et al., 1996; Heck et al., 2007). The marginal zone contains both GABAergic cells and bundles of GABAergic axons which may provide the required ambient GABA (Delrio et al., 1992). However, perinatal neuronal activity is rather low both in slices and in the whole brain (Schwartz et al., 1998; Aguilo et al., 1999). In addition, blockade of neuronal activity with TTX appears not to decrease ambient GABA concentration (Kirmse and Kirischuk, 2006a). Thus, despite the presence of GABAergic cells and axons, the main source of extracellular GABA seems to be non-synaptic. In the marginal zone of the neonatal neocortex blockade of GAT-1 and GAT-2/3 eliminates tonic GABA_B R-mediated inhibition of GABAergic transmission (Dvorzhak et al., 2010) suggesting that GATs represent the major mechanism of GABA release. Definitely, both extracellular GABA and glutamate are required to modulate cell migration in the neocortex (Heck et al., 2007; Reiprich et al., 2005), but one can not exclude the possibility that they operate in concert, i.e. one can substitute the other. In the immature hippocampus, for instance, GABA_A antagonists have been shown to affect cell migration more efficiently than NMDA antagonists (Manent et al., 2005). Moreover, early generated neurons in the marginal zone are highly vulnerable to excitotoxicity (Super et al., 1998). Thus, if NMDA- and GABA-mediated “stop” signals are redundant, the EAAT-GAT crosstalk may serve to replace potentially excitotoxic glutamate for less “dangerous” GABA preserving at the same time the

required level of the “stop” signal. Since the EAAT-GAT crosstalk was mainly mediated by glial GAT-3 and GLAST transporters. (Unichenko et al., 2013)

4.5 Does the glutamate-GABA exchange occur in astrocytes?

Interestingly, the EAAT-GAT crosstalk observed in this study is mediated by EAAT1 and GAT-2/3. Because GAT-2 was detected only in the arachnoid and in the subarachnoidal space (Minelli et al., 2003), probably only GAT-3 contributes to the GABA release. In adult neocortex both GAT-3 and EAAT1 are expressed exclusively in astrocytic processes (Voutsinos-Porche et al., 2003; Minelli et al., 1996). However, during the first two postnatal weeks many cells with ultrastructural features typical for neurons as well as axon terminals express GAT-3 (Minelli et al., 2003). Similar to GAT-3, in the prenatal mouse brain transient expression of EAAT1 has been reported on radial glial cells, while the other “glial” glutamate transporter EAAT2 was detected on neurons (Matsugami et al., 2006; Regan et al., 2007). Thus, glial location of EAAT-GAT interaction is highly probable. Therefore next we have investigated STCs in cortical layer 2/3 astrocytes. (Dvorzhak et al., 2012)

4.6 Paired-pulse plasticity of STCs

STCs in cortical layer 2/3 astrocytes were induced by electrical stimulation in layer 4. As STCs were blocked by TTX, Cd^{2+} , and DL-TBOA, they indeed represent EAAT-mediated removal of synaptically released glutamate. At room temperature, STCs showed the rise time (20-80%) of 2.1 ms and decayed exponentially with a time constant of 12.6 ms. Similar STC kinetics at room temperature were observed in the cerebellum (1.9 and 17.3 ms, (Bergles et al., 1997)) and in the hippocampus (3.7 and 17.8 ms - rise time and decay time constant, respectively, (Bergles and Jahr, 1997)). STCs recorded at near physiological (31 °C) temperature displayed faster decay kinetics (9.6 ms, a decrease by a factor of 1.31). Short-term plasticity reflects the modification of synaptic transmission during repetitive stimulation (Zucker and Regehr, 2002). Because low $[\text{Na}^+]_i$ pipette solutions were used in most studies devoted to STCs in astrocytes (Bellamy and Ogden, 2005; Bergles and Jahr, 1997; Clark and Barbour, 1997; Diamond and Jahr, 1997; Manita et

al., 2007), we first applied the low $[Na^+]_i$ pipette solution. At short ISIs (<250 ms) STCs demonstrated PPF, whereas PPD dominated at longer ISIs (Fig. 26). The observed PPF of STCs at short ISIs is, however, unexpected, because glutamatergic projections from layer 4 spiny neurons to their main targets in layer 2/3 - pyramidal cells and interneurons display mostly PPD (Feldmeyer et al., 2002; Helmstaedter et al., 2008). However, although paired-pulse ratio is generally believed to reflect presynaptic release probability, the postsynaptic site can also influence it (Zucker and Regehr, 2002). Because EAATs are Na^+ dependent, we hypothesized that astrocytic $[Na^+]_i$ may influence STC plasticity. To be closer to physiological conditions, we have measured the resting $[Na^+]_i$ in cortical astrocytes using the Na^+ -sensitive indicator SBFI. The latter amounted to 17 mM. This value is close to $[Na^+]_i$ levels (15 mM) measured in cultured hippocampal astrocytes (Rose and Ransom, 1996), although in cultured cortical astrocytes $[Na^+]_i$ was reported to be lower (Chatton et al., 2000). Elevation of $[Na^+]_i$ to 20 mM strongly influenced STCs (Fig. 26-29). However, Na^+ entry through EAATs was shown to reverse the NCX (Rojas et al., 2007). According to the Nernst equation, 20 mM $[Na^+]_i$ could switch the NCX into the reverse mode. Because the NCX is electrogenic, its reversal can potentially influence STCs. However, as KB-R7943, an antagonist of the NCX reverse mode, failed to affect STCs plasticity, arguing against the dominating role of the NCX in this case. (Unichenko et al., 2012)

4.7 $[Na^+]_i$ influences paired-pulse plasticity of STCs

Interestingly, astrocytic $[Na^+]_i$ elevations through the patch pipette or by exogenous GABA produced the following effects: 1) STC amplitudes were reduced (Fig. 28, 32), 2) STC kinetics was slowed down (Fig. 32), and 3) PPF of STCs at short ISIs was reduced (Fig. 28,32). GABA applied in the presence of $GABA_A$ and $GABA_B$ receptor blockers increased astrocytic $[Na^+]_i$ and decreased STC amplitudes (Fig. 32-34). Immunohistochemical

(Minelli et al., 1996) and electrophysiological (Kinney and Spain, 2002) data show that cortical astrocytes express GATs. Because GATs co-transport GABA with two Na^+ and one Cl^- ions (Attwell et al., 1993), the GAT-mediated Cl^- influx can potentially influence the EAAT-coupled anion conductance (Billups et al., 1996; Otis et al., 1997). However, exogenous GABA not only decreased STC amplitudes, it also slowed STC kinetics (Fig. 32, 33). Similar slowing of STC kinetics was observed when astrocytic $[\text{Na}^+]_i$ was elevated via patch pipette, i.e. without alteration of intracellular Cl^- concentration. Thus, the EAAT-coupled anion conductance makes a minor contribution to the GAT-mediated effects of STCs. As GATs are electrogenic, GABA uptake can depolarize the plasma membrane and reduce the driving force for EAATs, resulting in a reduction of STC amplitudes. In this work, exogenous GABA induced a small but detectable (<5 pA) inward current in somata of cortical astrocytes. As cortical astrocytes have low input resistance (about 20 M Ω), cell depolarization induced by such small currents should not exceed several mV. GAT-mediated depolarization should only slightly decrease the EAAT driving force. However, we can not exclude that local GAT-mediated depolarization may be strong enough to reduce STC amplitude. But even if this were the case, the GAT-mediated depolarization should equally decrease amplitudes of all STCs, i.e. it should not change PPR. Thus, we can assume that the GAT-mediated $[\text{Na}^+]_i$ increase underlies the observed effects. Indeed, because EAATs co-transport glutamate with 3 Na^+ ions, even small (2-5 mM) $[\text{Na}^+]_i$ changes induced by exogenous GABA could detectably reduce STC amplitudes. In addition, elevated $[\text{Na}^+]_i$ was shown to influence kinetics of EAAT-mediated currents in retinal Müller cells (Barbour et al., 1991) and in cerebellar Purkinje cells (Otis and Jahr, 1998; Wadiche et al., 2006). In cultured cortical astrocytes, the rate of EAAT-mediated Na^+ influx measured using the Na^+ -sensitive indicator SBFI was shown to decline during glutamate application with kinetics that correlated with the increase in $[\text{Na}^+]_i$ (Chatton et al., 2000; Wadiche et al., 2006) reported that high $[\text{Na}^+]_i$ slows the intrinsic kinetics of EAAT4 transporter in cerebellar Purkinje neurons. Taken together, these results obtained in different preparations

support the idea that the EAAT cycling rate is inversely dependent on $[Na^+]_i$. Slowing of glutamate transport may potentially reduce the number of available EAATs at short, i.e. cycling time comparable, ISIs, leading 1) to a decrease of PPR and 2) elevation of extracellular glutamate concentration. The latter was directly shown in brain slices by Okubo et al. (Okubo et al., 2009). In that study EOS, a new glutamate-sensitive fluorescence indicator, was used to trace extracellular glutamate concentration. A single stimulus did not induce any detectable signal in neocortical layer 2/3, whereas paired-pulse stimulation at 100 Hz was followed by a significant (several μM) increase of extracellular glutamate concentration. In this study, effects of single astrocyte dialysis on the field potentials in layer 2/3 were dependent on the pipette $[Na^+]_i$. If high $[Na^+]_i$ slows down EAATs, it is a bit surprising, however, that the reduction of astrocytic $[Na^+]_i$, i.e. expected EAAT acceleration, potentiated neocortical network activity instead of suppressing it (Fig. 41). However, astrocytes enwrap glutamatergic synapses on both excitatory and inhibitory neurons, and $[Na^+]_i$ dependent change of glutamate uptake definitely influences the excitation-inhibition balance. If the faster glutamate uptake stronger suppresses excitation of GABAergic neurons as compared to glutamatergic cells, a potentiation of network activity is actually expected. PPR reduction in the presence of elevated $[Na^+]_i$ was also observed (Fig. 28,32,34). Interestingly, elevated $[Na^+]_i$ reduced PPF at short ISIs, while PPD at longer ISIs remained unaffected. On the other hand, evoked $[Na^+]_i$ transients were reported to last for tens of seconds (Bennay et al., 2008; Langer and Rose, 2009), suggesting that the STC paired-pulse plasticity should be affected also at longer ISIs. However, all $[Na^+]_i$ measurements available in the literature were performed using SBFI, a Na^+ -sensitive fluorescence indicators. The latter reports cytosolic Na^+ concentration, whereas the glutamate uptake via EAATs is mainly determined by the transmembrane gradients, i.e. by near membrane concentrations of glutamate and co-transported ions. Because glutamate uptake is a relatively fast process, one could assume that the short-lasting EAAT-mediated near

membrane $[\text{Na}^+]_i$ transients would have much higher amplitudes than the 2-10 mM cytosolic $[\text{Na}^+]_i$ elevations obtained from the SBFi-based imaging data (Bennay et al., 2008; Kirischuk et al., 2007; Langer and Rose, 2009). Unfortunately, the relationship between $[\text{Na}^+]_i$ and EAAT cycling rate is not quantified yet, i.e. neither the threshold nor the half-maximal (IC_{50}) $[\text{Na}^+]_i$ have been reported. If a relatively high local $[\text{Na}^+]_i$ is required to affect the EAAT cycling rate, short-living near-membrane Na^+ transients would determine the $[\text{Na}^+]_i$ -mediated effects on the paired-pulse plasticity of STCs. Unfortunately, there is no technique available to measure near-membrane $[\text{Na}^+]_i$ transients, but if the hypothesis is true, our data allows proposing that their duration is shorter than 500 ms. (Unichenko et al., 2012)

4.8 GATs may affect glutamate uptake under physiological conditions

100 μM of exogenous GABA is, however, a non-physiological treatment. Can GATs influence EAAT functioning under more physiological conditions? It seems to be the case. Although GAT blockade failed to change the mean amplitude of the first STC, it reduced PPF of STCs at short ISIs in experiments with the low $[\text{Na}^+]_i$ intrapipette solution (Fig. 37,40). Given GATs operate in the uptake mode (but see (Kinney, 2005; Kirmse and Kirischuk, 2006a)), their blockade should result in a decrease of $[\text{Na}^+]_i$. Thus, it is surprising that both the $[\text{Na}^+]_i$ elevation by exogenous GABA and the $[\text{Na}^+]_i$ decrease by GAT blockers resulted in a PPF reduction at short ISIs. To explain the contradiction, we would again hypothesize that the near-membrane $[\text{Na}^+]_i$ transients are much larger than 2-10 mM reported by SBFi. The reversal potential of GATs was reported to be close to the cell resting potential (Richerson and Wu, 2003; Wu et al., 2007). If the EAAT-mediated $[\text{Na}^+]_i$ elevation induced by the first glutamate release is high enough to induce GAT reversal, GATs would contribute to Na^+ extrusion and their

blockade would slow down the decay of $[Na^+]_i$ transients, resulting in EAAT slowing. Because exogenous GABA presumably also prevents the GAT reversal; such hypothesis could explain similar effects observed in the presence of GABA and GAT blockers. If the above hypothesis is true, GATs may dynamically contribute to local $[Na^+]_i$ regulation, accelerating glutamate uptake via EAATs and in turn preventing glutamate spillover during periods of activity (Unichenko et al., 2012).

5 References

1. Achilles K, Okabe A, Ikeda M, Shimizu-Okabe C, Yamada J, Fukuda A, Luhmann HJ, Kilb W (2007) Kinetic properties of Cl⁻ uptake mediated by Na⁺-dependent K⁺-2Cl⁻ cotransport in immature rat neocortical neurons. *Journal of Neuroscience* 27:8616-8627.
2. Aguilo A, Schwartz TH, Kumar VS, Peterlin ZA, Tsiola A, Soriano E, Yuste R (1999) Involvement of Cajal-Retzius neurons in spontaneous correlated activity of embryonic and postnatal layer 1 from wild-type and reeler mice. *Journal of Neuroscience* 19:10856-10868.
3. Anderson CM, Swanson RA (2000) Astrocyte glutamate transport: Review of properties, regulation, and physiological functions. *Glia* 32:1-14.
4. Angulo MC, Kozlov AS, Charpak S, Audinat E (2004) Glutamate released from glial cells synchronizes neuronal activity in the hippocampus. *Journal of Neuroscience* 24:6920-6927.
5. Araque A, Sanzgiri RP, Parpura V, Haydon PG (1999) Astrocyte-induced modulation of synaptic transmission. *Canadian Journal of Physiology and Pharmacology* 77:699-706.
6. Arriza JL, Eliasof S, Kavanaugh MP, Amara SG (1997) Excitatory amino acid transporter 5, a retinal glutamate transporter coupled to a chloride conductance. *Proceedings of the National Academy of Sciences of the United States of America* 94:4155-4160.
7. Attwell D, Barbour B, Szatkowski M (1993) Nonvesicular Release of Neurotransmitter. *Neuron* 11:401-407.
8. Auger C, Attwell D (2000) Fast removal of synaptic glutamate by postsynaptic transporters. *Neuron* 28:547-558.

9. Bacci A, Verderio C, Pravettoni E, Matteoli M (1999) The role of glial cells in synaptic function. *Philosophical Transactions of the Royal Society of London Series B-Biological Sciences* 354:403-409.
10. Bannai S, Tateishi N (1986) Role of Membrane-Transport in Metabolism and Function of Glutathione in Mammals. *Journal of Membrane Biology* 89:1-8.
11. Barbour B, Brew H, Attwell D (1991) Electrogenic Uptake of Glutamate and Aspartate Into Glial-Cells Isolated from the Salamander (*Ambystoma*) Retina. *Journal of Physiology-London* 436:169-193.
12. Behar TN, Li YX, Tran HT, Ma W, Dunlap V, Scott C, Barker JL (1996) GABA stimulates chemotaxis and chemokinesis of embryonic cortical neurons via calcium-dependent mechanisms. *Journal of Neuroscience* 16:1808-1818.
13. Behar TN, Schaffner AE, Scott CA, Greene CL, Barker JL (2000) GABA receptor antagonists modulate postmitotic cell migration in slice cultures of embryonic rat cortex. *Cerebral Cortex* 10:899-909.
14. Behar TN, Scott CA, Greene CL, Wen XL, Smith SV, Maric D, Liu QY, Colton CA, Barker JL (1999a) Glutamate acting at NMDA receptors stimulates embryonic cortical neuronal migration. *Journal of Neuroscience* 19:4449-4461.
15. Behar TN, Scott CA, Greene CL, Wen XL, Smith SV, Maric D, Liu QY, Colton CA, Barker JL (1999b) Glutamate acting at NMDA receptors stimulates embryonic cortical neuronal migration. *Journal of Neuroscience* 19:4449-4461.
16. Bellamy TC, Ogden D (2005) Short-term plasticity of Bergmann glial cell extrasynaptic currents during parallel fiber stimulation in rat cerebellum. *Glia* 52:325-335.
17. Bennay M, Langer J, Meier SD, Kafitz KW, Rose CR (2008) Sodium signals in cerebellar Purkinje neurons and Bergmann glial cells evoked by glutamatergic synaptic transmission. *Glia* 56:1138-1149.

18. Bergles DE, Dzubay JA, Jahr CE (1997) Glutamate transporter currents in Bergmann glial cells follow the time course of extrasynaptic glutamate. *Proceedings of the National Academy of Sciences of the United States of America* 94:14821-14825.
19. Bergles DE, Jahr CE (1997) Synaptic activation of glutamate transporters in hippocampal astrocytes. *Neuron* 19:1297-1308.
20. Bergles DE, Jahr CE (1998) Glial contribution to glutamate uptake at Schaffer collateral-commissural synapses in the hippocampus. *Journal of Neuroscience* 18:7709-7716.
21. Billups B, Rossi D, Attwell D (1996) Anion conductance behavior of the glutamate uptake carrier in salamander retinal glial cells. *Journal of Neuroscience* 16:6722-6731.
22. Bowman CL, Kimelberg HK (1984) Excitatory Amino-Acids Directly Depolarize Rat-Brain Astrocytes in Primary Culture. *Nature* 311:656-659.
23. Cattani AA, Bonfardin VD, Represa A, Ben-Ari Y, Aniksztejn L (2007) Generation of slow network oscillations in the developing rat hippocampus after blockade of glutamate uptake. *Journal of Neurophysiology* 98:2324-2336.
24. Chatton JY, Marquet P, Magistretti PJ (2000) A quantitative analysis of L-glutamate-regulated Na⁺ dynamics in mouse cortical astrocytes: implications for cellular bioenergetics. *European Journal of Neuroscience* 12:3843-3853.
25. Clark BA, Barbour B (1997) Currents evoked in Bergmann glial cells by parallel fibre stimulation in rat cerebellar slices. *Journal of Physiology-London* 502:335-350.
26. Conti F, DeBiasi S, Minelli A, Rothstein JD, Melone M (1998) EAAC1, a high-affinity glutamate transporter, is localized to astrocytes and gabaergic neurons besides pyramidal cells in the rat cerebral cortex. *Cerebral Cortex* 8:108-116.

27. Conti F, Minelli A, Melone M (2004) GABA transporters in the mammalian cerebral cortex: localization, development and pathological implications. *Brain Research Reviews* 45:196-212.
28. Conti F, Zuccarello LV, Barbaresi P, Minelli A, Brecha NC, Melone M (1999) Neuronal, glial, and epithelial localization of gamma-aminobutyric acid transporter 2, a high-affinity gamma-aminobutyric acid plasma membrane transporter, in the cerebral cortex and neighboring structures. *Journal of Comparative Neurology* 409:482-494.
29. Cunningham J, Neal MJ (1981) On the Mechanism by Which Veratridine Causes A Calcium-Independent Release of Gamma-Aminobutyric Acid from Brain-Slices. *British Journal of Pharmacology* 73:655-667.
30. Danbolt NC (2001) Glutamate uptake. *Progress in Neurobiology* 65:1-105.
31. Danbolt NC, Chaudhry FA, Dehnes Y, Lehre KP, Levy LM, Ullensvang K, Storm-Mathisen J (1998) Properties and localization of glutamate transporters. *Glutamate Synapse As A Therapeutical Target: Molecular Organization and Pathology of the Glutamate Synapse* 116:23-43.
32. Delrio JA, Soriano E, Ferrer I (1992) Development of Gaba-Immunoreactivity in the Neocortex of the Mouse. *Journal of Comparative Neurology* 326:501-526.
33. Demarque M, Villeneuve N, Manent JB, Becq H, Represa A, Ben-Ari Y, Aniksztejn L (2004) Glutamate transporters prevent the generation of seizures in the developing rat neocortex. *Journal of Neuroscience* 24:3289-3294.
34. Denter DG, Heck N, Riedemann T, White R, Kilb W, Luhmann HJ (2010) Gaba(C) Receptors Are Functionally Expressed in the Intermediate Zone and Regulate Radial Migration in the Embryonic Mouse Neocortex. *Neuroscience* 167:124-134.

35. Diamond JS (2005) Deriving the glutamate clearance time course from transporter currents in CA1 hippocampal astrocytes: Transmitter uptake gets faster during development. *Journal of Neuroscience* 25:2906-2916.
36. Diamond JS, Bergles DE, Jahr CE (1998) Glutamate release monitored with astrocyte transporter currents during LTP. *Neuron* 21:425-433.
37. Diamond JS, Jahr CE (1997) Transporters buffer synaptically released glutamate on a submillisecond time scale. *Journal of Neuroscience* 17:4672-4687.
38. During MJ, Ryder KM, Spencer DD (1995) Hippocampal Gaba Transporter Function in Temporal-Lobe Epilepsy. *Nature* 376:174-177.
39. Dvorzhak A, Myakhar O, Unichenko P, Kirmse K, Kirischuk S (2010) Estimation of ambient GABA levels in layer I of the mouse neonatal cortex in brain slices. *Journal of Physiology-London* 588:2351-2360.
40. Dvorzhak A, Unichenko P, Kirischuk S (2012) Glutamate transporters and presynaptic metabotropic glutamate receptors protect neocortical Cajal-Retzius cells against over-excitation. *Pflugers Archiv-European Journal of Physiology* 464:217-225.
41. Eulenburg V, Gomez J (2010) Neurotransmitter transporters expressed in glial cells as regulators of synapse function. *Brain Research Reviews* 63:103-112.
42. Feldmeyer D, Lubke J, Silver RA, Sakmann B (2002) Synaptic connections between layer 4 spiny neurone-layer 2/3 pyramidal cell pairs in juvenile rat barrel cortex: physiology and anatomy of interlaminar signalling within a cortical column. *Journal of Physiology-London* 538:803-822.
43. Furuta A, Rothstein JD, Martin LJ (1997) Glutamate transporter protein subtypes are expressed differentially during rat CNS development. *Journal of Neuroscience* 17:8363-8375.

44. Gadea A, Lopez-Colome AM (2001a) Glial transporters for glutamate, glycine and GABA I. Glutamate transporters. *Journal of Neuroscience Research* 63:453-460.
45. Gadea A, Lopez-Colome AM (2001b) Glial transporters for glutamate, glycine, and GABA: II. GABA transporters. *Journal of Neuroscience Research* 63:461-468.
46. Giaume C (2009) Neuronal Control of Astroglial Networks. *Journal of Neurochemistry* 110:101.
47. Giaume C, McCarthy KD (1996) Control of gap-junctional communication in astrocytic networks. *Trends in Neurosciences* 19:319-325.
48. Halassa MM, Fellin T, Haydon PG (2007) The tripartite synapse: roles for gliotransmission in health and disease. *Trends in Molecular Medicine* 13:54-63.
49. Haycock JW, Levy WB, Denner LA, Cotman CW (1978) Effects of Elevated $[K^+]_o$ on Release of Neurotransmitters from Cortical Synaptosomes - Efflux Or Secretion. *Journal of Neurochemistry* 30:1113-1125.
50. Heck N, Kilb W, Reiprich P, Kubota H, Furukawa T, Fukuda A, Luhmann HJ (2007) GABA-A receptors regulate neocortical neuronal migration in vitro and in vivo. *Cerebral Cortex* 17:138-148.
51. Heja L, Barabas P, Nyitrai G, Kekesi KA, Lasztoczi B, Toke O, Tarkanyi G, Madsen K, Schousboe A, Dobolyi A, Palkovits M, Kardos J (2009) Glutamate Uptake Triggers Transporter-Mediated GABA Release from Astrocytes. *Plos One* 4.
52. Helmstaedter M, Staiger JF, Sakmann B, Feldmeyer D (2008) Efficient recruitment of layer 2/3 interneurons by layer 4 input in single columns of rat somatosensory cortex. *Journal of Neuroscience* 28:8273-8284.

53. Hirai K, Yoshioka H, Kihara M, Hasegawa K, Sakamoto T, Sawada T, Fushiki S (1999) Inhibiting neuronal migration by blocking NMDA receptors in the embryonic rat cerebral cortex: a tissue culture study. *Developmental Brain Research* 114:63-67.
54. Hu B, McDonald JW, Johnston MV, Silverstein FS (1991) Excitotoxic Brain Injury Suppresses Striatal High-Affinity Glutamate Uptake in Perinatal Rats. *Journal of Neurochemistry* 56:933-937.
55. Huang YHH, Bergles DE (2004) Glutamate transporters bring competition to the synapse. *Current Opinion in Neurobiology* 14:346-352.
56. Jakobs KH, Lasch P, Minuth M, Aktories K, Schultz G (1982) Uncoupling of Alpha-Adrenoceptor-Mediated Inhibition of Human-Platelet Adenylate-Cyclase by N-Ethylmaleimide. *Journal of Biological Chemistry* 257:2829-2833.
57. Kinney GA (2005) GAT-3 transporters regulate inhibition in the neocortex. *Journal of Neurophysiology* 94:4533-4537.
58. Kinney GA, Spain WJ (2002) Synaptically evoked GABA transporter currents in neocortical glia. *Journal of Neurophysiology* 88:2899-2908.
59. Kirischuk S, Kettenmann H, Verkhratsky A (2007) Membrane currents and cytoplasmic sodium transients generated by glutamate transport in Bergmann glial cells. *Pflugers Archiv-European Journal of Physiology* 454:245-252.
60. Kirischuk S, Parpura V, Verkhratsky A (2012) Sodium dynamics: another key to astroglial excitability? *Trends Neurosci.*
61. Kirischuk S, Verkhratsky A (1996) $[Ca^{2+}]_i$ recordings from neural cells in acutely isolated cerebellar slices employing differential loading of the membrane permeant form of the calcium indicator fura-2. *Pflugers Archiv-European Journal of Physiology* 431:977-983.

62. Kirmse K, Dvorzhak A, Henneberger C, Grantyn R, Kirischuk S (2007a) Cajal-Retzius cells in the mouse neocortex receive two types of pre- and postsynaptically distinct GABAergic inputs. *Journal of Physiology-London* 585:881-895.
63. Kirmse K, Dvorzhak A, Henneberger C, Grantyn R, Kirischuk S (2007b) Cajal-Retzius cells in the mouse neocortex receive two types of pre- and postsynaptically distinct GABAergic inputs. *Journal of Physiology-London* 585:881-895.
64. Kirmse K, Kirischuk S (2006a) Ambient GABA constrains the strength of GABAergic synapses at Cajal-Retzius cells in the developing visual cortex. *Journal of Neuroscience* 26:4216-4227.
65. Kirmse K, Kirischuk S (2006b) N-ethylmaleimide increases release probability at GABAergic synapses in layer I of the mouse visual cortex. *European Journal of Neuroscience* 24:2741-2748.
66. Kovacs R, Heinemann U, Steinhauser C (2012) Mechanisms underlying blood-brain barrier dysfunction in brain pathology and epileptogenesis: Role of astroglia. *Epilepsia* 53:53-59.
67. Kressin K, Kuprijanova E, Jabs R, Seifert G, Steinhauser C (1995) Developmental Regulation of Na⁺ and K⁺ Conductances in Glial-Cells of Mouse Hippocampal Brain-Slices. *Glia* 15:173-187.
68. Langer J, Rose CR (2009) Synaptically induced sodium signals in hippocampal astrocytes in situ. *Journal of Physiology-London* 587:5859-5877.
69. Lee SH, Kim MH, Park KH, Earm YE, Ho WK (2002) K⁺-dependent Na⁺/Ca²⁺ exchange is a major Ca²⁺ clearance mechanism in axon terminals of rat neurohypophysis. *Journal of Neuroscience* 22:6891-6899.
70. Lenhossek Mv (1891) Zur Kenntnis der Neuroglia des menschlichen Rückenmarkes. *Verh Anat Ges* 193-221.

71. Levy LM, Warr O, Attwell D (1998) Stoichiometry of the glial glutamate transporter GLT-1 expressed inducibly in a Chinese hamster ovary cell line selected for low endogenous Na(+)-dependent glutamate uptake. *Journal of Neuroscience* 18:9620-9628.
72. Lopez-Bayghen E, Ortega A (2011) Glial Glutamate Transporters: New Actors in Brain Signaling. *Iubmb Life* 63:816-823.
73. Lopez-Bendito G, Lujan R, Shigemoto R, Ganter P, Paulsen O, Molnar Z (2003) Blockade of GABA(B) receptors alters the tangential migration of cortical neurons. *Cerebral Cortex* 13:932-942.
74. Manent JB, Demarque M, Jorquera I, Pellegrino C, Ben-Ari Y, Aniksztejn L, Represa A (2005) A noncanonical release of GABA and glutamate modulates neuronal migration. *Journal of Neuroscience* 25:4755-4765.
75. Manita S, Suzuki T, Inoue M, Kudo Y, Miyakawa H (2007) Paired-pulse ratio of synaptically induced transporter currents at hippocampal CA1 synapses is not related to release probability. *Brain Research* 1154:71-79.
76. Matsugami TR, Tanemura K, Mieda M, Nakatomi R, Yamada K, Kondo T, Ogawa M, Obata K, Watanabe M, Hashikawa T, Tanaka K (2006) Indispensability of the glutamate transporters GLAST and GLT1 to brain development. *Proceedings of the National Academy of Sciences of the United States of America* 103:12161-12166.
77. Matyash V, Kettenmann H (2010) Heterogeneity in astrocyte morphology and physiology. *Brain Research Reviews* 63:2-10.
78. Mienville JM (1998) Persistent depolarizing action of GABA in rat Cajal-Retzius cells. *Journal of Physiology-London* 512:809-817.
79. Mienville JM, Pesold C (1999) Low resting potential and postnatal upregulation of NMDA receptors may cause Cajal-Retzius cell death. *Journal of Neuroscience* 19:1636-1646.

80. Minelli A, Barbaresi P, Conti F (2003) Postnatal development of high-affinity plasma membrane GABA transporters GAT-2 and GAT-3 in the rat cerebral cortex. *Developmental Brain Research* 142:7-18.
81. Minelli A, DeBiasi S, Brecha NC, Zuccarello LV, Conti F (1996) GAT-3, a high-affinity GABA plasma membrane transporter, is localized to astrocytic processes, and it is not confined to the vicinity of GABAergic synapses in the cerebral cortex. *Journal of Neuroscience* 16:6255-6264.
82. Nimmerjahn A, Kirchhoff F, Kerr JND, Helmchen F (2004) Sulforhodamine 101 as a specific marker of astroglia in the neocortex in vivo. *Nature Methods* 1:31-37.
83. Okubo Y, Sekiya H, Namiki S, Sakamoto H, Iinuma S, Yamasaki M, Watanabe M, Hirose K, Iino M (2009) Imaging extrasynaptic glutamate dynamics in the brain. *Neuroscience Research* 65:S142-S143.
84. Otis TS, Jahr CE (1998) Anion currents and predicted glutamate flux through a neuronal glutamate transporter. *Journal of Neuroscience* 18:7099-7110.
85. Otis TS, Kavanaugh MP, Jahr CE (1997) Postsynaptic glutamate transport at the climbing fiber Purkinje cell synapse. *Science* 277:1515-1518.
86. Owens DF, Kriegstein AR (2002) Is there more to GABA than synaptic inhibition? *Nature Reviews Neuroscience* 3:715-727.
87. Peghini P, Janzen J, Stoffel W (1997) Glutamate transporter EAAC-1-deficient mice develop dicarboxylic aminoaciduria and behavioral abnormalities but no neurodegeneration. *Embo Journal* 16:3822-3832.
88. Perea G, Navarrete M, Araque A (2009) Tripartite synapses: astrocytes process and control synaptic information. *Trends in Neurosciences* 32:421-431.

89. Porter JT, McCarthy KD (1997) Astrocytic neurotransmitter receptors in situ and in vivo. *Progress in Neurobiology* 51:439-455.
90. Poskanzer KE, Yuste R (2011) Astrocytic regulation of cortical UP states. *Proceedings of the National Academy of Sciences of the United States of America* 108:18453-18458.
91. Regan MR, Huang YH, Kim YS, Dykes-Hoberg MI, Jin L, Watkins AM, Bergles DE, Rothstein JD (2007) Variations in promoter activity reveal a differential expression and physiology of glutamate transporters by glia in the developing and mature CNS. *Journal of Neuroscience* 27:6607-6619.
92. Reiprich P, Kilb W, Luhmann HJ (2005) Neonatal NMDA receptor blockade disturbs neuronal migration in rat somatosensory cortex in vivo. *Cerebral Cortex* 15:349-358.
93. Represa A, Ben-Ari Y (2005) Trophic actions of GABA on neuronal development. *Trends in Neurosciences* 28:278-283.
94. Richerson GB, Wu YM (2003) Dynamic equilibrium of neurotransmitter transporters: Not just for reuptake anymore. *Journal of Neurophysiology* 90:1363-1374.
95. Rojas H, Colina C, Ramos M, Benaim G, Jaffe EH, Caputo C, DiPolo R (2007) Na⁺ entry via glutamate transporter activates the reverse Na⁺/Ca²⁺ exchange and triggers Ca²⁺-induced Ca²⁺ release in rat cerebellar Type-1 astrocytes. *Journal of Neurochemistry* 100:1188-1202.
96. Rose CR, Ransom BR (1996) Intracellular sodium homeostasis in rat hippocampal astrocytes. *Journal of Physiology-London* 491:291-305.
97. Rossi DJ, Oshima T, Attwell D (2000) Glutamate release in severe brain ischaemia is mainly by reversed uptake. *Nature* 403:316-321.
98. Rothstein JD, Dykes-Hoberg M, Pardo CA, Bristol LA, Jin L, Kuncl RW, Kanai Y, Hediger MA, Wang YF, Schielke JP, Welty DF (1996)

- Knockout of glutamate transporters reveals a major role for astroglial transport in excitotoxicity and clearance of glutamate. *Neuron* 16:675-686.
99. Rouach N, Koulakoff A, Abudara V, Willecke K, Giaume C (2008) Astroglial Metabolic Networks Sustain Hippocampal Synaptic Transmission. *Science* 322:1551-1555.
 100. Rouach N, Koulakoff A, Giaume C (2004) Neurons set the tone of gap junctional communication in astrocytic networks. *Neurochemistry International* 45:265-272.
 101. Sandoval ME (1980) Sodium-Dependent Efflux of [H-3]Gaba from Synaptosomes Probably Related to Mitochondrial Calcium Mobilization. *Journal of Neurochemistry* 35:915-921.
 102. Santello M, Cali C, Bezzi P (2012) Gliotransmission and the Tripartite Synapse. *Synaptic Plasticity: Dynamics, Development and Disease* 970:307-331.
 103. Schroder W, Hager G, Kouprijanova E, Weber M, Schmitt AB, Seifert G, Steinhauser C (1999) Lesion-induced changes of electrophysiological properties in astrocytes of the rat dentate gyrus. *Glia* 28:166-174.
 104. Schwartz EA (1982) Calcium-Independent Release of Gaba from Isolated Horizontal Cells of the Toad Retina. *Journal of Physiology-London* 323:211-&.
 105. Schwartz TH, Rabinowitz D, Unni V, Kumar VS, Smetters DK, Tsiola A, Yuste R (1998) Networks of coactive neurons in developing layer 1. *Neuron* 20:541-552.
 106. Shimamoto K, Sakai R, Takaoka K, Yumoto N, Nakajima T, Amara SG, Shigeri Y (2004) Characterization of novel L-threo-beta-benzyloxyaspartate derivatives, potent blockers of the glutamate transporters. *Molecular Pharmacology* 65:1008-1015.

107. Soda T, Nakashima R, Watanabe D, Nakajima K, Pastan I, Nakanishi S (2003) Segregation and coactivation of developing neocortical layer 1 neurons. *Journal of Neuroscience* 23:6272-6279.
108. Somjen GG (1988) Nervenkitz - Notes on the History of the Concept of Neuroglia. *Glia* 1:2-9.
109. Super H, Soriano E, Uylings HBM (1998) The functions of the preplate in development and evolution of the neocortex and hippocampus. *Brain Research Reviews* 27:40-64.
110. Tzingounis AV, Wadiche JI (2007) Glutamate transporters: confining runaway excitation by shaping synaptic transmission. *Nature Reviews Neuroscience* 8:935-947.
111. Unichenko P, Dvorzhak A, Kirischuk S (2013) Transporter-mediated replacement of extracellular glutamate for GABA in the developing murine neocortex. *European Journal of Neuroscience* 38:3580-3588.
112. Unichenko P, Myakhar O, Kirischuk S (2012) Intracellular Na⁺ concentration influences short-term plasticity of glutamate transporter-mediated currents in neocortical astrocytes. *Glia* 60:605-614.
113. Varoqueaux F, Sigler A, Rhee JS, Brose N, Enk C, Reim K, Rosenmund C (2002) Total arrest of spontaneous and evoked synaptic transmission but normal synaptogenesis in the absence of Munc13-mediated vesicle priming. *Proceedings of the National Academy of Sciences of the United States of America* 99:9037-9042.
114. Verhage M, Maia AS, Plomp JJ, Brussaard AB, Heeroma JH, Vermeer H, Toonen RF, Hammer RE, van den Berg TK, Missler M, Geuze HJ, Sudhof TC (2000) Synaptic assembly of the brain in the absence of neurotransmitter secretion. *Science* 287:864-869.
115. Volterra A, Steinhauser C (2004) Glial modulation of synaptic transmission in the hippocampus. *Glia* 47:249-257.

116. Voutsinos-Porche B, Knott G, Tanaka K, Quairiaux C, Welker E, Bonvento G (2003) Glial glutamate transporters and maturation of the mouse somatosensory cortex. *Cerebral Cortex* 13:1110-1121.
117. Wadiche JI, Tzingounis AV, Jahr CE (2006) Intrinsic kinetics determine the time course of neuronal synaptic transporter currents. *Proceedings of the National Academy of Sciences of the United States of America* 103:1083-1087.
118. Watase K, Hashimoto K, Kano M, Yamada K, Watanabe M, Inoue Y, Okuyama S, Sakagawa T, Ogawa S, Kawashima N, Hori S, Takimoto M, Wada K, Tanaka K (1998) Motor discoordination and increased susceptibility to cerebellar injury in GLAST mutant mice. *European Journal of Neuroscience* 10:976-988.
119. Wu YM, Wang WG, Diez-Sampedro A, Richerson GB (2007) Nonvesicular inhibitory neurotransmission via reversal of the GABA transporter GAT-1. *Neuron* 56:851-865.
120. Zerangue N, Kavanaugh MP (1996) Flux coupling in a neuronal glutamate transporter. *Nature* 383:634-637.
121. Zucker RS, Regehr WG (2002) Short-term synaptic plasticity. *Annual Review of Physiology* 64:355-405.

Acknowledgments

CV